Francisella tularensis ferric-siderophore and ferrous iron transport systems are necessary for iron acquisition and viability

Natalie Marie Pérez
Austin, Texas

B.A. Smith College, 2007

A Dissertation presented to the Graduate Faculty
of the University of Virginia in Candidacy for the Degree of
Doctor of Philosophy

Department of Microbiology, Immunology, and Cancer Biology

University of Virginia
December 2014

Abstract

Francisella tularensis is a Gram-negative intracellular bacterium and the causative agent of the disease tularemia. *F. tularensis* is designated by the CDC as a Tier One Select Agent, due to its low infection dose, aerosol transmissibility, lack of a licensed vaccine, and for its potential use as an agent of biological warfare. Virulent Schu S4 and the attenuated live vaccine strain (LVS) are model strains used to study *F. tularensis* pathogenesis in tissue culture and in the mouse model of disease. Despite the genetic similarities between LVS and Schu S4, these strains have differences in iron uptake capability and virulence. Within the host, iron is tightly controlled and sequestered by iron binding proteins. Pathogenic bacteria, include *F. tularensis,* have devised methods for acquiring available ferrous and ferric iron from their hosts and they are frequently associated with virulence.

A common method for ferric acquisition is the production of siderophores, which are low molecular weight iron binding chelators that are secreted into the environment and have high affinities for ferric iron. *F. tularensis* strains LVS and Schu S4 secrete an identical siderophore and encode genes required for siderophore biosynthesis and transport (*fslABCDEF* also referred to as *figABCDEF*). An in-frame deletion of *fslC* was generated in the LVS background (LVS Δ*fslC*), and similar to the previously published *fslA* mutant (LVS Δ*fslA*), this mutant was defective for siderophore production as determined by the liquid Chrome-Azurol S (CAS) assay. A *fslABCDEF* locus deletion mutant, LVS Δ*fsl,* was complemented with plasmids containing wild-type copies of the *fsl* genes

and was used to determine that *F. tularensis* siderophore biosynthesis requires FslA and FslC, and siderophore export requires FslB. The LVS *fsl* mutants were not defective for growth in tissue culture cells thus suggesting that another iron acquisition system is sufficient at acquiring necessary iron for *Francisella* growth and survival.

My dissertation studies also investigated the ferrous iron uptake system (Feo) in the *Francisella* strains Schu S4 and LVS as an alternative iron acquisition mechanism for growth and survival. The Feo system has been demonstrated in other bacterial systems to regulate the entry of available ferrous iron. Partial deletion mutants of *feoB* (Δ*feoB'*) were generated in LVS and Schu S4. ^{55}Fe uptake assays demonstrated that the Feo systems in both LVS and Schu S4 are dependent on FeoB for ferrous iron uptake at both high (0.1 μM) and low (3.0 μM) affinity iron concentrations. These Δ*feoB'* mutants did utilize the ferric-siderophore iron acquisition system which was observed through CAS and ^{55}Fe-siderophore uptake assays. My dissertation studies demonstrated that the Feo system is specific for ferrous iron transport and is the sole ferrous iron acquisition system in this bacterium.

Studies with Δ*fslA*, Δ*feoB'*, and Δ*fslA* Δ*feoB'* were used to delineate iron acquisition preferences and the potential presence of an unidentified iron acquisition system in *Francisella*. The double deletion mutants in both strains were only able to grow and survive in the presence of *F. tularensis* siderophore. Through intracellular replication assays and mouse infection studies it was observed that both iron acquisition systems contribute to optimal iron acquisition,

growth, and virulence of *F. tularensis* and each iron acquisition system can compensate for the loss of the other. Both LVS and Schu S4 double deletion mutants were attenuated for virulence in C57BL/6 mouse infection studies and provided protection upon lethal challenge with wild-type LVS and Schu S4, respectively. The work presented here clarifies our understanding of the iron acquisition mechanisms utilized by this pathogenic bacterium and their role in growth and virulence in the mouse model of infection. Additionally, the LVS and Schu S4 double deletion mutants are potential candidates for vaccine development.

Acknowledgements:

I would like to express my deepest gratitude to University of Virginia, especially the Department of Microbiology, Immunology, and Cancer Biology for allowing me the opportunity to study and to perform my dissertation studies at this prestigious University. Foremost, I would like to thank my mentor Dr. Girija Ramakrishnan and my co-mentor Dr. Barbara Mann for their patience, insight, and enthusiasm for my project. I would also like to thank my committee members Dr. Alison Criss, Dr. Ann Beyer, Dr. John Bushweller, Dr. Melissa Kendall, and my former committee member Dr. Joanna Goldberg. I especially want to thank Dr. William A. Petri for allowing me be an honorary member of the Petri lab and for your support and optimistic critiques of my work.

To my friends and family, I would like to thank you for your encouragement and support over the course of my graduate studies. I would especially like to thank my parents Sergio and Sylvia Pérez for their love and support; my dissertation is dedicated to you.

Table of Contents:

Chapter 2. The Live Vaccine Strain (LVS) encodes two iron acquisition systems essential for growth and virulence

Chapter 3. Type A *Francisella tularensis* mutant disrupted in the two major iron acquisition systems provides limited protection against subcutaneous Schu S4 challenge

Appendix. The *F. tularensis* siderophore locus (*fsl*) contains all the necessary genes for siderophore biosynthesis and siderophore export

List of Figures

List of Tables

List of Abbreviations:

ATP	Adenosine triphosphate
BHI	Brain heart infusion broth
CAS	Chrome Azurol S assay
CCCP	Carbonyl cyanide *m*-chlorophenyl hydrazone
CD	Circular dichroism
CDM	Chamberlain's chemically defined media
CFU	Colony forming units
CHAB	Cysteine heart agar plates
Che-CDM	Chelex-100 treated chemically defined media
Da	Dalton
DAP	Diaminopimelate
DAPDC	Diaminopimelate decarboxylase
DNA	Deoxyribonucleic acid
Fe	Iron
Fe^{2+}	Ferrous iron
Fe^{3+}	Ferric iron
^{55}Fe	Iron-55, radioactive isotope
Fe-Fur	Iron bound ferric uptake regulator protein
Feo	Ferrous iron transport system
FePPi	Ferric pyrophosphate
$FeSO_4$	Ferrous sulfate
fsl	*Francisella* siderophore locus
Fur	Ferric uptake regulator
FPI	*Francisella* pathogenicity island
FPN1	Ferroportin 1
G+C	Guanine-cytosine content
GDP	Guanosine diphosphate
GIS	Growth initiation substance
G-protein	Guanine nucleotide-binding protein
GTP	Guanosine triphosphate
H_2O_2	Hydrogen peroxide
ID_{50}	Infectious dose 50
IM	Inner membrane
IP	Intraperitoneal
LIP	Labile iron pool
LVS	Live Vaccine Strain
μ	Micro (10^{-6})
M	Molar
Mbp	Megabase pair, 1,000,000 base pairs
MFS	Major facilitator superfamily
MHA	Modified Muller-Hinton Agar
MHA+	Muller-Hinton Agar with ferric pyrophosphate
MHA-	Muller-Hinton Agar without additional iron
MOI	Multiplicity of infection

NCBI	National Center for Biotechnology Information
NIS	NRPS independent siderophore synthetase
NRPS	Nonribosomal peptide synthetase
OD_{595}	Optical density measured at Absorbance 595 nm
OD_{600}	Optical density measured at Absorbance 600 nm
ODC	Ornithine decarboxylase
-OH	Hydroxyl radical
OM	Outer membrane
OMP	Outer membrane protein
PLP	pyridoxal 5'-phosphate
S.D	Standard Deviation
SDS	Sodium dodecyl sulfate
S.E	Standard error
Tf	Transferrin
TfR1	Transferrin receptor 1
TfR2	Transferrin receptor 2
TMS	Transmembrane segments
TonB	TonB ExbB ExbD complex
TSB/c	Tryptic soy broth supplemented with cysteine

Chapter 1: Introduction

1.0 Iron necessity and human nutritional immunity

Iron, with the exception of a few organisms, is necessary for basic metabolic processes. Iron is present in two oxidation states, either the oxidized ferric form (Fe^{3+}) or the reduced ferrous form (Fe^{2+}), depending on the presence or absence of oxygen, respectively. While prevalent in nature, iron is highly insoluble in aerobic environments and forms ferric hydroxide and oxyhydroxide polymers [1]. In humans, iron is solubilized in complexes such as heme or iron sulfur clusters and is bound by various metalloproteins that require the redox capability of this metal for respiration, amino acid synthesis, and DNA synthesis [1,2]. When unbound by regulatory proteins or iron-complexes, iron can decompose hydrogen peroxide (H_2O_2) through the Fenton reaction to produce hydroxy radicals (-OH). These hydroxyl radicals can damage cellular membranes and DNA. Therefore, the uptake and transport of iron is highly regulated to maintain the concentration of free iron at approximately 10^{-18} M within the human host [3].

Iron enters humans through the ingestion of food and is absorbed by the small intestine either in the reduced ferrous iron form or bound by heme [4]. Absorbed iron is then trafficked through the blood by the transport protein, transferrin (Tf), and is typically received by iron starved cells through the transferrin receptor 1 (TfR1), which is present on most cell types [4]. Transferrin can also be received by transferrin receptor 2 (TfR2), which is predominately expressed on hepatocytes [5]. Iron within host cells is present as an enzymatic cofactor or is reserved in the large iron storage molecule, ferritin [4]. There are also

varying levels of iron present in the cytoplasm within the intracellular labile iron

pool (LIP), which makes iron readily available to meet the needs of the cell [6].

The host also regulates and sequesters essential metals like iron in the

body to prevent and limit the progression of bacterial infection, otherwise referred

to as nutritional immunity [7–9]. The efficiency of iron binding and transport by

regulatory molecules is necessary for basic host metabolism; however, iron

withholding is a key element to prevent the overgrowth of bacterial and

eukaryotic pathogens within the host. The hormone hepcidin, which is produced

by hepatocytes in the liver, negatively regulates the transport of iron from host

cells [10]. When pathogens are present in the blood, hepcidin binds to the host cell

iron transporter, ferroportin 1 (FPN1) and both hepcidin and FPN1 are

internalized and destroyed [11]. In addition, to prevent iron accessibility in blood,

transferrin receptors on cells continually remove iron bound transferrin (holo-

transferrin) which in turn starves extracellular bacteria [4]. During infection, iron is

also sequestered in macrophages, which characteristically recycle senescent

erythrocyte iron, to prevent the circulation of iron to pathogens [12].

1.1 Iron acquisition mechanisms of bacteria

Iron is essential for most bacteria and is an important cofactor.

Intracellular bacteria are able to sense the levels of metals, including iron, in the

host environment and regulate the transcription of metal dependent genes

required for iron acquisition and transport [13–15]. Bacteria have also evolved

various mechanisms to survive within the different metal restrictive niches of the

mammalian host. When iron levels drop below the bacterial threshold

requirement of ~10^{-6} M, bacteria increase expression of iron acquisition systems, which target the uptake of iron bound by heme, transferrin, and iron binding proteins [16,17]. These acquisition systems are necessary for acquiring iron, growth and survival, and are implicated as determinants of bacterial virulence mechanisms in a number of bacterial pathogens [13].

1.2 Iron regulation in bacteria

Extensive studies of bacterial pathogens have determined that the environmental stress of low-iron correlates with the expression of virulence factors [13,15,18]. These acquisition systems are managed by intracellular transcription protein regulators such as diphtheria toxin receptor, DtxR, in Gram-positive bacteria and the ferric uptake regulator, Fur, in Gram-negative bacteria [19]. Fur is a key determinant for the sensing and maintenance of the intracellular environment of Gram-negative bacteria [19]. In the presence of an iron rich environment, the Fur protein is bound by two iron molecules to form a complex which then binds to the Fur-box where it acts as a repressor [15]. The Fur-box is a 19 base pair conserved sequence motif that functions as a recognition signal upstream of iron-regulated genes [15]. When Fe-Fur is bound to the Fur-box, transcription of iron-regulated genes is prevented [15]. The Fe-Fur repressor has been shown in *Neisseria meningitides, Yersinia* species*, and *Pseudomonas* species to have a dual regulatory role as both an activator and a repressor of virulence genes [20,21]. This regulation at the level of transcription is important to limit the energy expensive synthesis of proteins when they are unnecessary [22]. Fur as a transcription regulator is capable of influencing the global intracellular

profile of an organism, including proteins necessary for but not restricted to energy metabolism, combating oxidative stress [23], biofilm formation, and quorum sensing [24].

1.3 Ferric iron acquisition

In aerobic environments, iron is present in the oxidized ferric form. Ferric iron is insoluble at neutral pH and is typically bound by proteins to increase solubility. To acquire this form of iron, bacteria and fungi produce siderophores, which are low molecular weight (500-1500 Da) iron binding molecules that are capable of chelating ferric iron [25]. Siderophore ligands coordinate with ferric iron to form multidentate Fe^{3+}-complexes [26]. Siderophores are secreted into the environment, bind ferric iron, and are retrieved through specific membrane receptors [27,28]. The energy for siderophore retrieval across the outer membrane is provided by the TonB ExbB ExbD complex in the inner membrane, also referred to as the TonB complex, which is able to harness the proton motive force [15,29]. Some bacterial systems lack the TonB homolog, such as *Legionella pneumophila* [30] and *Francisella tularensis* [31], though these bacteria are still fully capable of retrieving and utilizing ferric siderophores. The intracellular utilization of iron from ferric siderophore is predicted to occur by the action of ferric reductases or through the degradation of siderophores [32].

Siderophores are classified based on their structural ligands (hydroxymate, catecholate, α-hydroxycarboxylate), and the types of enzymes used for their biosynthesis [16]. Siderophores are synthesized by either nonribosomal peptide synthetases (NRPS) or NRPS independent siderophore

(NIS) synthetases [26]. NRPS systems catalyze the biosynthesis of mainly catechol and hydroxamate siderophores [21,26]. Both NRPS and NIS synthetases are required to synthesize some siderophores such as petrobactin [26]. NIS synthetases require the cofactor ATP to catalyze the formation of an amide bond between carboxylic acid and an amino group [26]. NIS synthetases are categorized based on their substrates, which include Type A and Type A' (citric acid), Type B (α-ketoglutaric acid), and Type C (succinic acid derivatives) [28]. Both Type A and Type A' require citric acid substrates but differ in their phylogeny lineage [28]. The substrates required for siderophore biosynthesis arise from intracellular bacterial metabolism and, in some cases, potentially from host derived sources. Depending on the siderophore structure and ligands, a siderophore can remove iron from a range of substrates (i.e. iron bound host proteins) to acquire nutritional iron.

Bacteria tend to encode a variety of siderophores that can support survival in various environments including aquatic, terrestrial, and even mammalian hosts. While most bacteria generate and acquire their own siderophores, some bacteria avoid siderophore biosynthesis and utilize siderophores secreted from neighboring bacteria [33–35]. Certain siderophores have also been characterized as virulence factors due to their ability to help pathogens colonize a host niche by facilitating the nutritional need for iron [13,16]. Some bacterial systems, independent of siderophores, are able to acquire iron directly from iron bound host proteins such as heme, ferritin, and lactoferrin through specific receptors [36]. Most bacteria that are capable of utilizing iron bound by these proteins have specific protein

receptors that acquire the whole molecule for entry into the bacterium [16]. In addition to siderophores, there are also proteins that are secreted to bind heme, called hemophores, present in in some bacterial systems [37]. The variety of ferric iron acquisition mechanisms produced by bacteria demonstrates the need for iron is crucial and having multiple means of acquiring iron may provide an advantage for bacteria in different environments.

1.4 Ferrous iron

The reduced ferrous iron form is found primarily in anaerobic and microaerobic environments. Free soluble ferrous iron is predicted to diffuse through porins in the outer membrane of Gram-negative bacteria and is then subsequently transported into the cytoplasm by the ferrous iron transport system (Feo) [38]. The Feo system has been best described in the enteric pathogens, *Escherichia coli* and *Salmonella enterica* serovar *typhimurium* [38–41]. Classically the Feo system is comprised of three components: FeoA, FeoB, and FeoC [38]; however, all three components are not always required for ferrous iron uptake. While there is conservation of the Feo system in different classes of bacteria [38], there are differences in the genes necessary for ferrous iron uptake and their location within bacterial genomes [38].

The consensus amongst bacteria that encode the Feo system is the requirement for the GTP-dependent inner membrane permease, FeoB. FeoB is predicted to contain a hydrophilic N-terminal G-protein and a C-terminal integral membrane domain constructed of 8-transmembrane α-helices [38,42]. The cytoplasmic N-terminus of FeoB contains a GTP binding domain with 4 out of the

21

5 characteristic G protein domains (G1-G5) [42]. It has been recently determined that the GTPase domain is very similar to the G protein domains of eukaryotic proteins and is required for binding GTP/GDP [42] as well as for interacting with FeoA in some systems [40]. The C-terminus of FeoB is comprised of α-transmembrane domains and allows for the recognition and entry of ferrous iron [39]. In *E coli,* FeoA and FeoB are both necessary for optimal ferrous iron entry, although ferrous iron is able to enter with just FeoB present [39]. To date little is known about FeoA and FeoC. Based on a bacterial hybrid assay, *S. typhimurium* FeoA was shown to interact with FeoB and found to be essential for ferrous iron uptake [40]. Also, FeoC in *Salmonella* is required for ferrous iron uptake in low oxygen and low iron conditions [41].

FeoA and FeoC are not essential for ferrous iron acquisition, and are even lacking in some bacteria, but the lack of these proteins can cause a reduced capacity for FeoB ferrous iron uptake [38,40,41,43]. Bacteria that do not encode for all three *feo* genes but have a functional Feo system include *Helicobacter pylori* [44], *Campylobacter jejuni* [23,45], and *Legionella pneumophila* [46]. These bacteria require ferrous iron acquisition through FeoB for effective colonization of the mammalian host. The Feo system, in combination with other iron acquisition systems, is required for intracellular growth and colonization of *Legionella pneumophila* [46], *Yersinia pestis* [47], *Shigella flexneri* [48], and *Campylobacter jejuni* [45]. Iron is crucial for bacterial growth and having the option to acquire it through a ferrous iron acquisition system may provide bacteria a survival advantage in an anaerobic or microaerobic environment.

1.5 Facultative intracellular bacteria

Facultative intracellular bacteria are a group of bacteria that are capable of surviving in both extracellular and intracellular niches. This category of bacteria is typically capable of being cultured through *in vitro* techniques, but they are also able to thrive intracellularly within host eukaryotic cells. *Shigella flexneri, Mycobacterium tuberculosis, Bacillus anthracis,* and *Yersinia pestis* are some examples of facultative intracellular pathogens. These species contain a variety of iron acquisition systems, and only when multiple iron acquisition systems are removed can noticeable virulence attenuation be recognized [47–51]. However, in *B. anthracis* [51] and *M. tuberculosis* [49,50], the removal of a single specific ferric siderophore system rendered these bacteria defective for intracellular growth within macrophages and were attenuated for virulence in animal models of infection. Iron acquisition is not necessarily an indicator of pathogenicity, but a bacterium's ability to acquire iron within the host can be a determinant of bacterial virulence potential [13]. Bacteria can only establish an infection if they are capable of obtaining the necessary nutrients for growth and survival. The iron limiting environment of the host provides a hurdle for these bacteria to obtain necessary iron resources and bacterial iron acquisition mechanisms can be the limiting factor for the ability to thrive within the host environment.

1.6 *Francisella tularensis*

F. tularensis is a Gram-negative γ-proteobacterium with a genome of ~1.9 Mbp and ~32.9% G+C content [31]. *F. tularensis* is classified as a facultative intracellular pathogen and is the causative agent of the zoonotic disease

tularemia, also referred to as rabbit fever [52]. *F. tularensis* is transmitted by inhalation of aerosolized bacteria and by the bite of arthropod vectors and is able to survive in a variety of small mammals [53–56]. *F. tularensis* has three subspecies that include *tularensis, holarctica,* and *mediasiatica,* which all cause varying degrees of disease in humans [57]. A related species, *F. novicida* is also studied in relation to *F. tularensis* genetics and pathogenicity.

F. tularensis subspecies *tularensis* causes the most severe disease in humans and is categorized by the United States Centers for Disease Control and Prevention (CDC) as a Tier One select agent. This classification is in effect due to the low 50% infectious dose (ID_{50}) of <10 colony forming units (CFU) [58], lack of a licensed vaccine, and the potential to cause significant harm to the public if misused. The subspecies *holarctica* causes a less virulent form of tularemia and is modeled by the live vaccine strain (LVS). LVS is an attenuated strain that has been extensively used as a preliminary organism to study prior to investigation of the virulent *tularensis* Schu S4 strain. While belonging to two different subspecies, both LVS and Schu S4 have very similar genomes with an average identity of 99.89% [59]. The study of both *holarctica* and *tularensis* strains are necessary for a complete understanding of *F. tularensis* and are essential for the study of this bacterium's metabolism and pathogenicity.

As an intracellular pathogen, *F. tularensis* is capable of entering both phagocytic and non-phagocytic cell types, which include but are not limited to macrophages, neutrophils, hepatocytes, and epithelial cells [58]. Entry and replication within innate immune macrophage cells has been best studied and

these cells are predicted to be the first cell type *F. tularensis* encounters during infection [60]. Over the course of infection, this bacterium targets the host's liver, spleen, and lung tissues [61].

    F. tularensis uptake into macrophages is characteristically achieved through the binding of host cell receptors that causes the host cell membrane to develop pseudoloops to phagocytose and acquire *F. tularensis* [62]. The intracellular lifecyle of *F. tularensis* within a macrophage is depicted in Figure 1. This entry into macrophages can occur with or without opsonization [62]. Upon phagocytosis, *F. tularensis* is initially sequestered in a phagosome [63]. This phagosome does not progress into the late endosomal stage, but rather an interruption occurs within 30 minutes to an hour of entry in which the phagosome becomes acidified and allows the escape of the bacterium into the cytosol [57,64,65]. This acidification of the phagosome was shown to be necessary for optimal *F. tularensis* growth and replication within the intracellular niche of peritoneal macrophages [57,65,66]. Bacterial genes located within the *Francisella* pathogenicity island (FPI) encode for a putative type VI secretion system and virulence effectors necessary for escape into the cytoplasm [67]. Deletion of the FPI genes *iglC* and *iglD* prevents *Francisella* escape from the phagosome, which limits bacterial intracellular replication and does not cause the host cell to undergo apoptosis as typically occurs [67]. The ability of *Francisella* to infect cells, escape the phagosome, and replicate within the host cell cytoplasm, are essential steps for growth and survival of this pathogen. Disruption of genes necessary for any of

these steps renders the bacterium unable to grow and replicate, and hence is attenuated for virulence.

The host cytoplasm provides a niche of essential nutrients that promote *F. tularensis* growth and replication. Like the mutants unable to escape the phagosome, the inability to grow and replicate has also been observed for *F. tularensis* metabolic auxotrophs such as the Schu S4 purine metabolism mutants (Schu S4 Δ*purMCD*) [68,69]. These mutants are able to infect macrophages and further enter the cytoplasm but lack key components to acquire essential nutrients and metabolites and thus are unable to replicate intracellularly. This inability to acquire nutrients can affect bacterial colonization, growth rate, and ultimately attenuate *F. tularensis*.

Wehrly *et al.* (2009) reported microarray data showing the upregulation of genes for siderophore biosynthesis early in the infection of bone marrow derived macrophages (BMM) by Schu S4 [70]. The ability of *F. tularensis* to replicate within macrophages is dependent on the availability of intracellular iron as shown by inhibition of this process by the iron chelator deferoxamine [66]. The presence of iron is also known to influence the *F. tularensis* FPI and thus by proxy may influence genes associated with *F. tularensis* virulence [71,72]. Bacterial sensing of host metabolite levels can also act as a cue to an intracellular bacterium to upregulate the expression of virulence mechanisms that promote growth and colonization [73]. The study of *F. tularensis* iron recognition and mechanisms necessary for iron acquisition may be essential for understanding the basis of pathogenesis and virulence of *Francisella* in the mammalian host.

1.7 *F. tularensis* siderophore structure is similar to rhizoferrin

Halman and Mager (1964) identified a growth initiation substance (GIS) in the supernatant of *Francisella* (previously named *Pasturella tularensis*) [74], which was found to promote bacterial growth from a small inoculum. A siderophore purified from *F. tularensis* grown under iron limiting conditions [71,75] is predicted to be the GIS initially discovered by Mager's group. This siderophore was confirmed by mass spectrometry to have the same configuration as the siderophore, rhizoferrin (Figure 2) [75]. Rhizoferrin is a symmetrical, α-hydroxycarboxylate siderophore with a putrescine backbone (1, 4-diamino butane) flanked by two citrate molecules through amide bonds [76–78]. The main components of rhizoferrin are byproducts of metabolic pathways found in eukaryotic and prokaryotic cells. It is produced by both fungi (zygomycetes family) and bacteria (*Ralstonia picketti*) under iron limiting conditions [27]. These siderophores were characterized by circular dichroism (CD) with regard to the chiral center of citric acid residues. While structurally similar, the fungal and bacterial forms produce distinct enantiomers (*R,R* and *S,S,* respectively) [77,78]. Rhizoferrin has also been demonstrated to be taken up by other bacteria including *Morganella morganii* [78] and *Staphylococcus aureus* [79], although chiral configuration is a required determinant for which structure can be utilized. The mechanism of retrieval of iron from Fe-rhizoferrin has not been determined to date, though ferric iron removal from other ferric-siderophore complexes occurs through ferric reduction by reductases and the catabolism of the ferric siderophore complexes with esterases [80].

Although siderophores have a high affinity for ferric iron, rhizoferrin has been demonstrated to bind other metals which in turn interfere with ferric-rhizoferrin acquisition [78]. Rhizoferrin's ability to bind other metals may act as a secondary mechanism for removing toxic metals from the environment, which has been demonstrated in other bacteria [81]. The biosynthesis of rhizoferrin has not been elucidated in fungi or bacteria nor have the genes required for siderophore biosynthesis been identified.

1.8 *F. tularensis* siderophore biosynthesis and transport

In 2005, Larsson *et al*. sequenced the genome of *F. tularensis* strain Schu S4 [31] and genes similar to other bacterial siderophore biosynthetic genes could be identified by amino acid sequence analysis searches. Genetic and biochemical studies have confirmed that the gene for the iron-responsive repressor Fur is present upstream of the siderophore biosynthetic operon, *fslABCDEF,* and a binding site for Fur is located within the promoter region of the first gene of the operon, *fslA* (Figure 3) [75]. Siderophore production is Fur-regulated and this regulation was shown to occur at the level of transcription control of the *fsl* genes [82]. Schu S4 infected macrophages showed upregulation of the *fsl* operon during cytosolic intracellular replication, thus suggesting the need for siderophore iron acquisition in a host intracellular environment [70]. In the *F. novicida* strain U112, signature-tagged mutagenesis identified siderophore acquisition genes as essential for bacterial survival in the mouse model of infection [83]. U112 mutant libraries [84–86] have also shown that the *fsl* genes are required for siderophore production, for *in vitro* growth under iron limited

conditions, and for growth and survival in murine RAW264.7 macrophages and

Drosophila Schneider (S2) macrophage-like cells [86,87]. The *F. holarctica* mutant

strain, LVS Δ*fslA,* is unable to produce siderophore under iron limitation and is

defective for growth in iron limiting chemically defined media [71,75]. This LVS Δ*fslA*

mutant was also defective for survival in lung infection in BALB/c mice [88].

However, Lindgren *et al.* and our unpublished studies determined that a Δ*fslA*

mutant in the virulent *tularensis* strains Schu S4 is not attenuated for virulence in

the mouse model of infection [89] [unpublished]. The ability of *F. tularensis* strain

Schu S4 to obtain iron without siderophore lead us to hypothesize that *F.*

tularensis uses multiple iron acquisition systems that additively contribute to

survival under low iron conditions.

We predicted that the *fur-fsl* operon, based on amino acid sequence

analysis and the genetic studies just described, encodes all the proteins required

for *F. tularensis* siderophore biosynthesis and transport as modeled in Figure 4.

The predicted roles of each of the Fsl proteins are described as follows:

i. Amino acid sequence analysis identified FslA as most similar to the NRPS-

independent (NIS) family of siderophore synthetases [75], which are exemplified by

the aerobic synthetases IucA and IucC [28]. FslA groups phylogenetically with the

Type A' NIS synthetases, which are enzymes that specifically recognize the

substrate citrate and incorporate it into the siderophore [28]. One of the

siderophores produced by *Staphylococcus aureus*, staphyloferrin A, is

structurally similar to rhizoferrin, but requires two Type A' NIS synthetases SfnaB

and SfnaD [28] for its biosynthesis. FslA is predicted to catalyze the formation of

amide bonds between putrescine and two citrate molecules to form the *F. tularensis* siderophore (Figure 2).

ii. Amino acid sequence analysis identified FslC as a pyridoxal 5'-phosphate (PLP) dependent diaminopimelate decarboxylase (DAPDC), an enzyme that is responsible for lysine biosynthesis from the intermediate diaminopimelate (DAP). There are no other known enzymes for lysine biosynthesis predicted in the *F. tularensis* genome, and lysine is a required media supplement to culture *F. tularensis* [90]. Therefore, it is hypothesized that FslC functions as a PLP dependent decarboxylase that is required for *F. tularensis* siderophore biosynthesis potentially as an ornithine decarboxylase (ODC). The prediction that FslC is a potential ODC comes from Mager's experiments where radiolabeled ornithine was incorporated into the GIS molecule (*F. tularensis* siderophore), thus identifying ornithine as a precursor for the siderophore [74]. When ornithine undergoes decarboxylation by an ODC it becomes the polyamine putrescine, which is found in the backbone of the *F. tularensis* siderophore structure.

iii. Amino acid sequence of FslB and FslD indicated these proteins to be most similar to inner membrane resistance associated permeases/efflux transporter proteins of the major facilitator superfamily (MFS) proteins. They both contain the characteristic 12 α-helical transmembrane segments (TMSs) [91]. MFS proteins can transport metabolites, organic and inorganic anions and siderophores like vibrioferrin (PvsC) [92] and enterobactin (EntS) [93], through the inner membrane of Gram-negative bacteria [16]. FslB is similar to *L. pneumophila* MFS protein LbtB, which is required for legiobactin inner membrane export [94], while FslD is most

similar to LbtC which was demonstrated to be necessary for *Legionella* inner

membrane import of siderophore [95]. Since FslB and FslD are only expressed

under iron limitation, it is less likely that these proteins export essential

metabolites and/or anions, and more likely to specifically target the transport of *F.*

tularensis siderophore. MFS proteins can export or import substrates across the

inner membrane of bacteria [91] and thus it is likely that FslB and/or FslD could be

important for either exporting synthesized siderophore or importing iron bound

siderophore.

iv. FslE in Schu S4 belongs to a family of five *Francisella*-specific proteins [31,96].

This family is found in the other *Francisella* subspecies and the related *F.*

novicida species [82]; however, the expression and presence of these proteins

differs between strains. The first to be extensively studied was the ferric-

siderophore receptor protein, FslE [82,85]. The *fslE* gene is transcribed in concert

with the other *fsl* locus genes that encode for siderophore biosynthesis and inner

membrane transport proteins [82]. FslE is predicted to fold as a 14-stranded β-

barrel [82] in the outer membrane and to bind ferric-bound siderophore. *F.*

tularensis does not encode a TonB homolog [31], which is required for ferric

siderophore mediated recognition and uptake in most Gram-negative bacteria.

Therefore, FslE is predicted to be part of an unknown TonB independent

siderophore uptake system. Even though *F. tularensis* does not encode TonB,

^{55}Fe-siderophore uptake is energy dependent as shown by the interruption of

^{55}Fe uptake via a proton motive force inhibitor, CCCP [97]. FslE functions as the

receptor for ferric-siderophore as demonstrated through siderophore bioassay

plate assays and ^{55}Fe uptake assays [82]. In the strain Schu S4, FslE is the only protein of this family required for ferric siderophore utilization. In the LVS strain, both FslE and its paralog FupA/B are necessary for ferric-siderophore acquisition [98]. There are five amino acid differences between the two FslE proteins in Schu S4 and LVS that could explain Schu S4 FslE being more efficient.

v. In LVS and Schu S4, FslF is predicted to be an unidentified transmembrane protein based on amino acid sequence analysis. While *fslF* is transcribed along with the other genes within the *fur-fsl* locus, extensive studies in our lab have not been able to elucidate a role for FslF in either siderophore biosynthesis or transport. Thus at this time, we are not including this FslF within our predicted *F. tularensis* biosynthesis and transport model.

Studies on the importance of ferric-siderophore iron acquisition in LVS and Schu S4 strains will be discussed in Chapters 2 and 3, respectively, including its role in virulence in tissue culture and the mouse model of infection. The initial studies of the *fsl* genes necessary for siderophore biosynthesis and transport are discussed in the Appendix.

1.9 *Francisella* specific proteins associated with iron acquisition and the ferrous iron transport system (Feo)

The outer membrane protein FupA also belongs to the previously mentioned family of five *Francisella*-specific proteins [31] and shares 63% identity and 79% similarity with FslE [96,97], though it is not regulated by iron [97]. While FslE and FupA are paralogs, they function separately and are extremely important for *F. tularensis* growth in iron limiting environments [97]. A defect in intracellular

replication within mouse peritoneal macrophages was shown in a *fupA* mutant in the Schu S4 strain [99]. Deletion of *fupA* in Schu S4 severely attenuated virulence in the mouse model of infection [89]. FupA was also demonstrated through ^{55}Fe uptake assays as necessary to specifically regulate ferrous iron entry as a high affinity iron acquisition outer membrane protein [97]. The FupA ortholog in *F. tularensis* strain LVS, FupA/B, is a hybrid protein resulting from a recombination event in the chromosome [82]. In LVS, FupA/B is required for ferric-siderophore mediated uptake along with FslE and is also necessary for high affinity ferrous iron uptake [98,100]. Single and double deletion mutants of the Schu S4 paralogs, Δ*fslE* and Δ*fupA*, demonstrated reduced growth on iron limiting CDM plates and in liquid culture [97].

FupA and FupA/B have recently been shown to regulate high affinity ferrous iron acquisition through the outer membrane of Schu S4 and LVS, respectively [97,100]. However, unlike LVS, the wild-type *holarctica* strains express FupA and FupB as independent proteins. Complementation studies of the LVS Δ*fupA/B* mutant with wild-type *holarctica fupA* showed a regain in virulence akin to wild-type in the mouse model of infection.

Schu S4 and LVS encode *feoA* and *feoB* orthologs of the Feo system are located in different regions of the chromosome. *F. tularensis* does not encode the *feoC* gene that is found in other bacterial genomes and its absence suggests it is not necessary for optimal ferrous iron acquisition. The predicted model for the entry of ferrous iron into *F. tularensis* is depicted in Figure 5. Ferrous iron enters *F. tularensis* through a high affinity outer membrane transporter, FupA (Schu S4)

or FupA/B (LVS). In the periplasm, ferrous iron is transported through the inner

membrane protein FeoB and this entry is potentially dependent on the

cytoplasmic protein FeoA. The studies revealing the importance of the Feo

system in LVS and Schu S4 strains in ferrous iron acquisition and its role in

virulence in tissue culture and the mouse model of infection are discussed in

Chapters 2 and 3, respectively.

2.0 *F. tularensis* vaccine development

Current antibiotics used to treat tularemia in the US include doxycycline

and ciproflaxin [101]. Antibiotic resistance is becoming a growing problem for health

care systems and it remains possible that *F. tularensis* may acquire resistance to

antibiotics. In addition, after the completion of antibiotic regimens, some

tularemia patients have been shown to relapse [101,102]. The Type B strain LVS

was derived from the subspecies *holarctica* and has been used as a vaccine in

Russia, primarily administered to laboratory individuals who have a high risk of

exposure for this organism [103]. While effective against low doses of *F. tularensis,*

there is little protection against large doses of aerosolized bacteria (>1000 CFU

[68]). Although Type A and Type B genomes are highly conserved, underlying

differences in virulence make the development of a live attenuated vaccine in a

Type A strain essential.

2.1 Dissertation research aims

Aim 1. Elucidate the relative importance of the *fsl* and *feo* systems in iron acquisition in *F. tularensis.*

1A. Generate deletion mutants of the ferrous iron transporter gene *feoB* and a double deletion mutant additionally deficient in siderophore production (Δ*fslA* Δ*feoB'*) in the LVS and Schu S4 backgrounds and construct complemented strains.

1B. Test mutants and complemented strains for growth under iron limitation, and iron transport using ^{55}Fe uptake assays.

Aim 2. Define the role of *fsl* and *feo* systems in *F. tularensis* virulence.

2A. Assess the virulence of LVS and Schu S4 mutants in tissue culture models for infection using murine-macrophage like cells (J774A.1) and human hepatic carcinoma cell line (HepG2).

2B. Assess the virulence of iron uptake mutants by intraperitoneal (LVS), and subcutaneous (Schu S4) routes of infection in the mouse model.

2.2 Chapter 1 Figures

Figure 1: *F. tularensis* entry, growth, and potential iron sources available within the intracellular environment of a macrophage.

F. tularensis undergoes phagocytosis into the macrophage and enters a phagosome. *F. tularensis* escapes the phagosome to access host nutrients available within the cytoplasm. Iron available to *F. tularensis* is predicted to be present in the labile iron pool, iron-sulfur clusters (Fe-S), heme, ferritin, and host iron requiring proteins. *F. tularensis* replicates and exits the macrophage when the host cell undergoes apoptosis. This figure is adapted from [104].

Figure 1
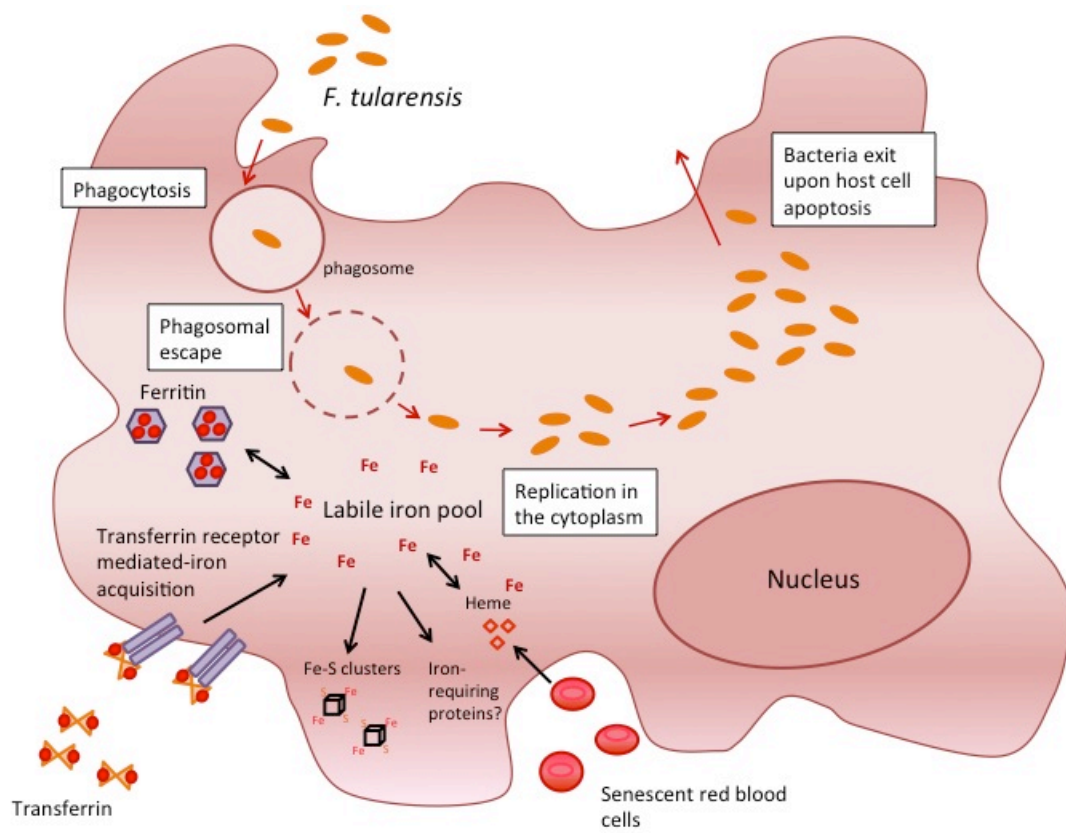
Figure 2: *F. tularensis* siderophore structure.

The structure of rhizoferrin contains a putrescine backbone bound by two citrate

molecules through amide bonds.

Figure 2
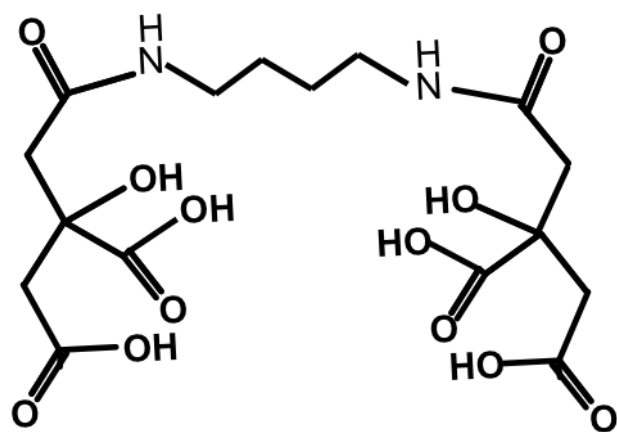
Figure 3: *F. tularensis* siderophore *fur-fsl* locus.

The *F. tularensis fsl* operon contains a *fur* gene upstream and a Fur binding site (Fur box) at the N-terminus of the first *fsl* gene. The *fsl* genes are predicted to function in siderophore biosynthesis, as well as export and import of siderophore.

Figure 3

Fur box
GATAATGATATTCGTTATC

fur fslA fslB fslC fslD fslE fslF

Closest homologs: siderophore synthetase | MFS transporter | diamino-pimelate decarboxylase | MFS transporter | siderophore receptor
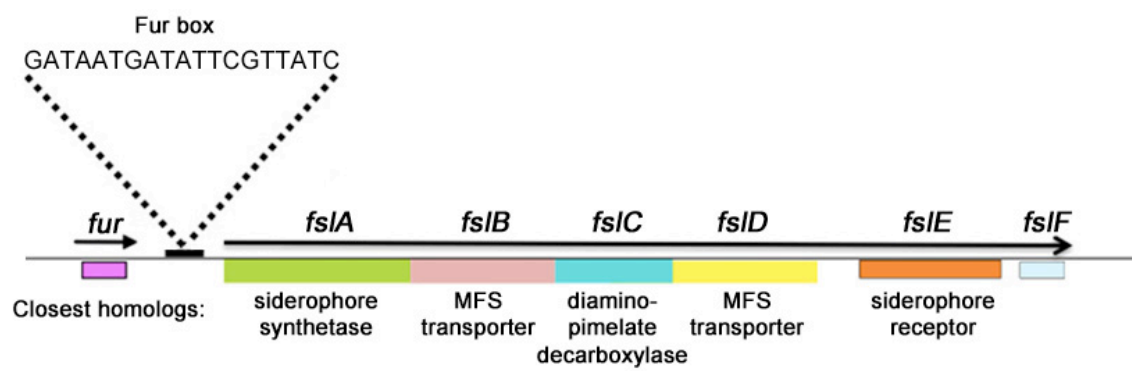
Figure 4: Predicted model for *F. tularensis* siderophore mediated iron uptake.

The model depicts the predicted roles of each of the Fsl proteins in siderophore synthesis and export. In the cytoplasm, FslA and FslC proteins synthesize the siderophore from the precursors ornithine and citrate. The siderophore is exported out of the cytoplasm through the inner membrane through FslB and out of the outer membrane through an unknown outer membrane protein (OMP). The siderophore receptor binds the ferric-bound siderophore and transports it through the outer membrane. The components of the siderophore receptor vary between LVS (FslE and FupA/B) and Schu S4 (FslE) strains, as shown. The ferric-siderophore is then transported through the inner membrane and into the bacterial cytoplasm, possibly by FslD.

Figure 4

Figure Legend:
- Biosynthesis enzyme
- Biosynthesis enzyme
- IM export protein
- OM protein
- Siderophore receptor
- IM import protein
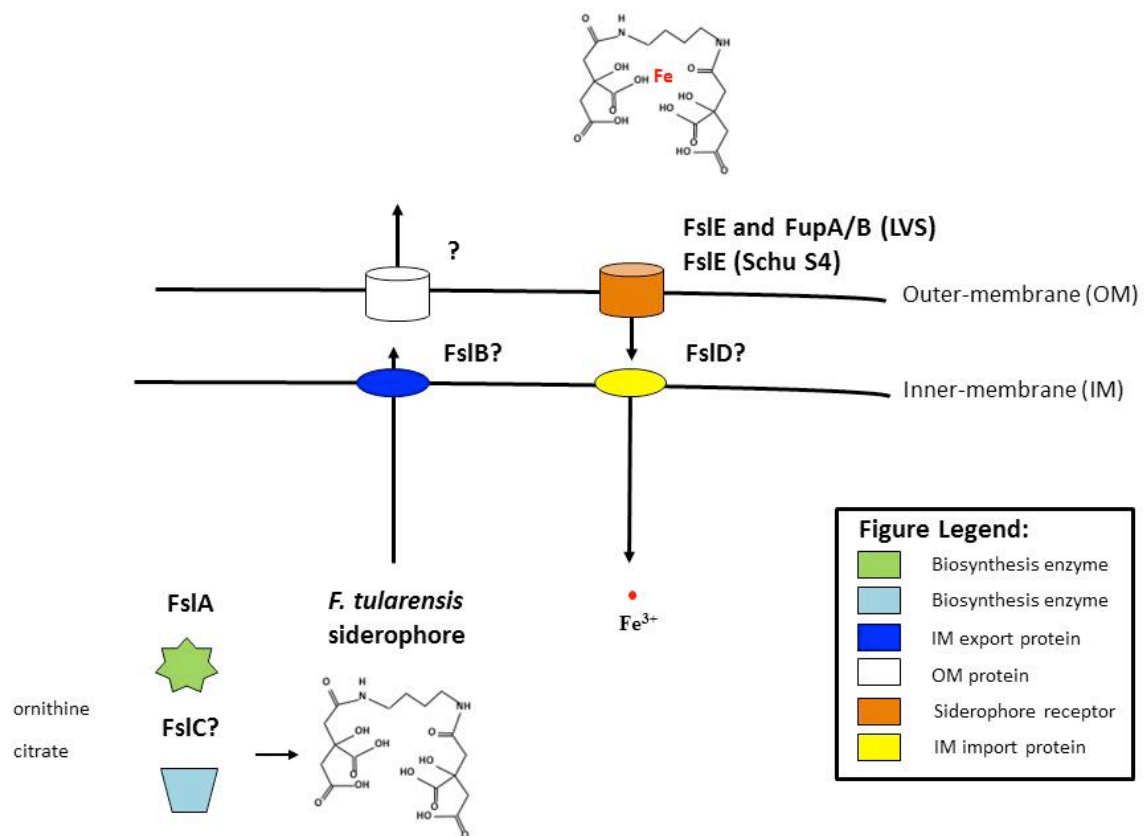
Figure 5: Predicted model for *F. tularensis* Feo mediated uptake.

Ferrous iron is predicted to enter *F. tularensis* through the outer membrane

ferrous iron transporter. This ferrous iron transporter's components vary between

the LVS (FupA/B) and Schu S4 (FupA) strains. Entry through the inner

membrane requires the inner membrane permease FeoB and potentially the

cytoplasmic protein FeoA, both of which are predicted components of the ferrous

iron transport system (Feo).

Figure 5
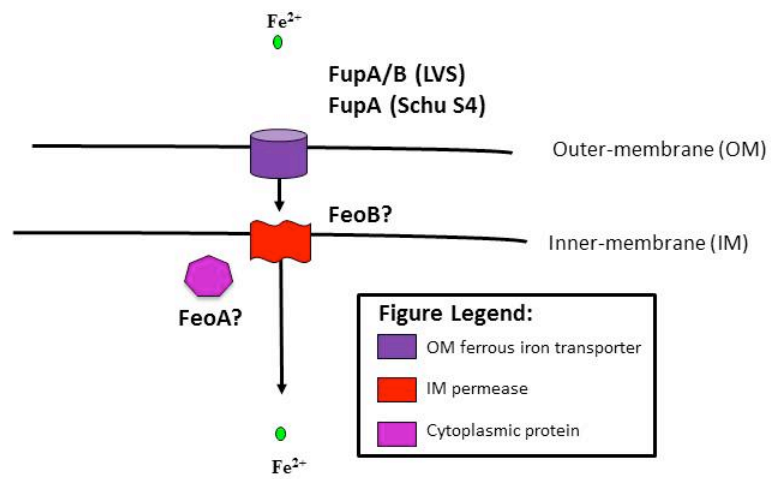
Chapter 2: The Live Vaccine Strain (LVS) encodes two iron acquisition systems essential for growth and virulence

Contents of this chapter were derived from the published research paper: Pérez, NM and Ramakrishnan, G. The reduced genome of the *Francisella tularensis* Live Vaccine Strain (LVS) encodes two iron acquisition systems essential for optimal growth and virulence *PLoS One* **9,** e93558 (2014).

2.0 Abstract:

Bacteria require various iron acquisition systems for optimal growth and survival. The environment of the mammalian host is kept at a low iron concentration to prevent the growth of bacteria; however, the human pathogen *F. tularensis* is fully capable of circumventing this barrier and replicating in multiple cell types. To study iron acquisition mechanisms and their contributing role in virulence, single and double deletion mutants within LVS were generated in the ferrous iron transport (*feo*) and ferric siderophore synthetase (*fslA*) genes. The single deletion mutants demonstrated the specificity of each system for ferrous or ferric iron, respectively. Only through the double deletion, (LVS Δ*fslA* Δ*feoB*'), was this strain unable to grow *in vitro*, in tissue culture, and in the mouse model of infection. These results demonstrated that both iron acquisition systems are capable of acquiring necessary iron intracellularly and *F. tularensis* requires both for optimal growth and virulence in the mouse model of infection.

2.1 Introduction:

Iron is a necessary element for growth and survival of a variety of
organisms including bacteria. In aerobic environments, iron is more prevalent in
the ferric form (Fe^{3+}) while in anoxic environments, iron is found in the reduced
ferrous form (Fe^{2+}). Within the mammalian host, free iron is kept at low levels (10^{-18} M) [3] and is bound by host proteins which regulate and transport iron. Like most
organisms, bacteria need iron for various aspects of homeostasis and express
multiple iron acquisition systems to acquire both ferric and ferrous iron.

F. tularensis is capable of entering multiple cell types through
phagocytosis and prior to fusion with a lysosome it is able to escape to the
cytoplasm where it acquires necessary nutrients for growth and replication [58]. *F.
tularensis* strain LVS is known to alter the intracellular environment of host cells
and to increase intracellular iron within J774A.1 murine macrophages by
modulating the expression of transferrin receptor 1 (TfR1). The increase in TfR1
expression results in an increase in the concentration of host iron within the
intracellular labile iron pool (LIP) [105].

In iron deplete conditions, the model strains of *F. tularensis* (LVS, Schu
S4) and the related *F. novicida* (U112) secrete a siderophore capable of
acquiring iron from the environment [71,75]. Siderophore biosynthesis and transport
require the genes located within the Fur regulated *Francisella* siderophore locus,
fur-fslABCDEF (also named the *fur-figABCDEF* locus). The *fslA* gene encodes a
putative siderophore synthetase that is necessary for siderophore production in

LVS [71,75]. In LVS, FslE is required along with the *F. tularensis* FupA/B outer membrane protein for optimal ferric siderophore acquisition [98].

In LVS, ferrous iron entry across the outer membrane occurs through the *Francisella* specific protein FupA/B [100]. In LVS, FupA/B was demonstrated by ^{55}Fe transport assays to be required for high affinity uptake (iron acquisition at low iron concentrations) and for ferric-siderophore uptake [100]. This suggests that FupA/B participates in a dual role in ferric siderophore and ferrous iron acquisition in LVS [100].

Entry of ferrous iron through the inner membrane of Gram-negative bacteria requires the action of the ferrous iron transport system, Feo [38]. The Feo system is a high affinity ferrous iron acquisition system present in a variety of Gram-negative bacterial genomes [38,106] and contains the proteins FeoA, FeoB, and FeoC [38]. FeoB is composed of a hydrophilic N-terminal G-protein domain and a C-terminal integral membrane domain predicted to have 8-transmembrane α-helices [38,42] and is essential for acquiring ferrous iron through the inner membrane [39]. The *F. tularensis* strain LVS encodes only the *feoA* (FTL_0660) and *feoB* (FTL_0133) orthologs, which are unlinked and map to different regions of the *F. tularensis* chromosome (NCBI Reference sequence NC_007880.1).

We have previously demonstrated that *F. tularensis* strain LVS requires siderophore production and ferric-siderophore acquisition under iron limiting conditions for optimal growth [75,98] and that the genes required for these mechanisms are encoded in the *fsl* locus. *F. tularensis* siderophore deficient mutant (Δ*fslA*) in the virulent *tularensis* subspecies is virulent in the mouse model

of infection [89]. In *F. tularensis,* deletion of genes for siderophore biosynthesis (Δ*fslA*) and transport (Δ*fslE*) in the strain Schu S4 did not reduce virulence of the bacteria in mouse studies [89,97]. The lack of virulence attenuation with the removal of *F. tularensis* siderophore is in contrast to studies of other siderophores in pathogenic bacteria, which are required for virulence, such as *Mycobacterium tuberculosis* [49,50] and *Bacillus anthracis* [51]. However, in Su *et al*. it was demonstrated with a signature-tagged mutagenesis screen that the *F. tularensis* iron acquisition associated genes *fslA* and *feoB* were independently necessary for virulence in BALB/c mouse lung infection [88]. Thus to study the roles of the *F. tularensis* iron acquisition systems, single and double deletion mutants were generated to evaluate the contributions of ferrous and ferric-siderophore iron uptake to intracellular survival and virulence of *F. tularensis* strain LVS. Our studies conclusively establish that these are the only two significant iron acquisition systems in the organism and highlight the reduced and minimalist nature of the iron uptake machinery for LVS survival and virulence. Our studies support the predicted model (Figure 6) that the siderophore biosynthesis and transport and Feo systems work in tandem to provide the necessary nutritional iron for *F. tularensis* growth and survival in the host.

2.2 Results:

Characterization of the LVS Δ*feoB'* mutant

To characterize the role of the Feo system in LVS iron transport, we generated a mutant LVS Δ*feoB'* strain with an 1100 bp deletion in the 2241 bp *feoB* gene using a two-step mutagenesis procedure. The Δ*feoB'* strain is predicted to

produce a 380 amino acid truncated protein lacking 6 of the 8 predicted C-terminal transmembrane sequences, including two of the four Gate regions that constitute the permease in the inner membrane [38].

The mutant Δ*feoB'* strain is defective for growth on MHA+ and MHA- agar plates

We tested growth of the wild- type LVS and LVS Δ*feoB'* strains in rich broth (TSB/c) as well as in iron-replete and iron limiting minimal liquid medium (che-CDM), but did not observe growth differences between the strains (Figure 7A and 7B). The similar growth of the two strains demonstrated that expression of a truncated FeoB protein did not have deleterious effects on general growth of the mutant. We then tested growth of ten-fold serial dilutions of each strain on modified Muller Hinton (MHA+) agar plates that are iron-replete and commonly used for non-selective maintenance and propagation of *F. tularensis* strains. The Δ*feoB'* mutant strain was able to form single colonies on these plates (Figure 8, MHA+), but had a delayed growth phenotype. On plates lacking iron supplementation (Figure 8, MHA-), wild-type LVS also demonstrated a growth delay but was able to form single colonies (out to 10^{-6} dilution) while the Δ*feoB'* mutant demonstrated a growth defect and was only able to grow out to 10^{-5} dilution compared to wild-type LVS. The observed colony size of the Δ*feoB'* mutant was small in comparison to wild-type LVS (MHA+) and this "small" colony phenotype was further accentuated on MHA- plates. Figure 8 also shows that the reduced size and growth defect phenotype of the Δ*feoB'* mutant was abrogated in the Δ*feoB' cis*-complemented strain, Δ*feoB'* (+p*feoB*). These results suggested

51

that the observed growth delay of the Δ*feoB'* mutant on agar was likely due to a deficiency in iron acquisition. Small colony morphology associated with reduced iron acquisition has been previously reported in LVS as well as in *E. coli feo* mutants [39,107]. The discrepancy in liquid and agar growth phenotypes may be explained by the fact that the iron is likely in the oxidized ferric form during growth with shaking in liquid, while the agar medium with a high concentration of cysteine (required supplement since *F. tularensis* is a cysteine auxotroph) would maintain much of the iron in the reduced ferrous form.

FeoB is required for high and low affinity iron transport

^{55}Fe uptake assays are the best platform to demonstrate ferrous iron transport in bacteria and have been used to establish that *F. tularensis* employs distinct outer membrane transport mechanisms for ferrous iron transport at limiting iron concentrations (high affinity transport) and at high iron concentrations (low affinity transport) [97,100]. We compared the ability of the Δ*feoB'* and wild-type LVS strains to take up ^{55}Fe^{2+} at two iron concentrations, 0.1 μM for high affinity iron acquisition and 3 μM reflecting low affinity transport [100]. Bacterial strains were grown overnight under iron-limitation and were then incubated with ^{55}Fe in the presence of ascorbate to keep the iron in the reduced form. As shown in Figure 9A, the Δ*feoB'* strain showed a negligible rate of ferrous uptake compared to wild-type LVS at 0.1 μM iron. Surprisingly, ferrous iron transport in the Δ*feoB'* mutant was also minimal at the 3 μM iron concentration (Figure 9B). These results indicated that *F. tularensis* strain LVS relies solely on FeoB for ferrous iron acquisition across the inner membrane.

FeoB is not required for siderophore production or siderophore-mediated iron acquisition

The Δ*feoB'* mutation was predicted to be competent for siderophore-mediated iron acquisition. We confirmed that the Δ*feoB'* mutant was capable of siderophore production using the universal Chrome Azurol S assay (CAS) [108] to assess levels of siderophore in supernatants of bacteria grown in iron-limiting che-CDM. The LVS Δ*fslA* strain lacking the siderophore synthetase gene [75] was used as a negative control. As shown in Figure 10A, the Δ*feoB'* strain, like wild-type LVS, was capable of secreting siderophore when grown under iron-limitation. We tested siderophore-mediated iron transport capability using ^{55}Fe uptake assays with purified siderophore incubated with ^{55}Fe, as previously described [97,100]. Optimal siderophore-mediated iron acquisition in LVS requires the siderophore receptor FslE [100] and therefore the Δ*fslE* mutant was used as a control in this assay. Wild-type LVS and the mutant Δ*feoB'* and Δ*fslE* strains were grown in iron-limiting liquid che-CDM and were evaluated for the ability to transport ^{55}Fe-bound siderophore. As shown in Figure 10B, the Δ*feoB'* mutant was capable of acquiring siderophore-bound ^{55}Fe at levels comparable to wild-type LVS, whereas the siderophore receptor mutant Δ*fslE* was defective in ^{55}Fe-siderophore uptake. These findings demonstrated that Feo-mediated ferrous iron transport and ferric-siderophore iron acquisition work independently in LVS.

The LVS Δ*feoB'* strain, like the LVS Δ*fslA* mutant, is capable of intracellular growth within J774A.1 murine cells

To test if ferrous iron uptake or siderophore-mediated iron acquisition is critical in supporting the intracellular lifecycle of *F. tularensis*, we compared the Δ*feoB'* and Δ*fslA* strains to wild-type LVS for their ability to enter and replicate within the murine macrophage-like cell line J774A.1. LVS and single deletion mutants were able to enter J774A.1 cells at comparable numbers. At 24 hours post infection (Figure 11A) the single deletion mutants were able to replicate to numbers slightly higher than wild-type LVS. However, by 48 hours post-infection, all the strains grew to similar intracellular levels (Figure 11A). The ability of both the Δ*feoB'* and Δ*fslA* strains to replicate within J774A.1 cells suggested that the *F. tularensis* ferric-siderophore and Feo-mediated ferrous iron acquisition systems were independent and could compensate for each other. Since bacteria typically possess multiple systems for iron acquisition, an alternative possibility was that an additional unidentified uptake system might compensate for the loss of either FeoB- or siderophore-mediated iron transport in LVS.

Generation of the LVS Δ*fslA* Δ*feoB'* mutant

To determine if an iron acquisition system was present in addition to the *fsl* and *feo* systems in LVS, a mutant carrying deletions in both *fslA* and *feoB* genes, LVS Δ*fslA* Δ*feoB'*, was generated. The process involved introduction of a suicide vector by electroporation into the Δ*feoB'* strain to generate an in-frame deletion of *fslA,* as described previously [75]. Diagnostic PCR of initial isolates indicated mixed populations of the parent Δ*feoB'* strain with the Δ*fslA* Δ*feoB'* mutant. Attempts to select for single colonies of the Δ*fslA* Δ*feoB'* mutant by plating on various agar media including CDM, cysteine heart agar plates with blood

(CHAB), tryptic soy agar with cysteine (TSB/c) or MHA plates supplemented with FePPi, FeSO$_4$, or horse blood were unsuccessful. The Δ*fslA* Δ*feoB'* strain was also unable to grow in liquid culture media including CDM supplemented with FePPi or ferrous sulfate (FeSO$_4$), Muller Hinton Broth, TSB/c and Brain Heart Infusion broth (BHI). We were able to finally isolate the strain using MHA agar topically supplemented with purified LVS siderophore. The purity of culture was confirmed on the basis of PCR analysis of genomic DNA.

The Δ*fslA* Δ*feoB'* strain requires the addition of siderophore for growth

To demonstrate the phenotypic growth differences between wild-type LVS and the Δ*fslA,* Δ*feoB',* and Δ*fslA* Δ*feoB'* mutants, bacteria grown on MHA+ plates were collected and resuspended in CDM and ten-fold serial dilutions of all the strains were spotted on MHA+ and MHA- plates. The Δ*fslA* Δ*feoB'* mutant was severely defective for growth on both MHA+ and MHA- plates but when spotted adjacent to the Δ*feoB'* mutant, the double deletion mutant grew to the 10^{-3} dilution after 3 days (Figure 12A). The growth of the double deletion mutant was densest in the region proximal to the adjacent Δ*feoB'* strain thus presenting a "half-moon" phenotype. This was consistent with the idea that the Δ*feoB'* strain was secreting siderophore which helped to support growth of the Δ*fslA* Δ*feoB'* mutant. To test this, the order of bacterial strains was switched (Figure 12B). When the siderophore-deficient Δ*fslA* strain was spotted adjacent to the Δ*fslA* Δ*feoB'* mutant, the growth restriction of the Δ*fslA* Δ*feoB'* mutant was more severe and was only able to reach the 10^{-1} dilution on both MHA+ and MHA- agar plates. The greater growth defect was likely due to the increased distance from the

55

siderophore source (LVS Δ*feoB'*). Ten-fold serial dilutions of the Δ*fslA* Δ*feoB'*

mutant were spotted adjacent to a dense streak of siderophore producing LVS

(Figure 13A, top) or siderophore deficient Δ*fslA* strain (bottom) on an MHA+ agar

plate. After two days, only the Δ*fslA* Δ*feoB'* strain spotted in the vicinity of LVS

was able to grow out to single colonies. To confirm that growth was specifically

dependent on exogenous siderophore, ten-fold dilutions of the Δ*fslA* Δ*feoB'* strain

were spotted on top of concentrated *F. tularensis* siderophore or on a region on

the MHA+ plate without siderophore (Figure 13B). After two days, only the

bacteria spotted over *F. tularensis* siderophore were able to grow. The

Δ*fslA'*Δ*feoB'* strain was also able to grow on CHAB and CDM agar if provided

with *F. tularensis* siderophore (data not shown). The *F. tularensis* double deletion

mutant growth on MHA+ agar was restored with the complementation of *feoB* in

cis (Figure 14) and *fslA* in trans (data not shown). Thus, the only way to

potentiate growth of the double deletion mutant was in the presence of *F.

tularensis* siderophore.

It was previously shown that the addition of siderophore as an iron

supplement promoted growth of LVS and Schu S4 double deletion mutants for

both ferric-siderophore biosynthesis and ferrous iron transport (Feo) [109]

[unpublished]. To determine whether the addition of purified siderophore could

promote the growth of single LVS mutants, different concentrations (1.5 mM,

0.15 mM, 15 µM siderophore) of siderophores were applied to ten-fold serially

diluted mutants, LVS Δ*feoB'* and LVS Δ*fslA* on MHA+ (with the addition of FePPi)

and MHA- plates (without the addition of iron) (Figure 15). The LVS Δ*feoB'*

mutant has a delayed growth phenotype on MHA+ and MHA- plates [109]. With the addition of increasing concentrations of siderophore, the LVS Δ*feoB*' mutant was able to grow out to single colonies with the addition of purified siderophore. The LVS Δ*fslA* mutant did not display a growth defect on MHA+ agar plates. The LVS Δ*fslA* mutant did have a slight growth defect on MHA- plates but this defect in growth was alleviated with the addition of increasing concentrations of *F. tularensis* siderophore. These results demonstrate the importance of *F. tularensis* siderophore on MHA+/- plates for the promotion of growth of these LVS single iron acquisition mutants.

The Δ*fslA* Δ*feoB*' strain is defective for ferrous transport but is still capable of siderophore-bound ⁵⁵Fe uptake

The Δ*fslA* Δ*feoB*' strain growth defects were predicted to be due to the loss of both iron uptake systems. Its ability to grow on MHA+ with added *F. tularensis* siderophore suggested that this mutant was dependent on the ferric-siderophore acquisition system for survival. ⁵⁵Fe uptake assays were used to analyze the iron transport capability of the Δ*fslA* Δ*feoB*' strain in comparison to wild-type LVS and the Δ*fslA* and Δ*feoB*' mutants. For this experiment, all the strains were grown on iron-rich plates similar to the double deletion mutant, followed by resuspension and a three-hour incubation with shaking in liquid che-CDM lacking iron. As expected, the Δ*fslA* Δ*feoB*' mutant was defective for ⁵⁵Fe ferrous iron uptake at both high and low ⁵⁵Fe concentrations, just like the single deletion mutant Δ*feoB*' mutant (Figure 16A and 16B). The Δ*fslA* Δ*feoB*' strain complemented in *cis* with

feoB, Δ*fslA* Δ*feoB'* (+p*feoB*) regained the ability to acquire ferrous iron at both ferrous iron concentrations (Figure 16C and 16D).

The mutants were then examined for siderophore-mediated ferric iron transport. As might be expected following growth in iron-replete media, the LVS and single deletion mutants displayed a range of low, but detectable rates of [55]Fe-siderophore transport that were consistent across experiments. The Δ*fslA* Δ*feoB'* mutant however demonstrated a significantly greater rate of siderophore-bound [55]Fe transport (Figure 17A), suggesting that the siderophore transport genes were more highly expressed in this strain. To explore this possibility, the levels of the FslE and FupA/B proteins (required for siderophore-iron transport) were tested by western blotting of bacterial lysates. GroEL was used as the loading control (Figure 17 B). The *fslE* gene is Fur regulated and is only expressed under iron-limitation [82]. As expected, lysates from wild-type LVS and single deletion mutants grown on iron-replete MHA+ plates did not contain FslE. However, FslE was detectable in lysates prepared from the Δ*fslA* Δ*feoB'* strain and the level resembled expression of LVS grown under iron-limiting conditions. The observed expression of the siderophore receptor FslE suggested that the Δ*fslA* Δ*feoB'* strain was in a state of iron starvation. FupA/B is not iron-regulated (unpublished data) and as expected, was produced in all strains at comparable levels (Figure 17 B).

The Δ*fslA* Δ*feoB'* strain is attenuated for intracellular replication and for virulence in C57BL/6 mice

Agar plate studies of the Δ*fslA* Δ*feoB'* strain described above showed that the double deletion mutant was capable of growth only with the addition of exogenous *F. tularensis* siderophore, indicating the absence of a third active iron acquisition mechanism in culture. Several genes important for *in vivo* survival and replication are induced following invasion of the macrophage [70] and we considered the possibility that these could include additional iron acquisition mechanisms. To test if an unidentified iron acquisition mechanism may be induced in the intracellular niche, the ability of the Δ*fslA* Δ*feoB'* mutant to infect and replicate within J774A.1 cells was tested in comparison to LVS wild-type, Δ*fslA*, and Δ*feoB'* strains (Figure 11). All the strains, including the Δ*fslA* Δ*feoB'* mutant, were able to infect the J774A.1 cells equally. The Δ*fslA* Δ*feoB'* mutant, in contrast to the single deletion mutants Δ*fslA* and Δ*feoB',* showed no increase in intracellular CFU at 24 and 48 hours post infection. This defect in intracellular replication was abrogated when the Δ*fslA* Δ*feoB'* strain was complemented with the wild-type gene *feoB* (Figure 11B). Thus, there appeared to be no alternative iron acquisition system to support growth of the Δ*fslA* Δ*feoB'* mutant in J774A.1 cells.

  To test the impact of iron acquisition defects on virulence, we evaluated the bacterial mutants in a mouse model of tularemia. The number of LVS bacteria required to cause disease in the mouse model varies depending on the route of infection [110]. Infection with wild-type LVS at even a low dose (<10 CFU) by the intraperitoneal route (IP) has been demonstrated to produce a disease akin to human tularemia in mice [110]. Groups of C57BL/6 mice were infected with

1000 CFU of LVS and iron acquisition mutants by the IP route. Mice were monitored for two weeks (Figure 18). All mice infected with LVS (5/5) and the majority of mice infected with the Δ*fslA* strain (4/5) died within 6 days of infection. The Δ*feoB'* mutant was partially attenuated for virulence, with 3/5 mice surviving the infection. All mice infected with the Δ*fslA*Δ*feoB'* strain survived. Survivors of the initial infection were challenged with a lethal dose of LVS (1000 CFU by IP) to determine protection and all the mice survived up to 14 days, at which point the experiment was terminated. These experiments indicated that both siderophore-iron acquisition and ferrous iron acquisition contribute to virulence although ferrous iron acquisition likely played a more significant role. The attenuation of the double deletion mutant indicated that, as seen also in the intracellular replication assay, no alternative iron acquisition strategies existed to support *in vivo* survival of the bacteria.

2.3 Discussion:

Our study compared the contribution of the ferric siderophore and ferrous iron transport system in *F. tularensis.* The use of single and double deletion mutants in siderophore biosynthesis and ferrous iron uptake has established that the *F. tularensis* strain LVS possesses only two mechanisms for iron acquisition: the *fsl*-locus encoded ferric-siderophore and *feoB*-mediated ferrous iron acquisition systems. ^{55}Fe uptake assays clearly demonstrated that the LVS Δ*feoB'* mutant is completely deficient in ferrous iron uptake, revealing the Feo system as the sole transporter of ferrous iron across the inner membrane of *F. tularensis*. However the LVS Δ*feoB'* mutant is capable of siderophore production

and siderophore-mediated iron acquisition. The siderophore biosynthesis mutant ∆*fslA* is unable to synthesize siderophore [75] but is proficient at ferrous iron acquisition based on the ^{55}Fe assays. The ^{55}Fe assays have demonstrated that these two iron acquisition systems are specific to different forms of iron and function independently.

Ex vivo the LVS ∆*feoB'* and LVS ∆*fslA* strains were capable of entering and replicating within J774A.1 macrophage-like cells to CFUs on par with and exceeding the wild-type LVS strain. These results suggest that while free iron is limited within mammalian cells, both ferric and ferrous iron sources are available to LVS within the cytoplasm of J774A.1 cells and that the *F. tularensis* siderophore and ferrous iron uptake mechanisms work in concert to provide enough iron for growth and replication of the pathogen. To determine if another iron acquisition system is available to LVS, a double deletion mutant was generated. The LVS ∆*fslA* ∆*feoB'* mutant could only be cultivated by providing *F. tularensis* siderophore on MHA+ plates. While the LVS ∆*fslA* ∆*feoB'* mutant was able to enter and survive in J774A.1 cells, it showed no increase in intracellular CFUs. This is similar to LVS mutants defective in purine [111] and guanine nucleotide biosynthesis [112], which are unable to replicate due to an inability to acquire necessary nutrients. The inability of the double deletion mutant to replicate intracellularly and its lack of virulence in mice demonstrate unequivocally that the ferric-siderophore and Feo systems are the only significant means of iron acquisition and are both necessary for full virulence in the mouse model of infection.

Intracellular growth capability may be influenced by differences in iron metabolism within different cell types. A strain lacking *feoB* was shown to have a deficient growth phenotype in epithelial and hepatic tissue culture cells [107]. However, macrophages are important for *Francisella* dissemination [60] and we confirmed by our study that a LVS Δ*feoB'* mutant is still capable of growing within macrophage-like J774 cells [107]. Loss of siderophore production as with the Δ*fslA* mutant in our study, or a LVS Δ*fslC* mutant [107], does not affect the ability to replicate within a macrophage. Intra-macrophage growth is hampered only if both FeoB function and siderophore biosynthesis are disrupted.

The lack of another iron acquisition system in *F. tularensis* strain LVS demonstrates the effectiveness of the *F. tularensis* siderophore and Feo systems for survival and pathogenesis. Our analysis indicates that J774A.1 macrophage-like cells contain sufficient amounts of ferrous and ferric iron to satisfy the needs of LVS. The iron available within the cytoplasm is thought to include iron bound by host proteins such as ferritin and heme as well as within the transitional LIP. It has been shown that *F. tularensis* LVS co-localizes with transferrin receptor 1 (TfR1) during the initial stages of internalization and also promotes the host cell's expression of the transferrin receptor [105]. The TfR1 transferrin receptor pathway delivers iron into the cytoplasmic LIP through the action of the iron transporter Dmt1 and the reducing action of the Steap3 ferrireductase and thus makes iron available for *F. tularensis* in the cytoplasm [105]. It has also been suggested that *F. tularensis* siderophore is capable of removing iron from transferrin [113]. The ability to switch and/or simultaneously use both iron transport systems gives *F.*

tularensis an advantage to survive within the iron-limiting environment of the host.

We found using an intraperitoneal infection model that the LVS Δ*fslA* mutant was unaffected in virulence but the LVS Δ*feoB'* mutant was partially attenuated. In an intradermal model of infection, however, a Δ*feoB* mutant did not demonstrate virulence attenuation following administration of a lethal dose, although differences in tissue burden were detected with a sublethal dose [107]. Both the route of infection and mouse genotype could lead to the differences in our results. We found that the double deletion mutant was avirulent following administration of CFUs corresponding to a lethal LVS dose. Interestingly, all mice in our study that survived the challenge with single Δ*feoB'* or double deletion mutant were resistant to subsequent rechallenge with a lethal dose of LVS.

While the role of FeoA was not examined in our study, we anticipate that this predicted cytoplasmic protein could interact with FeoB as recently shown in the bacterial systems of *S. typhimurium* [40,41] and *Vibrio cholera* [43]. The Fur protein is known to regulate expression of iron acquisition systems and studies of an LVS Δ*fur* mutant (G. Ramakrishnan, unpublished data) have demonstrated that *feoB* is regulated by Fur. Since the Feo system is the sole inner membrane ferrous transport system in LVS, Fur and FeoA may also play significant roles in the FeoB-mediated transport of ferrous iron.

F. tularensis includes the less studied *mediasiatica* subspecies in addition to *tularensis* and *holarctica*, all of which are human pathogens and have reduced genomes in comparison to the near ancestral relative *F. novicida* within the same

evolutionary clade [59,114,115]. *F. novicida* is not normally a human pathogen but is capable of intracellular replication in murine and human macrophages and can cause a tularemia-like disease in mice [116]. Interestingly, the *fsl* and *feo* genes are conserved among all of these isolates (www.patricbrc.org), suggesting that the iron acquisition systems may play an important role in supporting survival in the pathogenic intracellular milieu, although it is possible that the more metabolically competent *F. novicida* may encode additional iron acquisition systems. Conservation of the *fsl* and *feo* iron acquisition systems does not necessarily suggest that both systems are equally utilized in different scenarios. Similar studies in the virulent *tularensis* subspecies may weigh the importance of both iron acquisition systems and their necessity for survival and virulence. Additionally, the ability of the LVS Δ*fslA* Δ*feoB'* mutant to generate resistance to subsequent lethal LVS challenge suggests that a similar mutant may also be generated in the *tularensis* subspecies as an effective live vaccine strain.

2.4 Experimental Methods

Bacterial strains:

Francisella tularensis subspecies *holarctica*, live vaccine strain (LVS) was
obtained from K. Elkins (CBER). The bacteria (Table 1) were maintained at $37°C$
on modified Muller Hinton agar, MHA (Difco), supplemented with 2.5% horse
serum, 1% glucose, 0.1% cysteine, and 0.025% ferric pyrophosphate (FePPi).
For the purpose of this study, iron rich MHA plates were supplemented with
FePPi and annotated as MHA+. Iron-limiting MHA plates were not supplemented
with iron (MHA-) but contained an undetermined amount of iron from horse
serum and agar. *F. tularensis* strains were grown in liquid Chamberlin's defined
media (CDM) [117] at $37°C$ with shaking. Bacterial optical densities were read at
600 nm (OD_{600}) using a plate reader (BioTek ELx800). For growth comparisons
in liquid, we used tryptic soy broth (TSB/c) supplemented with 0.1% cysteine,
0.1% glucose, and 0.025% ferric pyrophosphate (FePPi) and chelex-100
(BioRad) treated CDM (che-CDM) [14] supplemented with $MgSO_4$ (0.55 mM), $CaCl_2$
(5 μM) and FePPi to make the medium either iron replete (2.5 $\mu g/mL$, 3.36 μM)
or iron limiting (0.125 $\mu g/mL$, 0.168 μM) [75,97]. Bacteria in the exponential stage of
growth were inoculated to an OD_{600} of 0.01 in the respective liquid growth media.
For growth in iron-limiting and iron-replete che-CDM, the bacteria were first
washed three times in che-CDM without iron. To maintain the LVS Δ*fslA* Δ*feoB'*
mutant, *F. tularensis* siderophore-active culture supernatant (determined by the
Chrome Azurol S assay as described below in "Detection of *F. tularensis*
siderophore") was obtained from LVS cultures grown in iron limiting che-CDM

liquid and 100 μL of this filter sterilized (0.22 μm) supernatant was topically added to MHA+ agar plates. A *F. tularensis* siderophore stock was obtained from siderophore-active supernatants of LVS by chromatography on AG1X-8 columns (as described in [75]). Column eluates were lyophilized and dissolved in water. A final concentration of 1.5 mM was determined by a Cu-CAS assay [118] and compared to deferoxamine standards. This siderophore stock was used in some experiments to promote growth of the LVS Δ*fslA* Δ*feoB'*, LVS Δ*fslA,* and LVS Δ*feoB'* mutants. For complementation studies, kanamycin was added at 15 μg/ml. Bacterial stocks used for *in vitro* assays, intracellular replication and mouse infection studies were stored at -80°C. *Escherichia coli* strain MC1061.1 (araD139 Δ(ara-leu)7696 galE15 galK16 Δ(lac)X74 rpsL(Str^r) hsdR2 (rK$^-$mK$^+$) mcrA mcrB1 recA) was received from Chang Hahn (University of Virginia) and used for cloning purposes [75]. *E. coli* bacteria were grown in Luria broth (LB) and on agar plates supplemented with ampicillin, 50 μg/ml and 100 μg/ml respectively.

Growth of serial dilutions on plates

Bacterial strains were routinely grown overnight in CDM liquid at 37°C with shaking. In experiments involving the LVS Δ*fslA* Δ*feoB'* mutant, bacteria were grown overnight on a MHA+ plate and directly inoculated into CDM liquid on the day of the experiment. Bacterial cultures were adjusted to an OD$_{600}$ of 1 and ten-fold serially diluted in CDM to the 10^{-6} dilution. A multichannel pipette was used to spot 5 μL of each dilution onto MHA+ or MHA- plates. Growth was assessed after 3 days at 37°C under normal aerobic conditions.

Detection of *F. tularensis* siderophore

The liquid Chrome Azurol S (CAS) assay developed by Schwyn and Neilands (1987) [108] was adapted to assess the production of siderophore (as detailed in [75]). Bacterial strains were grown in CDM overnight to mid-logarithmic phase. Bacteria were then washed in che-CDM without iron and inoculated into che-CDM supplemented with low concentration of FePPi (0.125 μg/mL). At mid-logarithmic growth, bacteria were centrifuged at 9,000 x g. Supernatant (100 μL) was collected and added to equal parts CAS solution (100 μL) and 2μL of shuttle solution in wells of a 96-well plate. After a thirty-minute incubation at room temperature, absorbance was read at 630 nm (A_{630}) on a plate reader (BioTek ELx800). CAS activity was calculated using water as a reference blank with the formula ((A_{630} water-A_{630} sample)/ A_{630} water). CAS activity was normalized to bacterial cell density (OD_{600}) to obtain Specific CAS activity (CAS activity/OD_{600}). All strains were tested in triplicate.

Construction of LVS Δ*feoB'* and LVS Δ*fslA* Δ*feoB'* strains and complements

A partial deletion mutant of the *feoB* gene (Δ*feoB'*) was generated through the use of a suicide vector in a two-step mutagenesis procedure [82]. The 3' flanking sequence corresponding to the last ten codons and 1.828 kb downstream of the stop codon was amplified using primers F55 and F89 and was cloned as a *Not*I-*Sac*I fragment in plasmid pGIR459 [98]. The 5' homologous sequence consisting of 480 bp upstream of the *feoB* start codon and 1.066 kB of the amino-terminal coding sequence was obtained by PCR amplification using *Pfu* DNA polymerase

(Stratagene) and primers F56 and F11. The 5' sequence was cloned as an *Xba*I-*Hind*III fragment with a 100 bp *Hind*III-*Not*I linker sequence derived from pCK155 [119] to generate the Δ*feoB'* suicide plasmid pGIR473. Plasmid pGIR473 was introduced into LVS by electroporation as previously described [75]. LVS was grown at 37°C with shaking in 5 mL of CDM overnight to mid-log phase of growth. The bacterial growth was determined at OD_{600} and spun at 10,000 rpm for 8 minutes. Cells were washed three times in 0.5 M sucrose and incubated with the suicide plasmid. Cells were electroporated with a Bio Rad Gene Pulser II Electroporation System set at 2.5 kV, 600 ohms resistance, and 10 µF conductance in 0.1 cm cuvettes (Bio Rad). Cells were incubated in rich liquid media (TSB/c) for 4-6 hours and then plated on MHA (FePPi) supplemented with kanamycin. Kanamycin resistant colonies were screened by PCR to confirm integration of the plasmid in the chromosome. Integrants were plated on sucrose plates without kanamycin and colonies arising from this were screened for loss of plasmid sequences and for presence of the deletion by PCR analysis of genomic DNA. The primer sets F12/F335 and F10/F94 were used to confirm the 5' and 3' flanking region of the *feoB* gene, respectively.

LVS Δ*feoB'* was used as the parental strain with the suicide plasmid pGIR457 [75] to generate LVS Δ*fslA* Δ*feoB'* bearing an in-frame *fslA* deletion in addition to the *feoB'* deletion. Potential Δ*fslA* Δ*feoB'* colonies were isolated initially on MHA+ plates and were found to contain a mixed population of the parental LVS Δ*feoB'* and LVS Δ*fslA* Δ*feoB'* cells by diagnostic PCR. The primer sets F123/F116 and F115/F126 were used to confirm the 5' and 3' flanking

region of the *fslA* gene, respectively. The LVS Δ*fslA* Δ*feoB'* strain was ultimately isolated in pure culture by supplementing plates with purified LVS siderophore applied topically to the solidified agar.

The Δ*feoB'* and Δ*fslA* Δ*feoB'* mutants were complemented in *cis* with *feoB* by integrating a suicide plasmid bearing a kanamycin cassette at the *feoB'* locus on the chromosome. The integrative plasmid carried a wild-type copy of *feoB* under control of the promoter of *fslA*. The *feoB* gene was amplified with primers F158 and F357 using Fast Start High Fidelity polymerase (Roche Applied Science). The PCR fragment was digested with *Nde*I and *BspE*I and ligated into the corresponding sites in plasmid pGIR463 [82] to generate the in *cis* complementing plasmid pGIR463_*feoB* (p*feoB*). Plasmids were introduced by electroporation and selection with kanamycin as described above [75]. Complements were confirmed by PCR analysis of isolated DNA from the bacteria.

Intracellular Replication Assay

Bacterial intracellular replication was assessed in murine macrophage like cells J774A.1 (ATCC TIB-67) as previously described [98]. J774A.1 cells were maintained in high glucose Dulbecco's modified Eagle's medium (DMEM) supplemented with 10% FBS and grown at 37°C with 5% CO_2 and split 1:10 per passage. J774A.1 cells were counted on an automated cell counter (BioRad TC 10) and seeded at a concentration of 2×10^5 cells per well in 24-well plates the day before the assay. Bacteria were added at a multiplicity of infection (MOI) of 15 or 5 into four wells per group and plates were centrifuged at 950 x g for 10

minutes at room temperature to promote the bacterial invasion process. Cells

were incubated at 37°C for one hour, washed twice with PBS and incubated with

50 μg/mL of gentamicin in DMEM+FBS for 1 hour at 37°C. At two hours post-

infection, wells were washed twice with PBS and cells in one set of wells lysed

with distilled water and vigorous pipetting. Fresh media was added to remaining

wells and incubation at 37°C continued. Lysates were prepared at 2, 24, and 48

hours and were serially diluted in CDM and plated on MHA plates to determine

intracellular bacterial numbers as colony-forming units (CFU). Concentrated *F.

tularensis* siderophore was additionally topically spread on MHA+ agar to

promote growth of the double deletion mutant at each time point. Intracellular

replication assays were repeated three times to ensure consistency in results.

^{55}Fe uptake assays

^{55}Fe uptake assays were accomplished as previously described [97,100]. For the

initial ^{55}Fe uptake studies with LVS, Δ*feoB'*, and Δ*fslE* mutants, were grown

overnight in iron-limiting che-CDM. For studies involving LVS Δ*fslA* Δ*feoB'*, all

strains were grown overnight on MHA+ plates with topical supplementation of *F.

tularensis* siderophore for the Δ*fslA* Δ*feoB'* mutant strain. Bacteria collected from

these plates were washed once in che-CDM and then inoculated in che-CDM

containing no iron, followed by incubation at 37°C with shaking for 3 hours to

induce expression of iron acquisition systems. Cell pellets were brought to an

OD_{600} of 0.2 and 0.1 mL of the suspensions were added to an equal volume of

che-CDM in 96 well filter plates (Millipore). For $^{55}Fe^{2+}$ (ferrous iron) uptake

studies, the final transport assay contained $^{55}FeCl_3$ (PerkinElmer Life Sciences;

21.95 mCi/mg, 38.59 mCi/mL) at concentrations of 0.1 μM (high affinity transport) or 3 μM (low affinity uptake) in the presence of 5 mM ascorbate. For assessing $^{55}Fe^{3+}$-siderophore uptake, the transport reaction contained 1.5 μM $^{55}Fe^{3+}$ complexed to siderophore in the presence of 10 mM citrate. Uptake was initiated by addition of ^{55}Fe to bacteria in filter wells, and accumulation was assessed at 5 and 10 minutes by scintillation counting of filtered cells. Bacterial protein content was analyzed by BCA assay (Pierce). All strains were tested in either triplicate or quadruplicate and rates of transport were normalized to protein concentration (pmol/min/mg). Transport assays were repeated three times to ensure consistency in results.

Western Blotting

LVS and Δ*fslA,* Δ*feoB',* and Δ*fslA* Δ*feoB'* mutant strains were grown overnight on MHA+ plates at 37°C and resuspended in che-CDM. For comparison to growth under iron-limitation, LVS was also grown in iron limiting che-CDM liquid overnight. Bacteria were normalized to cell density (OD_{600}) and lysed in 1X SDS page loading dye. Lysates were separated on 10% SDS-PAGE gels and protein was transferred onto polyvinylidene difluoride (PVDF) at 100V. The PVDF membrane was incubated with primary and HRP-conjugated secondary antibodies for detection by chemiluminesence. The FslE peptide antibody [98] was used at a dilution of 1: 2,500 and secondary goat anti-rabbit-peroxidase conjugate antibody (Sigma) at 1:10,000. GroEL expression was used as a loading control and was detected by the rabbit primary antibody GroEL(Sigma) was used at 1:10,000 dilution and the secondary goat anti-rabbit-peroxidase

71

conjugate antibody (Sigma) at 1:10,000. FupA/B expression was detected with the FupA peptide antibody at 1:100,000 dilution [97] and the secondary anti-guinea pig in goat 1:50,000 (Sigma).

Mouse infection

Frozen stocks of LVS strains were diluted in 0.9% sterile saline solution to 10,000 CFU/mL and 100 μL (1000 CFU) was injected by intraperitoneal (IP) route into seven-week-old C57BL/6 male mice (five mice per group) (Jackson laboratories, Bar Harbor, ME) [98]. The CFUs administered were determined by plating bacterial dilutions on MHA+ plates, topically supplemented with *F. tularensis* siderophore in order to promote growth of LVS Δ*fslA* Δ*feoB'* strain. Mice were observed each day for symptoms of disease and mice were euthanized at a humane endpoint if symptoms of irreversible morbidity were observed. Survivors were subsequently challenged by IP delivery with 1000 CFU of LVS and monitored for a period of 14 days.

Statistical Analysis

Data were analyzed using Prism 4.0 software (GraphPad Software, Inc., San Diego, CA). Statistical comparison of values was accomplished using *t* test function and the Logrank Test function was used to evaluate mouse survival curves.

2.5 Chapter 2 Tables

Table 1: *F. tularensis* LVS strains

Genotype	Strain Name	Alternative Strain Name	Source
LVS	Wild-type		K. Elkins (CBER)
LVS Δ*fslA*	GR7		[75]
LVS Δ*feoB'*	GR28	NMP088, NMP089, NMP090	[109]
LVS Δ*fslA* Δ*feoB'*	GR46	NMP091, NMP092	[109]
LVS Δ*fslA* Δ*feoB'* + pNMP095 (+*feoB*)	GR70	NMP111	[109]

Table 2: *F. tularensis* plasmids

Genotype	Plasmid name	Source
pFNLTP6_*fslA* (*fslA* complement)	pGIR458	[75]
p463_feoB (*feoB* complement)	pNMP095	[109]
pUC plasmid pSL1180	pUC	[120]
pFNLTP6 (empty vector)	pFNLTP6	Tom Zhart [121]
pGIR457 (*fslA* suicide vector)	pGIR457	[75]
pGIR458 (+pfslA with Schu S4) (*fslA* complement)	pGIR458	[75]
pGIR473 (*feoB'* suicide vector)	pGIR473	[109]

Table 3: Primers used in this study

Name	Sequence
F55	5' ctactggcggccgcTTCGTGGCAAATCTTACTGG 3'
F89	5' ctactggagctcGTAGCATGAAAAGCTTACC 3'
F56	5' ctactgtctagaAGCCAATCCAAGATATGGTG 3'
F11	5' CAATTAACGGTACAAAAGCTTTGC 3'
F158	5' ctactgtccggaGCCAATCCAAGATATGGTG 3'
F357	5' ctactgcatatgATTCAAATTAGAATTTTAAGAGC 3'
F12	ctactggtcgacCTGTGAGAGTAGAATTAGTAGC
F335	TCAAGAACAACAAATAACTGAC
F10	TATATGTCTCGAGCTGCTTTTG
F94	GCCTTCTTTAGCCATATCAACTGC
F123	GCCATCACATAAGCATGCTC
F116	ctactggagctcCTGCTATGATTATAAGCTGAC
F115	ctactggcggccgcTGTTAAATGCAAATCCTGTCG
F126	TCGACCAAACTACGTCCTAG

2.6 Chapter 2 Figures

Figure 6: Predicted model of the *F. tularensis* strain LVS siderophore mediated and ferrous iron transport (Feo) systems.

The left side of the model depicts siderophore biosynthesis and transport while the right side of the model demonstrates the predicted components of the ferrous iron transport system (Feo). For ferric iron transport, the FslA and FslC proteins synthesize the siderophore from the precursors ornithine and citrate. The siderophore is exported out of the cytoplasm through the inner membrane by FslB and out of the outer membrane through an unknown outer membrane protein (OMP). The siderophore receptor binds the ferric siderophore through the dual effect of FslE and FupA/B. FslD is required for transport of the ferric-siderophore through the inner membrane. For ferrous iron, entry occurs at the outer membrane of LVS through an outer membrane ferrous iron transporter FupA/B. Entry through the inner membrane requires the inner membrane permease FeoB and potentially the cytoplasmic protein FeoA.

Figure 6
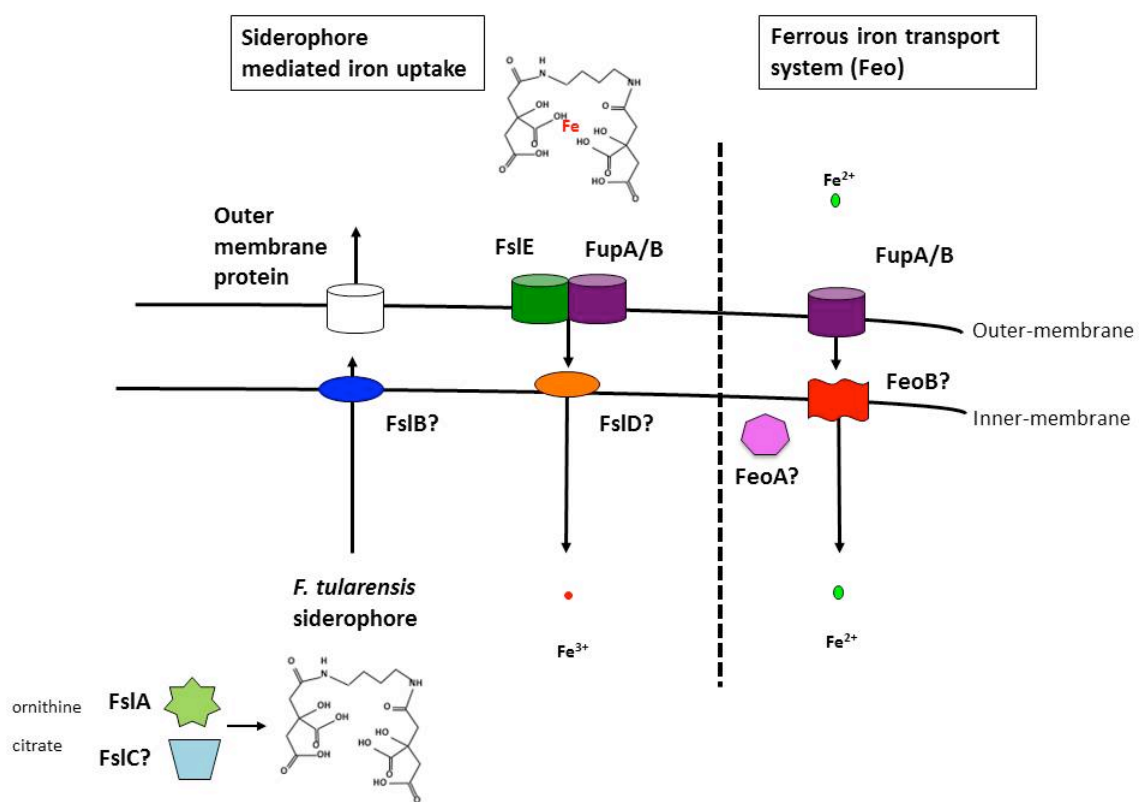
Figure 7: Growth of LVS Δ*feoB'* in liquid.

LVS and LVS Δ*feoB'* were inoculated in either iron rich TSB/c (**A**) or in che-CDM

supplemented with FePPi at 2.5 µg/mL (High Fe) or 0.125 µg/mL (Low Fe) (**B**).

Growth was followed over time by a change in optical density at 600 nm (OD$_{600}$).

Values were plotted as the means ± S.E.

Figure 7
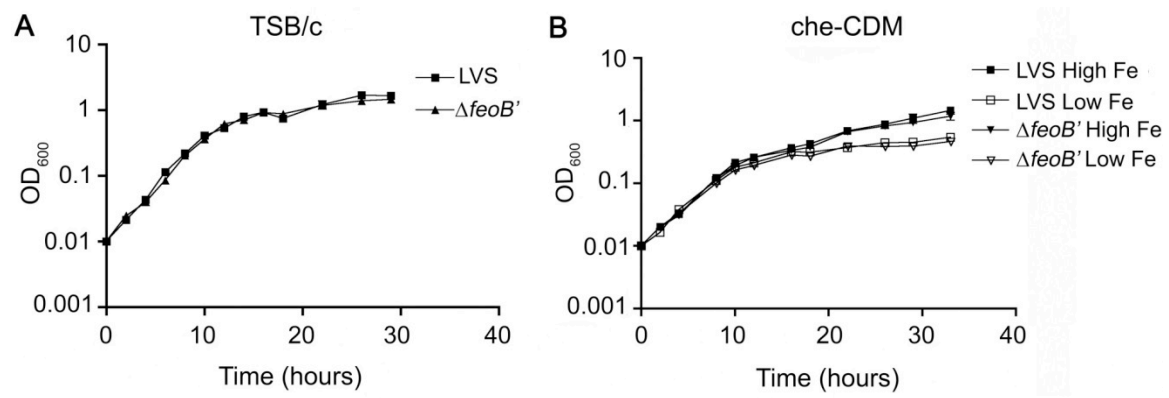
Figure 8: Growth of LVS Δ*feoB'* on MHA with (+) or without (-) additional iron supplementation.

LVS Δ*feoB'* bacterial strains were ten-fold serially diluted in liquid che-CDM, spotted on MHA agar with (MHA+)(left) or without (MHA-) (right) iron supplementation and grown for 3 days at 37°C under aerobic conditions.

Figure 8

MHA+

| 10^0 | 10^{-1} | 10^{-2} | 10^{-3} | 10^{-4} | 10^{-5} | 10^{-6} |

LVS

$\Delta feoB'$

$\Delta feoB'$ (+p$feoB$)

MHA-

| 10^0 | 10^{-1} | 10^{-2} | 10^{-3} | 10^{-4} | 10^{-5} | 10^{-6} |
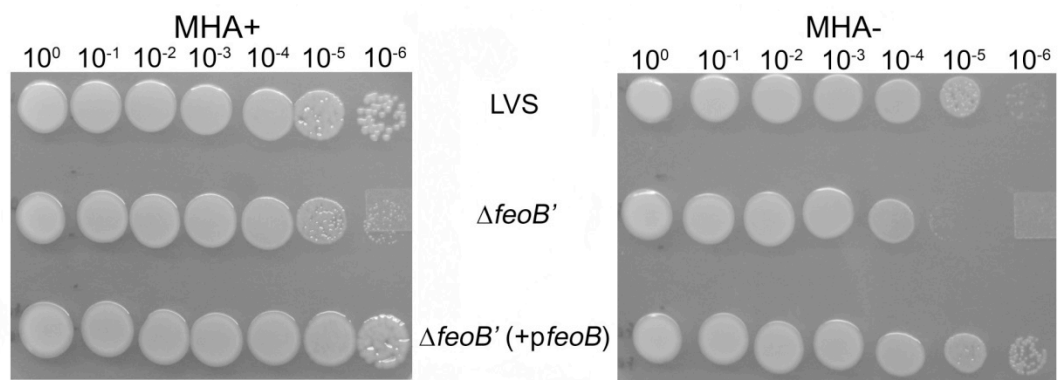
Figure 9: LVS Δ*feoB'* is defective for ferrous iron uptake.

LVS and LVS Δ*feoB'* strains were grown overnight to mid-logarithmic phase in iron-limiting che-CDM broth and rates of ferrous iron uptake were determined at 0.1 (**A**) and 3 μM (**B**) [^{55}Fe^{2+}] in the presence of ascorbate. Values were expressed as the mean ± S.D. Significance was calculated relative to LVS values. ***p<0.001.

Figure 9

A   0.1 µM $^{55}Fe^{2+}$

B   3 µM $^{55}Fe^{2+}$
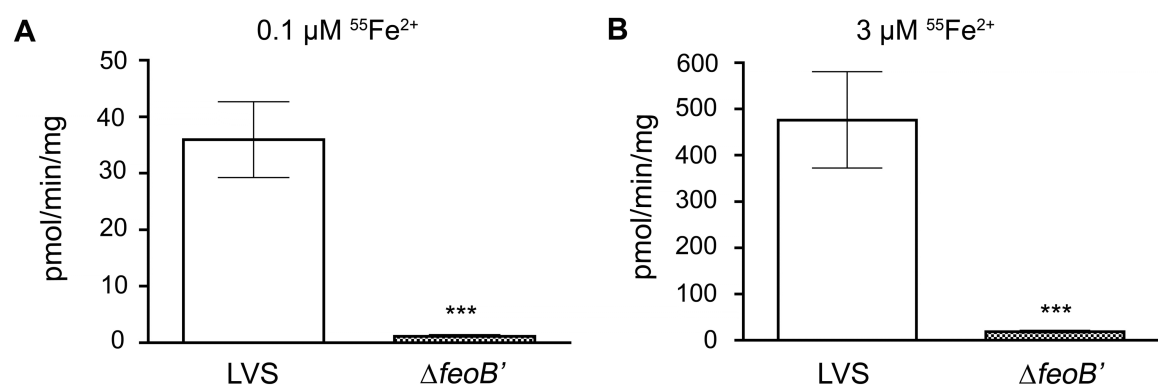
Figure 10: LVS Δ*feoB'* is capable of siderophore production and ^{55}Fe-siderophore utilization.

Culture supernatants of LVS, Δ*fslA*, Δ*feoB'* strains were grown overnight under iron-limitation and subsequently tested by the CAS assay (**A**). The measured siderophore activity was normalized to the OD_{600} for each culture. ^{55}Fe-bound siderophore was incubated with bacteria grown in iron-limiting che-CDM and the rate of ^{55}Fe uptake was determined, (**B**). Values were expressed as the means ± S.D. Significance was calculated relative to LVS values. ***$p < 0.001$.

Figure 10

A Siderophore expression

B ^{55}Fe-siderophore
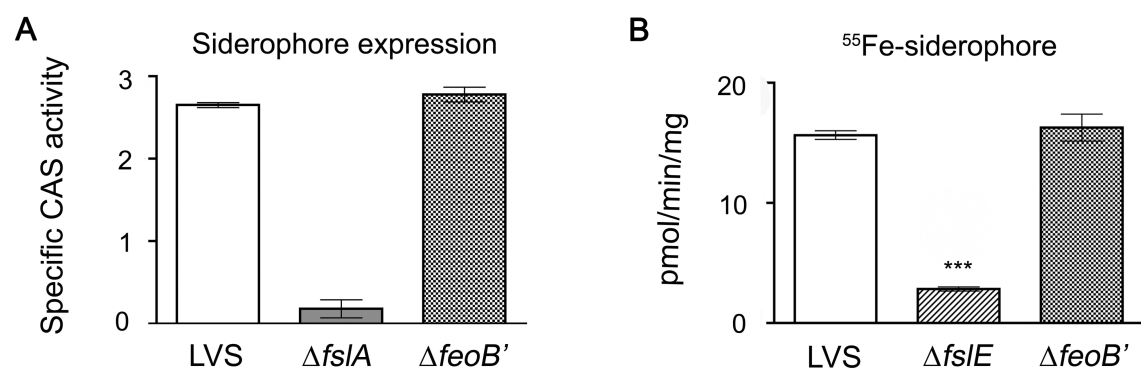
Figure 11: Intracellular replication of LVS iron acquisition mutants in J774A.1 murine macrophage-like cells.

LVS and iron acquisition mutants were tested for intracellular replication in J774A.1 macrophages. Bacteria from frozen stocks were used at an MOI of 15 (**A**) and 5 (**B**). Infected cells were lysed at the times indicated and plated on MHA with FePPi (MHA+) agar to determine CFU/mL. The LVS Δ*fslA* Δ*feoB'* mutant CFU/mL concentrations were determined on MHA+ agar topically supplemented with *F. tularensis* siderophore. LVS and single and double deletion mutant CFU were compared at 2, 24 and 48 hours post infection (**A**). The wild-type LVS, LVS Δ*fslA* Δ*feoB',* and LVS Δ*fslA* Δ*feoB'* (+p*feoB*) were compared at 2 and 24 hours post infection (**B**). Values were expressed as the means ± S.D. Significance was calculated relative to LVS values. Values of the complemented strain were also compared to the mutant. *$p<0.05$, **$p<0.01$, ***$p<0.001$.

Figure 11
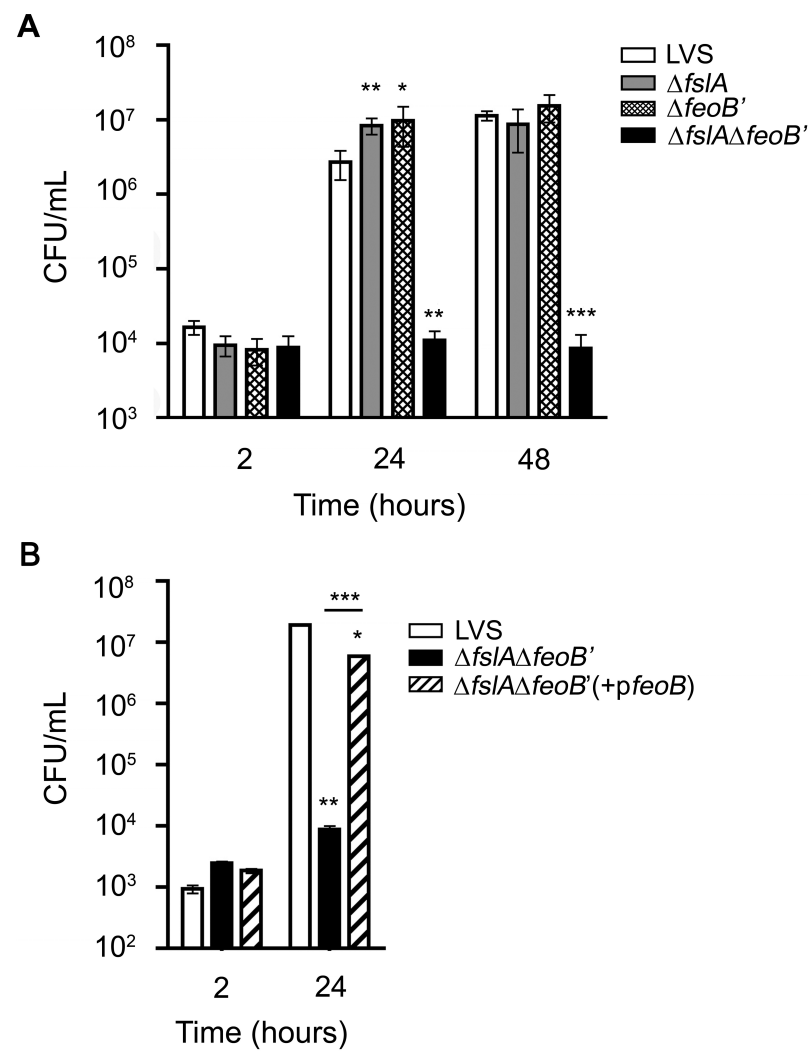
Figure 12: The LVS Δ*fslA* Δ*feoB'* mutant is defective for growth on iron replete and iron limiting MHA agar.

LVS, Δ*fslA,* Δ*feoB',* and Δ*fslA* Δ*feoB'* strains grown on MHA+ agar plates were suspended and brought to an OD_{600} of 1 in che-CDM. Strains were further ten-fold serially diluted and spotted on MHA+ and MHA- plates. The order in which Δ*fslA* and Δ*feoB'* were spotted are switched in **A** and **B**.

Figure 12
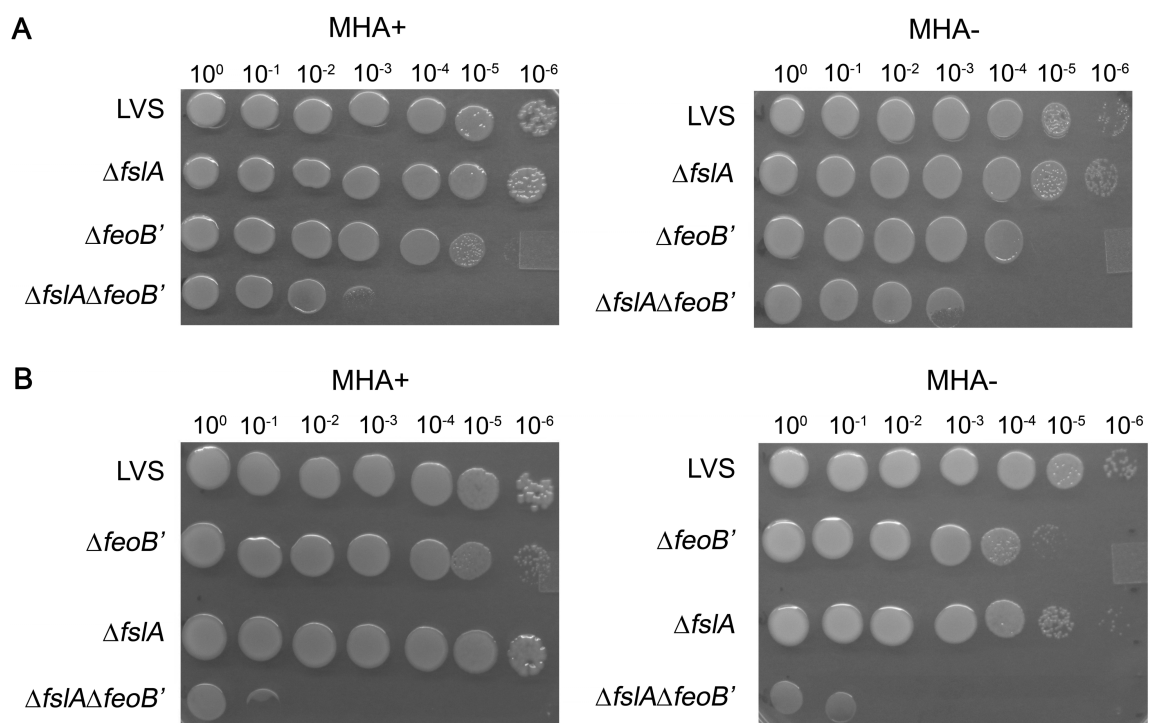
Figure 13: The LVS Δ*fslA* Δ*feoB'* mutant requires *F. tularensis* siderophore for growth.

Ten-fold serial dilutions of the Δ*fslA* Δ*feoB'* strain were spotted near dense streaks of LVS or ΔfslA strains on MHA+ plate and grown for two days under aerobic 37°C conditions (**A**). Ten-fold serial dilutions of the Δ*fslA* Δ*feoB'* strain were spotted with (top) or without (bottom) 5 µL of 1.5 mM *F. tularensis* siderophore and grown for two days under aerobic 37°C conditions (**B**).

Figure 13

A

LVS

$\Delta fslA \Delta feoB'$ →

$\Delta fslA \Delta feoB'$ →

$\Delta fslA$

B

+*F. tularensis* sideropore

$\Delta fslA \Delta feoB'$ →

$\Delta fslA \Delta feoB'$ →

-*F. tularensis* siderophore
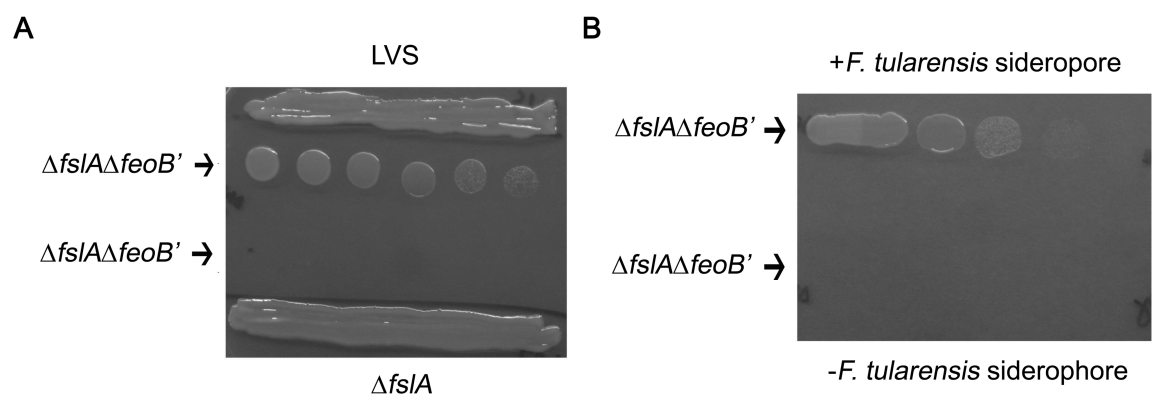
Figure 14: Growth of the LVS Δ*fslA* Δ*feoB'* mutant and complement strain on MHA agar.

LVS, Δ*feoB'*, Δ*fslA* ΔfeoB'+ p*feoB,* and Δ*fslA* Δ*feoB'* strains that were grown on MHA+ agar plates were suspended and brought to an OD_{600} of 1 in che-CDM. Strains were further serially diluted and spotted on MHA+ plates. Growth was observed after 3 days at 37°C under aerobic conditions.

Figure 14
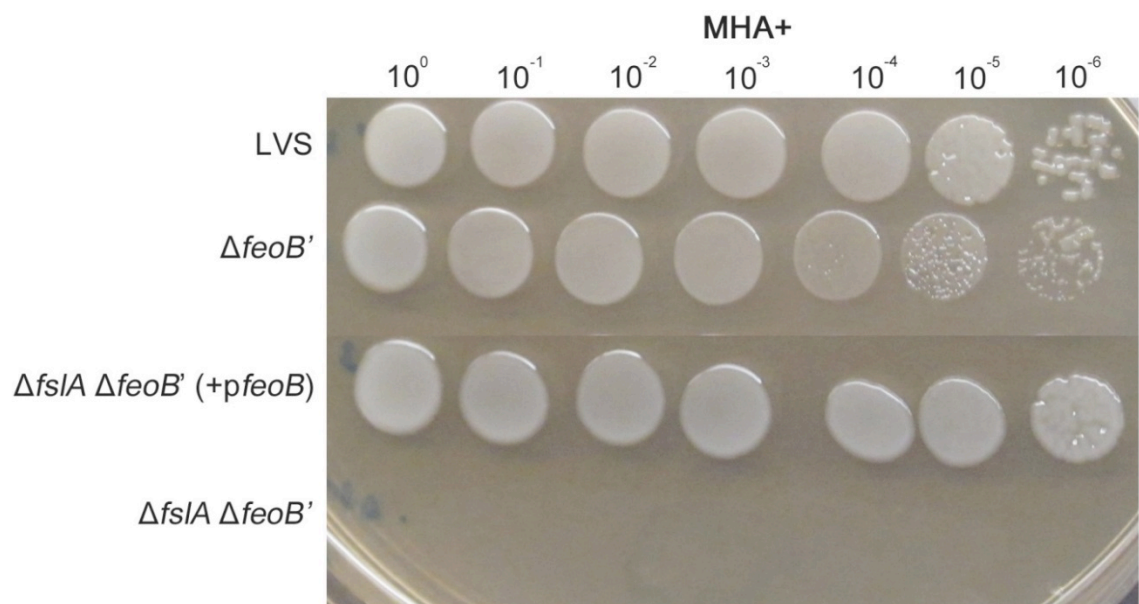
Figure 15: The LVS Δ*fslA* and Δ*feoB'* mutants can utilize *F. tularensis* siderophore for growth on MHA agar.

Three different concentrations of purified *F. tularensis* siderophore (1.5, 0.15, 0.015 mM) were lined across MHA plates with (MHA+) or without (MHA-) FePPi iron supplementation. LVS Δ*feoB'* (**A**) and LVS Δ*fslA* (**B**) was then ten-fold serially diluted over these different concentrations of purified siderophore. Growth was observed after 2 days of incubation and grown for 3 days in aerobic 37°C conditions.

Figure 15

A

MHA+   MHA-

| | 10^0 | 10^{-1} | 10^{-2} | 10^{-3} | 10^{-4} | 10^{-5} | 10^{-6} |

1.5 mM

0.15 mM

0.015 mM

LVS Δ*feoB'*   LVS Δ*feoB'*

B

MHA+   MHA-

1.5 mM

0.15 mM

0.015 mM

LVS Δ*fslA*   LVS Δ*fslA*
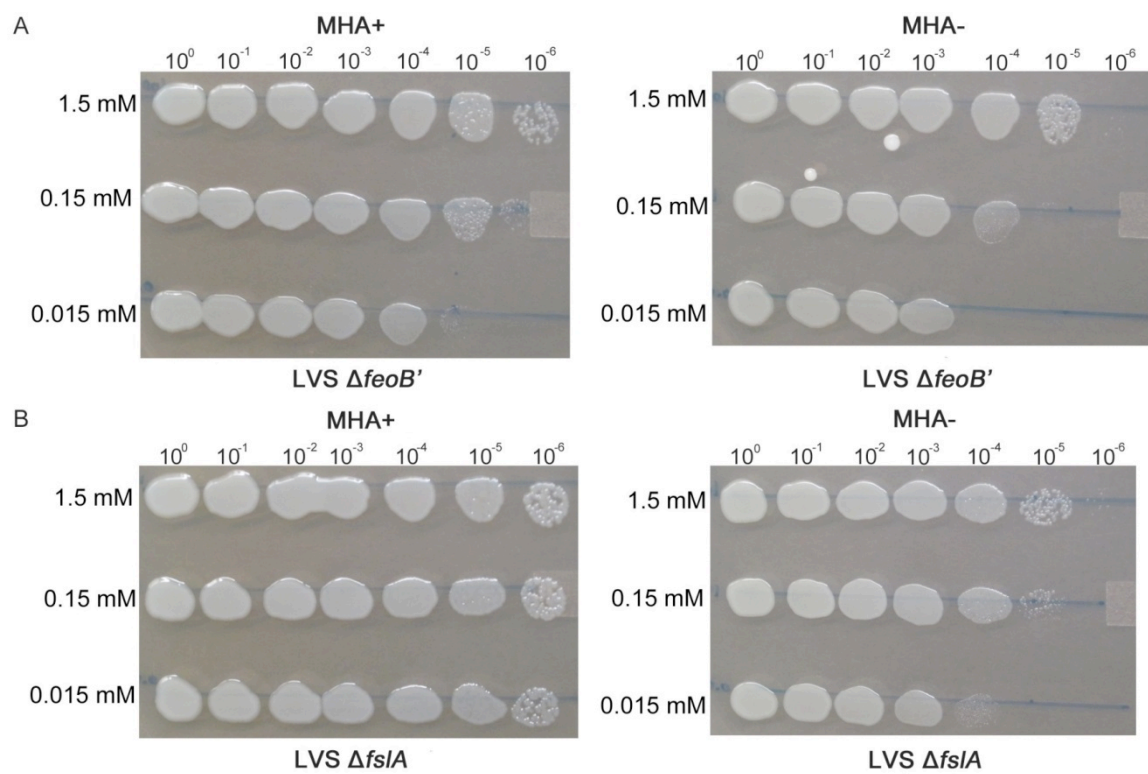
Figure 16: Ferrous iron acquisition by LVS single and double mutants and complementing strains.

LVS, the Δ*fslA* and Δ*feoB'* mutants and in *cis* complements were grown overnight on fresh MHA+ plates (with additional siderophore supplementation to the Δ*fslA* and Δ*feoB'* mutant) at 37°C and further inoculated into che-CDM without FePPi for three hours with shaking. The single mutants and the Δ*feoB'* complement were assessed for ferrous iron uptake as shown in **A** and **B**, and the complement of the double deletion mutant was tested as shown in figures **C** and **D**. Values are expressed as the means ± S.D. Significance was calculated relative to LVS values. *p<0.05, ***p<0.001.

Figure 16
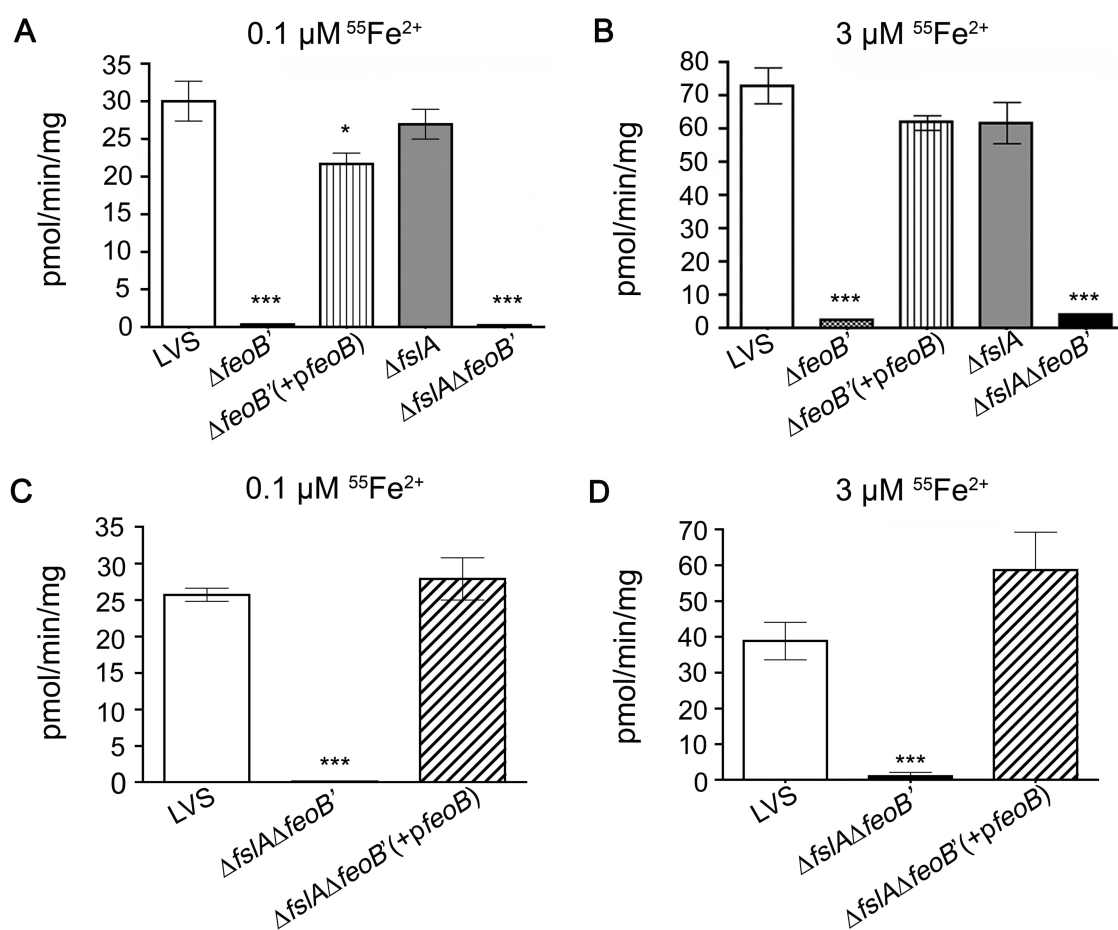
Figure 17: The LVS Δ*fslA* Δ*feoB'* mutant is capable of ^{55}Fe-siderophore uptake through the overexpression of FslE.

LVS, Δ*fslA*, Δ*feoB'*, Δ*feoB'* (+p*feoB*), and Δ*fslA* Δ*feoB'* were incubated with ^{55}Fe bound siderophore and rate of ^{55}Fe uptake was determined (**A**). The expression levels of FslE and FupA/B were analyzed by western blot (**B**) in bacteria grown on MHA+ plates. Comparisons were made to LVS grown under iron-limiting conditions. GroEL was used as a loading control. $*p < 0.05$, $***p < 0.001$.

Figure 17

A

^{55}Fe-siderophore

pmol/min/mg

LVS $\Delta fslA$ $\Delta feoB'$ $\Delta feoB'(+pfeoB)$ $\Delta fslA\Delta feoB'$

B

$\Delta fslA$ $\Delta feoB'$ $\Delta fslA\Delta feoB'$ LVS (plate) LVS (low iron)

FslE

FupA/B

GroEL
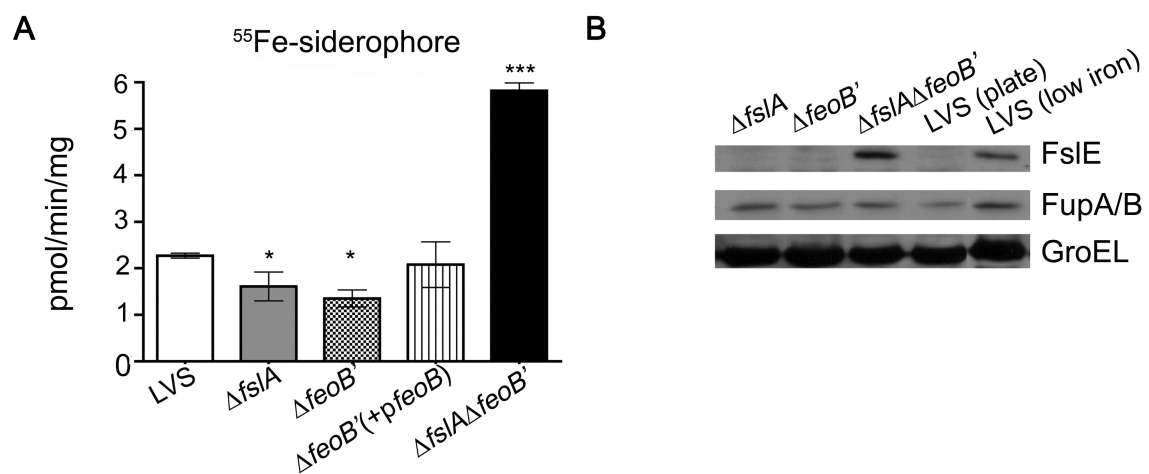
Figure 18: The LVS Δ*fslA* Δ*feoB'* strain is attenuated for virulence.

LVS, Δ*fslA*, Δ*feoB'*, and Δ*fslA* Δ*feoB'* were analyzed for virulence in 7-week-old C57BL/6 mice (5 per group). The mice were infected by the intraperitoneal route with 1000 CFU of bacteria from frozen stocks. The CFU administered was determined by plating on MHA+ with additional supplementation of *F. tularensis* siderophore for growth of the Δ*fslA* Δ*feoB'* mutant. The differences in survival curves of LVS Δ*feoB'* and LVS Δ*fslA* Δ*feoB'* relative to LVS were statistically significant, $p<0.05$ and $p<0.01$, respectively. All survivors (Δ*fslA*, Δ*feoB'*, and Δ*fslA* Δ*feoB'*) were challenged with 1000 CFU LVS at day 14 and all mice survived for greater than 14 days.

Figure 18
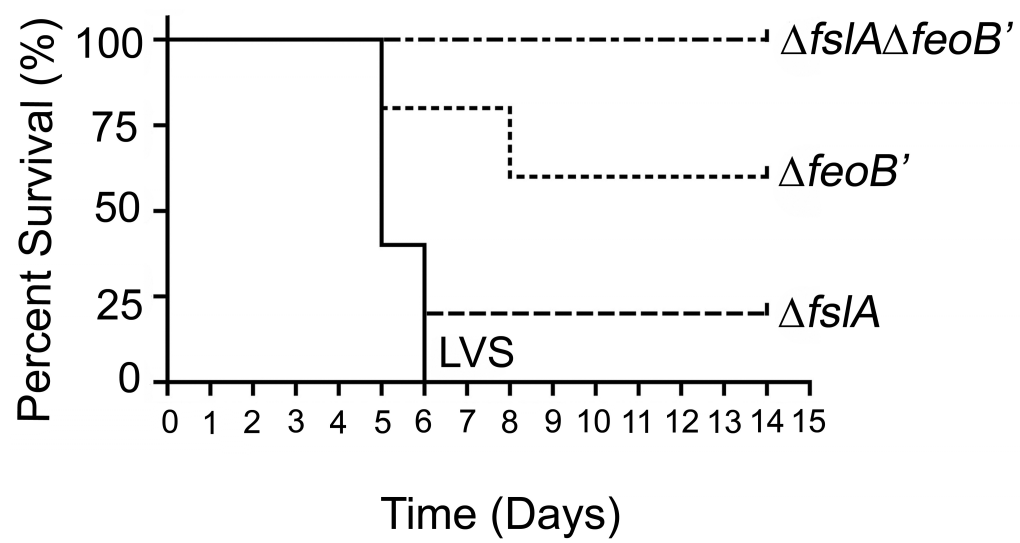
Chapter 3: Type A *Francisella tularensis* mutant disrupted in the two major iron acquisition systems provides limited protection against subcutaneous Schu S4 challenge

3.0 Abstract

F. tularensis is a facultative intracellular pathogen that is capable of rapid growth and proliferation within a multitude of human host cells. Bacteria typically express multiple iron acquisition mechanisms; however, in the previous chapter we demonstrated that the *F. tularensis* subspecies *holarctica* strain LVS encodes only two major iron acquisition mechanisms: ferrous iron (*feo*) and ferric-siderophore (*fsl*) systems. The focus of this study was concentrated on the iron preferences and iron acquisition mechanisms that potentially contribute to the virulence of the *F. tularensis* subspecies *tularensis* strain Schu S4. Both the Feo and ferric siderophore systems are conserved between the LVS and Schu S4 strains. Schu S4 single and double deletion mutants including Schu S4 Δ*feoB'*, Schu S4 Δ*fslA* and Schu S4 Δ*feoB'* Δ*fslA* were used to determine iron preferences that may provide an advantage for *F. tularensis* subsp. *tularensis* to survive and grow within the mammalian host. Metabolic differences were observed *in vitro* with the single deletion Schu S4 mutants on MHA agar without iron supplementation and in broth culture. However, similar to LVS, the Schu S4 single deletion mutant was not defective for growth within *ex vivo* cell lines or for virulence in the C57BL/6 mouse model of infection. The Schu S4 double deletion mutant, like LVS, was also unable to grow and replicate without the addition of endogenous *F. tularensis* siderophore and was attenuated for virulence in the

mouse model of infection. The results described in this chapter details the necessity for both Feo and ferric-siderophore systems for optimal growth and virulence of *F. tularensis* strain Schu S4 *in vitro* and within the mouse model of infection.

3.1 Introduction:

Iron is essential for basic metabolism and homeostasis for most organisms including bacteria. While iron is one of the most prevalent metals in nature, it is mainly found in the oxidized ferric form, which is very insoluble [38]. The reduced ferrous iron form is more prevalent in anaerobic and microaerobic environments. Bacteria utilize iron as a cofactor for many metabolic processes that include electron transfer, and amino acid and DNA synthesis [2]. The ability to transition between both the oxidized and reduced iron states can be both advantageous and detrimental depending on the state of iron. Unbound iron in the presence of oxygen can form hydroxyl radicals through the Fenton reaction that can destroy bacterial membranes and DNA [122,123]. To prevent these events from occurring, bacteria have developed highly regulated mechanisms to sequester and transport iron in order to limit the deleterious effects of this metal while maximizing iron's capabilities [15].

F. tularensis is a Gram-negative bacterium that replicates intracellularly within the iron limiting environment of the mammalian host cells [58]. *F. tularensis* contains three subspecies, which include *tularensis, holarctica* and *mediasiatica,* with the most virulent subspecies *tularensis* categorized by the CDC as a Tier One select agent. Both *tularensis* and *holarctica* subspecies are naturally found

in North America with the *holarctica* strains causing a mild disease in comparison to the *tularensis* subspecies [57]. *F. tularensis* pathogenesis and virulence mechanisms have been best studied in the model organisms the Live Vaccine Strain (LVS) and Schu S4, representing the subspecies *holarctica* and *tularensis*, respectively. While LVS and Schu S4 belong to two different subspecies, both encode genomes with an average identity of 99.89% [59] and are both studied to better understand *F. tularensis.*

In a transcriptional profile of Schu S4 bacteria that were allowed to infect bone marrow derived macrophages [70], genes within *Francisella* siderophore locus (*fsl*) were up-regulated early during the course of infection [70]. The *fsl* locus contains all the genes necessary for *F. tularensis* siderophore biosynthesis, export and import. These genes have previously been shown to produce a siderophore similar to fungal siderophore rhizoferrin [71,75]. Siderophores are small molecules that bind iron and are secreted under iron limiting conditions in order to obtain ferric iron in both bacteria and fungi. Siderophores have been implicated as virulence factors in some bacterial systems, which include *Pseudomonas aeruginosa* [124], *Bacillus anthracis* [51], *Mycobacteria tuberculosis* [49], *Escherichia coli* [125], *Yersinia pestis* [126], and *Campylobacter jejuni* [23]. However, a siderophore deficient mutant, Schu S4 Δ*fslA,* demonstrated no attenuation for virulence in the mouse model of infection [89] [unpublished]. This lack of attenuation was also demonstrated in the intraperitoneal mouse model of infection with an LVS Δ*fslA* mutant [109]. The *F. tularensis* genome also encodes another iron acquisition system, the ferrous iron transport system, *feo.* We and

others have shown that disruption of the *feoB* gene in LVS leads to only minor changes in virulence [107,109]. However, through the disruption of both the iron transport system (Feo) and ferric-siderophore system, severe attenuation was demonstrated in the LVS strain [109]. When mice infected with the LVS Δ*fslA* Δ*feoB'* strain were subsequently challenged with a lethal dose of LVS, they were protected [109]. These results suggest that the LVS Δ*fslA* Δ*feoB'* double deletion mutant is a potential candidate as a live vaccine strain.

The ferric-siderophore and Feo iron acquisition systems are encoded by both LVS and Schu S4; however, the two strains encode iron related proteins within their genomes that are inherently similar in sequence but functionally different. Schu S4 and the wild type strains of *tularensis* and *holarctica* encode for related proteins FupA and FupB, which belong to a family of *Francisella* specific proteins [96]. FupA was initially identified as a virulence factor [89,97] and is necessary for high affinity ferrous iron entry through the outer membrane [97]. The attenuation of Schu S4 Δ*fupA* in the mouse is potentially due to iron deficiency in the initial course of infection in the mammalian host rather than loss of a bacterial virulence-specific factor. In LVS, the *fup* genes produce a hybrid FupA/B protein that is necessary for siderophore receptor mediated uptake in addition to high affinity ferrous iron acquisition through the outer membrane [98,100]. FupA/B's role in association with FslE in LVS may be due to 5 amino acid differences between *fslE* genes in Schu S4 and LVS. When a wild-type *holarctica* copy of *fupA* was introduced into an LVS Δ*fupA/B* mutant, the complemented mutant regained virulence in the mouse model of infection [127].

Differences in iron acquisition capabilities may provide an advantage for *F. tularensis* subsp. *tularensis* that allows for survival and growth within the mammalian host. The contribution of siderophore for *F. tularensis* Schu S4 has been previously discussed; however, the need for ferrous iron acquisition through the Feo iron transport system has not been addressed in the virulent strain. Our predicted model for ferric siderophore and Feo iron acquisition systems in the virulent Schu S4 strain is depicted in Figure 19. We have generated single and double deletion mutants in both iron acquisition systems and have tested them *in vitro* liquid and agar plates, as well as for growth within *ex vivo* cell lines and within the subcutaneous C57BL/6 mouse model of infection.

3.2 Results

Characterization of the Schu S4 Δ*feoB'* mutant

The suicide plasmid used to generate the partial *feoB'* mutant in LVS, pGIR473 [109], was used to achieve a partial deletion in the Schu S4 strain, Schu S4 Δ*feoB'*. This mutant was maintained on MHA plates supplemented with ferric pyrophosphate, FePPi (MHA+). In Figure 20, growth of the Schu S4 Δ*feoB'* mutant was compared to iron acquisition mutants Schu S4 Δ*fupA* and Schu S4 Δ*fslA,* previously shown to be defective in high affinity ferrous iron uptake and siderophore biosynthesis, respectively. Ten-fold serial dilutions on MHA+ plates of the wild-type and single deletion mutants were grown for two days and showed no discernible differences (Figure 20A). When these strains were grown on MHA without the addition of iron (MHA-), there was a dramatic difference in growth

patterns (Figure 20B). Wild-type Schu S4 was able to grow out to single colonies at the 10^{-6} dilution. The Schu S4 $\Delta feoB'$ mutant was able to grow out to 10^{-2} dilution, which is in between the growth patterns of Schu S4 $\Delta fslA$ and Schu S4 $\Delta fupA$ mutants. These observations indicate that both the ferric-siderophore and Feo iron acquisition systems are required for normal growth on iron limiting MHA plates. Surprisingly the Schu S4 $\Delta feoB'$ mutant is not as defective for growth as the Schu S4 $\Delta fupA$ mutant (Figure 20B). This observation suggests that FupA is important not only for ferrous iron acquisition but also potentially for another essential function. The Schu S4 $\Delta feoB'$ mutant was then complemented with a wild-type copy of *feoB* in cis (Schu S4 $\Delta feoB'$ (+p*feoB*)), and was able to regain the growth phenotype of wild-type Schu S4 on MHA- plates (Figure 20C).

Due to the deficient growth in iron limiting MHA plates, we next monitored the ability of the Schu S4 $\Delta feoB'$ mutant to secrete siderophore using the liquid Chrome Azurol S (CAS) assay. We compared siderophore production in iron replete and iron limiting CDM of wild-type Schu S4 and the Schu S4 iron acquisition mutants (Figure 21). As expected, Schu S4 $\Delta fslA$ mutant is unable to produce siderophore [75] while the Schu S4 $\Delta fupA$ mutant is able to secrete siderophore in both iron replete and iron limiting conditions [97]. The Schu S4 $\Delta feoB'$ mutant was also found to secrete siderophore under both high and low ferric iron conditions, thus demonstrating the use of ferric-siderophore as its source of iron acquisition.

Iron can transition between the reduced ferrous and oxidized ferric states; however, under aerobic conditions the oxidized ferric form is more prevalent. Liquid growth was compared between Schu S4 and the Schu S4 Δ*feoB'* mutant in high and low ferric and ferrous iron conditions in chelex treated CDM (Figure 22). The Schu S4 Δ*feoB'* mutant was significantly defective for growth in both high and low ferric and ferrous iron conditions in comparison to Schu S4. Even in the presence of high ferric (Figure 21A) and ferrous (Figure 21B) iron, growth of the Schu S4 Δ*feoB'* mutant was slower than the growth of wild-type Schu S4. These observations show the importance of the Feo system for Schu S4 growth in liquid culture.

The capability for Schu S4 ferrous iron uptake was studied using the ^{55}Fe uptake assay previously described [97,100]. In Figure 23, Schu S4 was compared to Schu S4 Δ*feoB'*, Schu S4 Δ*fupA*, and the Schu S4 Δ*feoB'* complemented with a wild-type copy of *feoB* in cis, Schu S4 Δ*feoB'* + (+p*feoB*). As expected, the Schu S4 Δ*fupA* mutant is defective specifically for iron uptake at the high affinity iron concentration (Figure 23A). The Schu S4 Δ*feoB'* mutant on the other hand was defective in both high and low iron affinity ^{55}Fe uptake concentrations, 0.1 μM (Figure 23A) and 3.0 μM (Figure 23B), respectively. This uptake phenotype was abrogated by the complementation with a wild-type copy of *feoB.* These observations demonstrate that the Feo system is the major ferrous iron transport system in Schu S4, which is unable to acquire ferrous iron through another mechanism.

Characterization of the Schu S4 Δ*feoB'* Δ*fslA* mutant

A double deletion mutant, Schu S4 Δ*feoB'* Δ*fslA,* was generated from the parent strain Schu S4 Δ*feoB'* (Figure 24)*.* Like the LVS Δ*feoB'* Δ*fslA* mutant [109], the Schu S4 double deletion mutant required siderophore from a nearby siderophore producing strain Schu S4 (Figure 24A) or exogenous purified siderophore (Figure 24C) for growth on MHA+ agar. The use of siderophore secreted by LVS is able to promote growth of the Schu S4 double deletion mutant (Figure 24B). With the addition of a wild-type copy of *feoB,* the double deletion mutant regained the ability to grow on MHA+ without the addition of siderophore as an iron source (Figure 24A).

The Schu S4 iron acquisition mutants were then tested for their ability to enter and replicate within J774A.1(Figure 25A) and HepG2 cell lines (Figure 25B). In the murine macrophage J774A.1 cell line, the single deletion mutants of Schu S4 Δ*fslA* and Schu S4 Δ*feoB'* were able to replicate to numbers comparable to wild-type up to 24 hours post infection (Figure 25A). In the human hepatocyte cell line, HepG2, the *fslA* mutant was able to grow to levels comparable to wild-type Schu S4. The *feoB'* mutant was able to replicate within this cell line but not to the robust levels of wild-type at 24 hours post infection. Since the Δ*feoB'* mutant relies on the ferric-siderophore for meeting iron acquisition needs, the level of ferric iron is likely to be limiting in this cell line. The Schu S4 Δ*feoB'* Δ*fslA* mutant was unable to grow in either the J774A.1 or HepG2 strains up to 24 hours post infection. This defect for growth indicates that *fsl* and

feo are the only two major iron acquisition systems required for Schu S4 to grow intracellularly.

A lethal dose of Schu S4 has previously been shown to be <10 CFU by any route of infection in C57BL/6 mice. We infected these mice by subcutaneous infection with wild-type Schu S4, Schu S4 Δ*feoB'* and Schu S4 Δ*feoB'* Δ*fslA* with a dose of approximately 25 CFU (Figure 26). Mice in the wild type and Schu S4 Δ*feoB'* mutant groups all died between 4 and 6 days post infection. The mice infected with the Schu S4 Δ*feoB'* Δ*fslA* strain however lived past 21 days post infection. These mice were subsequently challenged with 25 CFU Schu S4 and monitored for 14 days. Out of the 5 surviving Δ*feoB'* Δ*fslA* mice, 4/5 mice survived lethal Schu S4 challenge. In an accompanying experiment, we infected mice with increasing doses of the Schu S4 Δ*feoB'* Δ*fslA* and found that mice remained resistant to the highest dose tested- 25,000 CFU.

3.3 Discussion

As an intracellular bacterium, *F. tularensis,* like *Listeria, Shigella, Salmonella,* and *Rickettsia,* is capable of entering the cytoplasm of host cells and utilizing host metabolites to grow and replicate [73]. These bacteria require iron and are capable of acquiring it through siderophores and ferrous iron transport systems. Unlike many bacteria, *F. tularensis* requires only two iron acquisition systems for survival within the iron-limiting environment of the mammalian host.

The Schu S4 *F. tularensis* ferric siderophore system was previously shown not to be essential for virulence in the mouse model of infection [89]. While

110

this observation suggests that another iron acquisition mechanism is capable of acquiring iron for *F. tularensis* survival within host cells, it does not indicate that the *F. tularensis* siderophore is irrelevant. To delineate the contribution of the Feo uptake system for *F. tularensis* viability and survival, a partial deletion within the inner membrane permease, FeoB, was generated in Schu S4. The Schu S4 Δ*feoB'* mutant was defective for ferrous iron uptake in ^{55}Fe uptake assays compared to the Feo-intact wild-type Schu S4 and regained ferrous iron function with its complement, Schu S4 Δ*feoB'* (+p*feoB*) (Figure 23). The Schu S4 Δ*feoB'* mutant was not defective for siderophore production as demonstrated by the CAS assay, and was capable of secreting siderophore under iron rich and iron limiting conditions (Figure 21). This has also been demonstrated in the Schu S4 Δ*fupA* mutant [97], which is defective for ferrous iron acquisition across the outer membrane. The production of siderophore under high iron conditions suggests that the Schu S4 Δ*feoB'* mutant is iron starved and relies on the ferric-siderophore iron acquisition system to acquire available iron. While the Schu S4 Δ*feoB'* mutant is capable of growing under iron limitation with the use of the ferric-siderophore, it is defective for optimal growth on both under iron replete and iron limiting ferric and ferrous iron liquid media as well as on iron limiting MHA- plates (Figure 22 and Figure 20B). The severity of the Schu S4 Δ*feoB'* growth defect demonstrates the necessity of the ferrous iron acquisition system for both liquid and agar plate growth. The siderophore, while present, is not able to promote growth of the bacteria at the rate of wild-type Schu S4. The Schu S4

Δ*fslA* mutant was also defective for growth on MHA- plates (Figure 20B); this demonstrates the need for both iron acquisition systems for optimal growth.

We tested both murine and human established cell lines, J774A.1 murine macrophages and HepG2 human hepatic carcinoma cells, to observe potential intracellular growth differences in phagocytic and non-phagocytic cells, respectively. Macrophages are considered important cells for the initiation of *F. tularensis* infection, but are not the sole cell type that *F. tularensis* is capable of infecting [58]. The infection of J774A.1 cells with Schu S4 and Schu S4 mutants demonstrated there was no growth defect for the Schu S4 Δ*feoB'* mutant, or for the siderophore defective Schu S4 Δ*fslA* mutant (Figure 25A). This ability of the bacteria to grow and replicate within macrophages with either the Feo or siderophore acquisition systems may allow for a robust early advantage to the progression of growth and survival in the mammalian host. Interestingly, there was a different growth outcome for the Schu S4 Δ*feoB'* mutant in human hepatocyte HepG2 cells (Figure 25B). Both Schu S4 Δ*fslA* and Schu S4 Δ*feoB'* mutants were able to grow intracellularly within HepG2 cells but the Schu S4 Δ*feoB'* mutant was significantly defective for growth at 24 hours post infection. This significant decrease in growth within HepG2 cells was also demonstrated within an LVS Δ*feoB* mutant [107] and in our own LVS Δ*feoB'* mutant [unpublished]. HepG2 cells are derived from human liver cancer cells and have been shown in comparison to another hepatocellular carcinoma cell line (Huh7) and to human derived liver cells, to be down-regulated in expression of transferrin receptor 2 (TfR2) [5]. It was shown in Pan *et al.* (2010) that in macrophages infected with LVS

112

there is an increase in the expression of transferrin receptor 1 (TfR1) [105], which is the more dominant protein form in the human body, while TfR2 is predominately expressed on hepatocytes [5]. This decrease in Schu S4 Δ*feoB'* growth within HepG2 cells could give supporting evidence that *F. tularensis* modulates host proteins for acquiring maximum iron for survival intracellularly and shows that *F. tularensis* requires the Feo system to acquire ferrous iron within specialized tissues such the liver.

We further determined by the generation of a double deletion iron acquisition mutant, Schu S4 Δ*feoB'* Δ*fslA*, that the Feo and ferric-siderophore systems are the major mechanisms utilized by *F. tularensis* strain Schu S4. This double deletion mutant was unable to grow without the supplementation of *F. tularensis* siderophore or had to be grown in the presence of a siderophore producing strain (Figure 24), as previously shown for our LVS Δ*fslA* Δ*feoB'* mutant (Figure 13) [109]. Only with the complementation of a wild-type copy of *feoB* in *cis* did the double deletion mutant regain the ability to grow without iron supplementation. In contrast to the Schu S4 Δ*feoB'* and Schu S4 Δ*fslA* mutants, the Schu S4 Δ*feoB'* Δ*fslA* mutant was unable to grow in either J774A.1 or HepG2 cells although it was able to enter both cell types (Figure 25). This further suggests that there are no other major or minor iron acquisition systems that can promote the growth of this mutant intracellularly.

The inability of *F. tularensis* to replicate in host cells has been demonstrated in specific Schu S4 mutants, especially the studied Schu S4

Francisella pathogenicity island mutants (*iglABC*) [128], Δ*fipB* mutant [129], and also

the purine auxotroph, Schu S4 Δ*purMCD* [68], which have further indicated the

attenuated virulence of these Schu S4 mutants in the mouse model of infection.

Somewhat surprising was the finding that the ferric-siderophore system in the

Schu S4 Δ*feoB'* mutant was capable of acquiring necessary iron for *F. tularensis*

within the mouse model of infection and further capable of causing disease and

death at comparable times to wild-type Schu S4 (Figure 26). This suggests that

the ability to acquire iron through either the ferric siderophore or Feo iron

acquisition can support growth and progression of disease.

At a low dose, approximately 25 CFU is capable of causing disease and

death with a wild-type Schu S4; however, our Schu S4 Δ*feoB'* Δ*fslA* double

deletion mutant at this concentration did not cause disease (Figure 26). This was

also demonstrated in our LVS Δ*feoB'* Δ*fslA* mutant (Figure 18) [109]. Challenge of

all of the Schu S4 Δ*feoB'* Δ*fslA* mice with a lethal dose of Schu S4 demonstrated

4/5 mice surviving thus demonstrating that only partial protection is provided to

mice infected with the Schu S4 Δ*feoB'* Δ*fslA* mutant. This confirms the results

established in the LVS model, that these are the two major systems of iron

acquisition and no minor iron acquisition system can rescue *F. tularensis* in both

ex vivo systems or within a mammalian host.

Our studies with the iron acquisition mutants were carried out in J774A.1

cells and in C57BL/6 mice. Both of these systems are defective for the divalent

metal transporter, natural resistance-associated macrophage protein (Nramp1) [11]

found primarily in professional phagocytes [130]. Nramp1 -/- mice have been shown to have decreased levels of intracellular iron content within hepatocytes [131]. Nramp1 is present in macrophages that actively recycle erythrocytes, and it appears that without this protein functioning in J774A.1 and C57BL/6 mice, the *F. tularensis* and the single deletion mutants can readily receive iron available from other sources intracellularly and within the iron-limiting environment of the mouse.

Inactivating iron acquisition systems in bacteria has been suggested as potential strategy for treating bacterial diseases. Recently, targeting of siderophore biosynthesis genes is a target for inhibitors and was shown recently that if the recycling of mycobactin in *Mycobacteria tuberculosis* is inhibited it affects the viability and virulence of this pathogen [132]. However, in the context of *F. tularensis* which has two equally effective iron acquisition mechanisms, inactivating a single system appears insufficient for decreasing the rapid growth and dissemination of this pathogen.

3.4 Experimental methods

Bacterial strains and media:

Francisella tularensis subspecies *tularensis,* Schu S4 (from the Centers for Disease Control and Prevention, Fort Collins, CO), and mutant derivatives were maintained on modified Mueller-Hinton agar (MHA) supplemented with horse serum, cysteine, and defined amounts of iron salts including ferrous sulfate ($FeSO_4$) and ferric pyrophosphate (FePPi). *F. tularensis* strains were grown in liquid Chamberlin's defined medium (CDM) [97,117] at 37°C with shaking overnight to reach late exponential phase. Bacterial culture optical densities were determined at 595 nm (OD_{595}) using a microplate reader (BioRAD iMark). For growth determinations in defined iron growth media, bacterial cultures were grown initially in iron replete media overnight. Cultures were then washed in chelex treated CDM (che-CDM) three times and then inoculated into che-CDM supplemented with known quantities of replete or iron deplete FePPi (2.5 μg/mL and 0.125 μg/mL) and $FeSO_4$ (2 μg/mL and 0.2 μg/mL). Bacteria in the exponential growth stage were inoculated to an OD_{595} of 0.01 in the respective growth media and grown at 37°C with shaking for 24 hours. The Schu S4 Δ*feoB*' Δ*fslA* was maintained on MHA agar supplemented with *F. tularensis* strain LVS purified siderophore (as previously described in [109]). Supernatant collected from LVS grown under iron limiting conditions was purified through a series of columns to obtain *F. tularensis* siderophore [75]. Supernatants were passed through gravity columns containing: XAD-2 (Amberlite) methanol activated beads, and further through cation exchange Dowex 50W-X8 beads. Collected

flow through was adjusted to a pH of 7 with sodium hydroxide, this extract was then run on an anion exchange AG1-X8 formate column. Column beads were then washed with water and *F. tularensis* siderophore was purified off with 1.5 M ammonium formate, lyophilized, and resuspendend in MilliQ water (Millipore). Siderophore concentration was determined by the Cu-CAS assay in comparison to deferoxamine standards [118].

Generation of Schu S4 single and double deletion iron acquisition mutants:
Schu S4 single and double deletion mutants (Table 4) were generated as previously described through a two-step mutagenesis procedure in Chapter 2 experimental methods [75]. Suicide vectors (Table 5) were introduced into Schu S4 through electroporation [82]. The suicide vector pGIR473 was used to generate a partial deletion of the *feoB* gene (Schu S4 Δ*feoB'*) and pGIR457 was used to generate an in-frame deletion of *fslA* (Schu S4 Δ*fslA*). Schu S4 was spread on an MHA plate supplemented with FePPi (MHA+) overnight. The lawn of Schu S4 was resuspendend into 5 mL of 0.5 M sucrose. The OD_{595} was determined and cultures were spun at 10,000 rpm for 8 minutes and the supernatant was discarded. This washing procedure was accomplished 3 times to remove excess salts. Cells were then incubated with respective plasmids and electroporated using Bio-Rad micropulser set at 2.5 kV, 600 Ω resistance, and 10 μF conductance. Cells were resuspendend in TSB/c and plated on MHA+ for 4-6 hours and then plated on MHA+ supplemented with kanamycin. The generation of the double deletion mutant required the supplementation of purified siderophore to be plated on MHA+ kanamycin. Mutants were screened by PCR

analysis of genome purified DNA. As described in Chapter 2 Experimental

methods, the primer sets F12/F335 and F10/F94 were used to confirm the 5' and

3' flanking region of the *feoB* gene, respectively. The primer sets F123/F116 and

F115/F126 were used to confirm the 5' and 3' flanking region of the *fslA* gene,

respectively.

F. tularensis siderophore detection with the Chrome Azurol S (CAS) assay:

As previously described [109] the Schwyn and Neilands 1987 adaptation of the

liquid CAS assay was used to determine the presence of the *F. tularensis*

siderophore under iron limitation [108] and was previously described in Chapter 2

experimental methods. Bacterial cultures were grown in iron replete or iron-

limiting FePPi (2.5 μg/mL and 0.125 μg/mL) supplemented che-CDM overnight at

37°C with shaking. Cultures were centrifuged at 9,0000 x G for 5 minutes and

supernatants were collected and added to equal parts CAS solution (100 μL) and

2 μL of the shuttle solution in a 96-well flat bottom plate. These were incubated

for 30 minutes at room temperature and absorbance was detected at 630 nM

(A_{630}) on a plate reader (BioRAD iMark). CAS activity values were calculated to a

reference water blank using the formula ((A_{630} water- A_{630})/A_{630} water). Specific

CAS activity was normalized to bacterial cell density (OD_{595}) with the formula

(CAS Activity/OD_{595}). All strains were tested in triplicate.

Growth on agar plates.

To assess the growth of Schu S4 and Schu S4 iron acquisition mutants on agar,

the OD_{595} was determined, overnight cultures were washed in che-CDM, ten-fold

serially diluted and spotted on modified Muller Hinton agar plates supplemented

with FePPi and FeSO$_4$, or on CDM plates without supplemented iron.

Intracellular replication:

Intracellular replication of Schu S4 and mutants was assessed in murine

macrophage-like cells J774A.1 (ATCC TIB-67) as previously described [98,109].

J774A.1 cells were maintained in high glucose Dulbecco's modified Eagle's

medium (DMEM) supplemented with 10% FBS and grown at 37°C with 5% CO$_2$

and split 1:10 per passage. Cells were counted on an automated cell counter

(BioRad TC10) and seeded at a concentration of 2 x 10^5 cells per well in 24-well

plates the day before the assay. Bacteria were added at a multiplicity of infection

(MOI) of 10 into four wells per group. Human liver carcinoma cell line (HepG2)

was also used to assess intracellular replication within a non-phagocytic cell line.

HepG2 cells were maintained in DMEM supplemented with 10% FBS, 5%

glutamate, and grown at 37°C with 5% CO$_2$ and split 1:10 per passage. Cells

were seeded at a concentration of 2 x 10^5 per well in a 24-well plate the day

before the assay. Bacteria were added at an MOI of 100 into four wells per

group. At one hour (J774A.1) and two hours (HepG2) post infection, cells were

washed twice in PBS and incubated with 50 µg/mL of gentamicin in DMEM+FBs

for 1 hour at 37°C. Cells were washed with media to remove gentamicin and then

one set of cells were lysed with 0.1% saponin and the other cells continued to

incubate in fresh media at 37°C. Lysed cells were immediately serially diluted in

CDM and plated on MHA+ plates to determine intracellular bacterial numbers as

colony-forming units (CFU). The double deletion mutant was supplemented with

purified *F. tularensis* siderophore to promote growth. Intracellular replication assays were repeated to ensure consistency of results.

Mouse infection studies

All animal protocols were approved by the Animal Care and Use Committee (ACUC) of the University of Virginia (protocol #3512). The University of Virginia's Animal Welfare Assurance number is #A3245-01, and the vivarium is accredited by the Association for Assessment Accreditation of Laboratory Animal Care International. Mice were anesthetized with a cocktail of ketamine-HCL-xylazine. Previously tittered frozen bacterial cultures were thawed to room temperature and diluted in 0.9% sterile saline solution to 250 CFU/mL and 100 μL (25 CFU) aliquots were subcutaneously (S.C) injected into 4-6 week old C57BL/6 male mice (five mice per group) (Jackson laboratories, Bar Harbor, ME) [97]. CFU's were determined after plating bacterial dilutions on MHA plates. MHA topically supplemented with *F. tularensis* siderophore was used to determine CFU's of the double deletion mutant. Clinical scores were determined for mice over the course of infection and were euthanized at a humane endpoint if symptoms of irreversible morbidity were observed. Survivors were subsequently challenged by S.C. by delivery of 25 CFU of wild-type Schu S4 and monitored over 21 days.

   LD$_{50}$ studies: Three groups of male C57BL/6 (4-6 weeks old) mice were S.C. injected with 0.1 mL saline solution containing either 250 CFU, 2,500 CFU, and 250 CFU of the $\Delta feoB'\Delta fslA$ bacteria. CFU's were determined by plating bacterial dilutions on MHA plates supplemented with *F. tularensis* siderophore.

Mice were monitored for 21 days and then challenged with 33 CFU of wild-type

Schu S4. CFUs were determined by plating on MHA plates.

Statistical Analysis:

Prism 4.0 software (GraphPad Software, Inc., San Diego, CA). Statistical

comparison of values was accomplished using *t* test function and the Logrank

Test function was used to evaluate mouse survival curves.

3.5 Chapter 3 Tables

Table 4. *F. tularensis* **Schu S4 strains**

Strain Description	Strain Name	Source
Schu S4	Schu S4	Centers for Disease Control and Prevention, Fort Collins, CO
Schu S4 Δ*feoB'*	GR288	This study
Schu S4 Δ*fslA*	GR206	[97]
Schu S4 Δ*feoB'* Δ*fslA*	GR292	This study
Schu S4 Δ*fupA*	GR218	[97]
Schu S4 Δ*feoB'* + pNMP095 (+*feoB*)	GR295	This study
Schu S4 Δ*feoB'* Δ*fslA* + pNMP095 (+*feoB*)	GR296	This study
Schu S4 Δ*fslE*	GR211	[82]

Table 5. Plasmids

Genotype	Plasmid name	Source
pGIR473 (suicide plasmid for deletion of *feoB*)	pGIR473	[109]
pGIR463_*feoB*	pNMP095	[109]
pGIR457 (suicide plasmid for the in-frame deletion of *fslA*)	pGIR457	[75]
pGIR458 (pFNLTP6 with *fslA*)	pGIR458	[75]

Table 6. Primers used in this study

Name	Sequence[1]
F12	ctactggtcgacCTGTGAGAGTAGAATTAGTAGC
F335	TCAAGAACAACAAATAACTGAC
F10	TATATGTCTCGAGCTGCTTTTG
F94	GCCTTCTTTAGCCATATCAACTGC
F123	GCCATCACATAAGCATGCTC
F116	ctactggagctcCTGCTATGATTATAAGCTGAC
F115	ctactggcggccgcTGTTAAATGCAAATCCTGTCG
F126	TCGACCAAACTACGTCCTAG

---

[1] Uppercase letters signify sequences corresponding to genomic DNA.

3.6 Chapter 3 Figures

Figure 19: Predicted model of the *F. tularensis* strain Schu S4 siderophore mediated and ferrous iron transport systems.

The model depicts the predicted roles of each of the Fsl proteins in siderophore synthesis and export (left) as well as the Feo transport system (right). For ferric iron transport, the FslA and FslC proteins synthesize the siderophore from the precursors ornithine and citrate. The siderophore is exported out of the cytoplasm through the inner membrane through FslB and out of the outer membrane through an unknown outer membrane protein (OMP). The siderophore receptor FslE binds the ferric siderophore. FslD is required for transport of the ferric-siderophore through the inner membrane. Ferrous iron entry occurs through the outer membrane ferrous iron transporter, FupA. Entry through the inner membrane requires the ferrous iron transport system (Feo) components including the inner membrane permease FeoB and potentially the cytoplasmic protein FeoA.

Figure 19
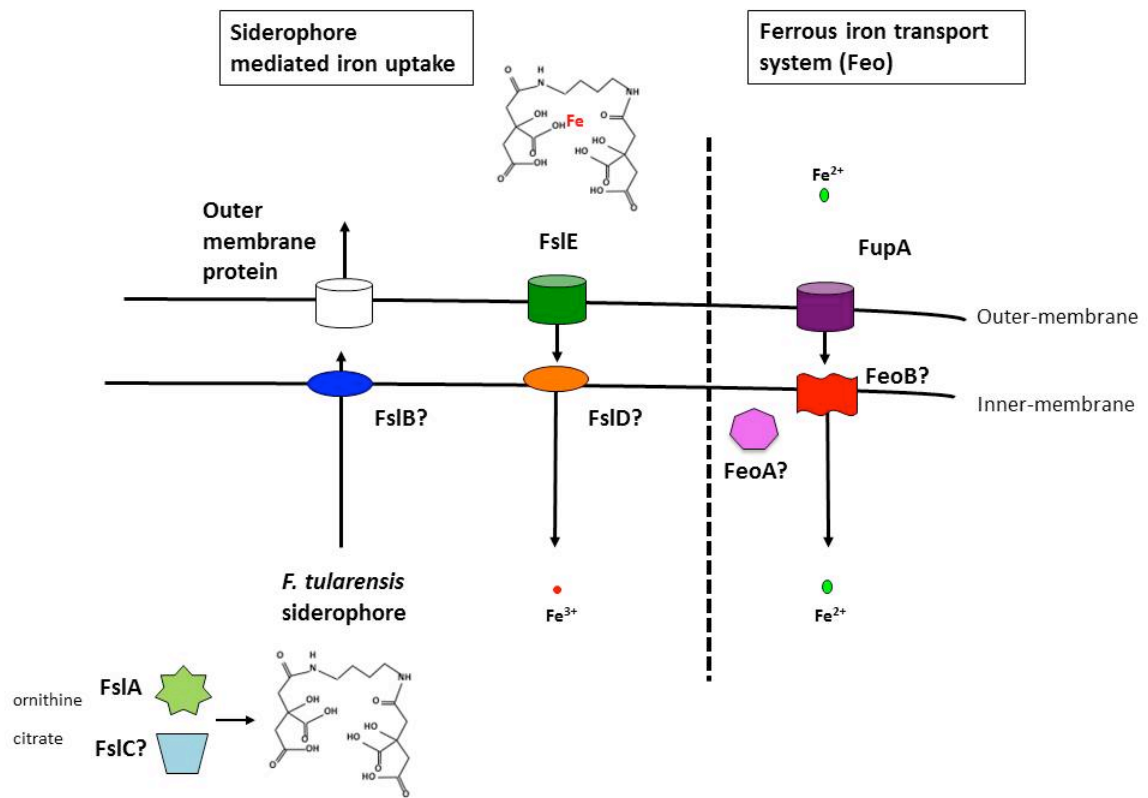
Figure 20: Growth of Schu S4 and iron acquisition mutants on MHA+/- iron plates.

Schu S4, Δ*fupA,* Δ*fslA*, Δ*feoB'*, and Δ*feoB'* Δ*fslA* were grown overnight in CDM supplemented with high ferric and ferrous iron to mid-logarithmic phase. Schu S4 Δ*feoB'* Δ*fslA* was grown overnight on an MHA+ plate supplemented with *F. tularensis* siderophore. All bacterial strains were washed in che-CDM and suspended to an OD_{595} of 1 in che-CDM. Bacteria were then ten-fold serially diluted in che-CDM and spotted on respective agar plates which include MHA with ferric pyrophosphate (MHA+) (**A**), MHA without addition of iron (MHA-) (**B**) and grown at 37°C in aerobic conditions. The order in which Schu Δ*feoB'* and Schu Δ*fslA* were spotted was switched between the left and right panel in **A** and **B**. Ten-fold serial dilutions of Schu S4, Δ*feoB'*, and the Δ*feoB'* (+p*feoB*) cis complement were spotted on MHA+ (**C**)*.*

Figure 20
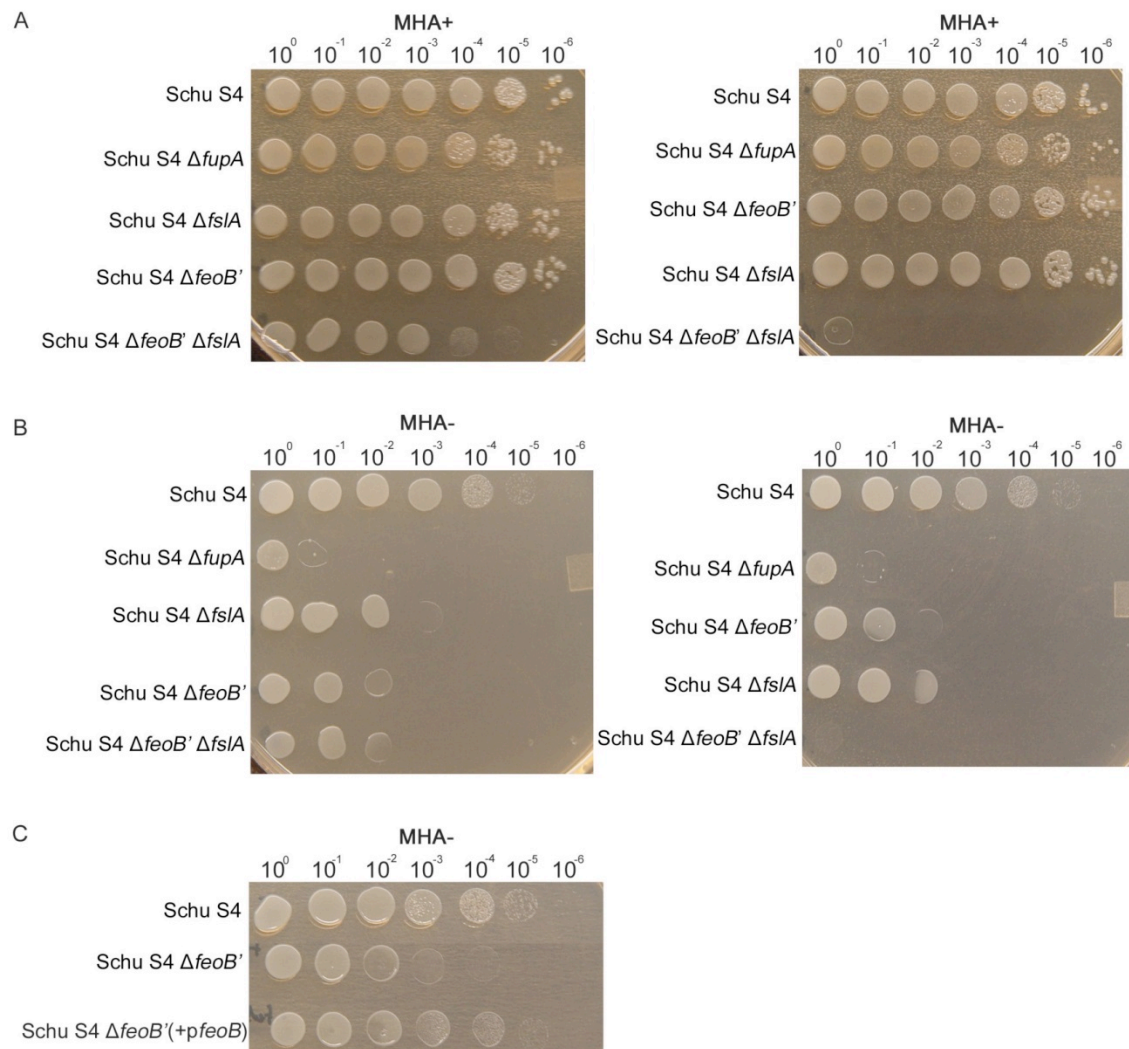
**Figure 21: Siderophore production is not defective in the Schu S4 Δ*feoB'*
mutant compared to wild-type Schu S4.**

Schu S4, Δ*fslA*, Δ*fslE,* Δ*fupA,* and Δ*feoB'* were grown in either high or low ferric
iron che-CDM overnight. Culture supernatants were analyzed with the Chrome
Azurol S assay (CAS) and siderophore activity was normalized to bacterial cell
densities (OD_{595}) to provide specific CAS values. Values were graphed as the
means ± S.E. Significance calculations were made relative to Schu S4. *$p<0.05$,
**$p<0.01$, ***$p<0.001$.

Figure 21
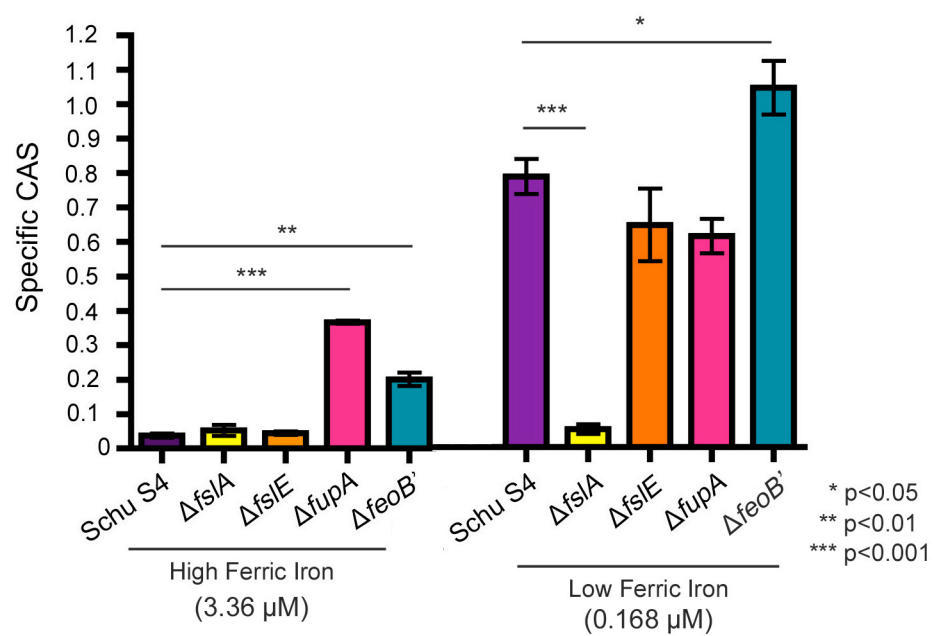
Figure 22: Schu S4 and Schu S4 Δ*feoB'* liquid growth in chemically defined liquid media.

Schu S4 and Δ*feoB'* were grown in che-CDM supplemented with either high (H) or low (L), ferric (FePPi) (**A**) or ferrous (FeSO$_4$) (**B**) iron. Cultures were washed in chelex treated CDM, inoculated into respective media conditions, and growth was monitored as a change in optical density of 595 nm (OD$_{595}$). Values were graphed as the means ± S.E. Significance calculations were made relative to Schu S4. *$p < 0.05$,

Figure 22

A

Ferric Iron

B

Ferrous Iron
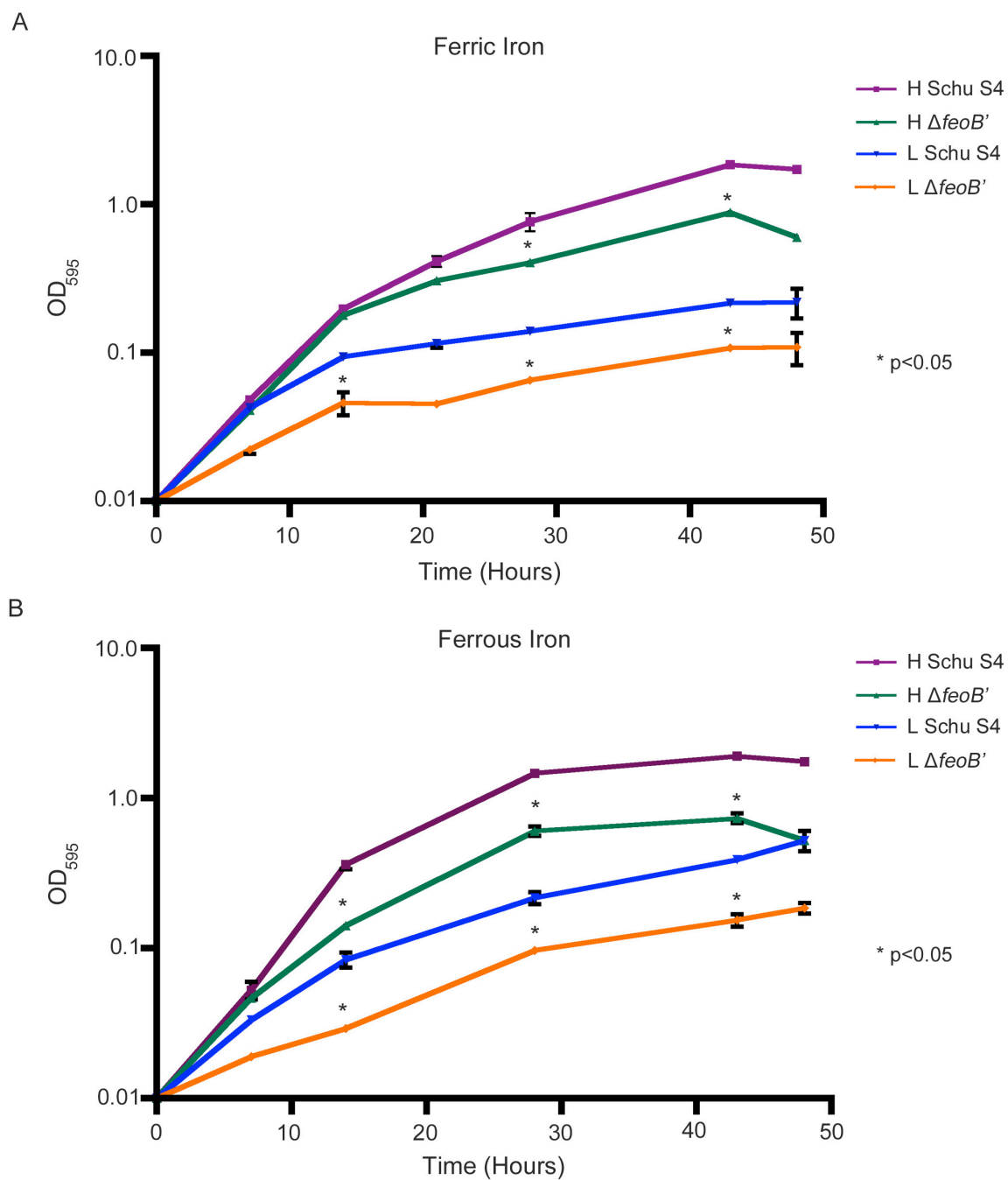
Figure 23: Schu S4 Δ*feoB'* is defective for ^{55}Fe uptake at high and low affinity iron concentrations.

^{55}Fe uptake abilities were assessed for Schu S4, Schu S4 Δ*fupA,* Schu S4 Δ*feoB',* and Schu S4 Δ*feoB'* (+p*feoB*) at high (0.1 μM) (**A**) and low (3.0 μM) (**B**) affinity ^{55}Fe uptake concentrations. Schu S4 strains were inoculated from MHA plates into iron limiting che-CDM broth and grown to mid-logarithmic phase. Rates of ^{55}Fe uptake were determined in the presence of ascorbate to maintain a reducing environment. Values were expressed as the means ± S.E. Significance calculations were made relative to Schu S4. *p<0.05, ***p<0.001.

Figure 23

A   0.1 µM $^{55}Fe^{2+}$

***p<0.001

B   3.0 µM $^{55}Fe^{2+}$

***p<0.001
*p<0.05

134

Figure 24: Schu S4 Δ*feoB' ΔfslA* mutant requires *F. tularensis* siderophore for growth.

Schu S4 Δ*feoB' ΔfslA* was grown overnight on an MHA+ plate supplemented with *F. tularensis* siderophore. Bacteria were then washed in che-CDM and suspended to an OD$_{595}$ of 1 in che-CDM. The culture was ten-fold serially diluted in che-CDM and spotted on respective agar plates which include MHA with ferric pyrophosphate (MHA+). Ten-fold serial dilutions of Schu S4, Schu S4 Δ*feoB' ΔfslA,* and the complemented in cis *feoB* strain Δ*feoB' ΔfslA*(+p*feoB*), were spotted on MHA+ agar (**A**). Schu S4 Δ*feoB' ΔfslA* was spotted near a dense streak of a siderophore producing strain (top, wild-type LVS) or without (bottom) (**B**). Schu S4 Δ*feoB' ΔfslA* was ten-fold serially diluted and spotted with purified siderophore (top) or without (bottom) (**C**).

Figure 24

A

MHA+

10^0 10^{-1} 10^{-2} 10^{-3} 10^{-4} 10^{-5} 10^{-6}

Schu S4

Schu S4 $\Delta feoB$' $\Delta fslA$

Schu S4 $\Delta feoB$' $\Delta fslA$ (+p$feoB$)

B

MHA+

10^0 10^{-1} 10^{-2} 10^{-3} 10^{-4} 10^{-5} 10^{-6}

LVS

Schu S4 $\Delta feoB$' $\Delta fslA$

Schu S4 $\Delta feoB$' $\Delta fslA$

C

+*F. tularensis* siderophore

10^0 10^{-1} 10^{-2} 10^{-3} 10^{-4} 10^{-5} 10^{-6}

Schu S4 $\Delta feoB$' $\Delta fslA$

Schu S4 $\Delta feoB$' $\Delta fslA$

-*F. tularensis* siderophore
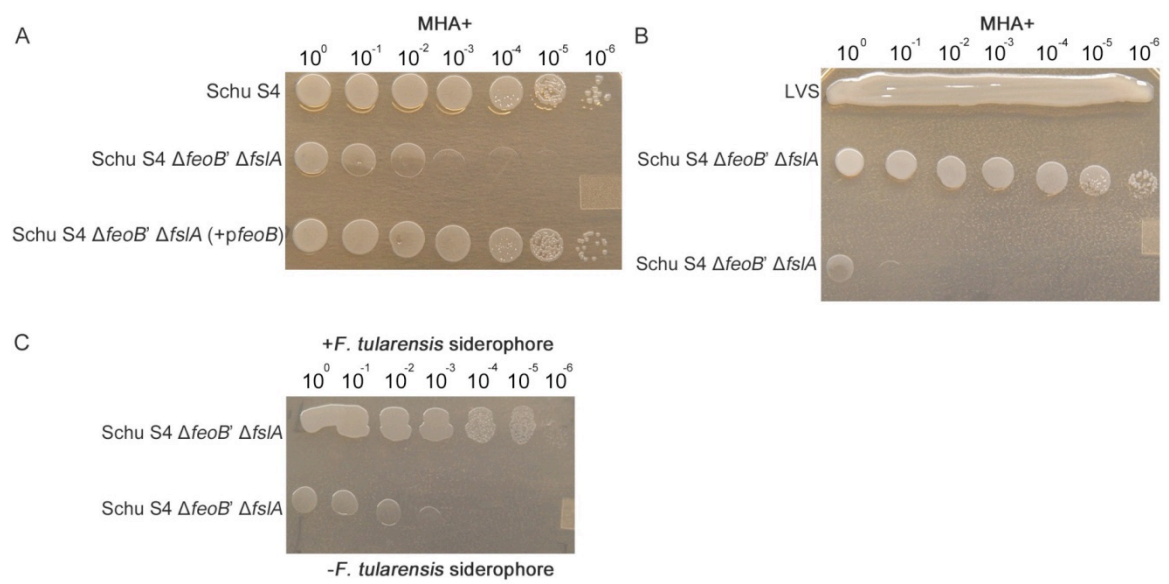
Figure 25: Intracellular replication capabilities of Schu S4 iron acquisition mutants.

Schu S4 and iron acquisition mutants were examined for their capabilities of intracellular replication in J774A.1 macrophages (**A**) and HepG2 hepatocytes (**B**). Frozen bacterial stocks were thawed and used at an MOI of 10 (**A**), and 100 (**B**). Tissue culture cells were lysed and plated on MHA agar at 2 and 24 hours post infection to determine bacterial load and intracellular replication capability, respectively. Purified *F. tularensis* siderophore was topically applied to MHA agar plates for Schu S4 Δ*feoB*' Δ*fslA* CFU/mL concentration determinations. Values were expressed as the means ± S.E. Significance calculations were made relative to Schu S4. **p<0.01, ***p<0.001.
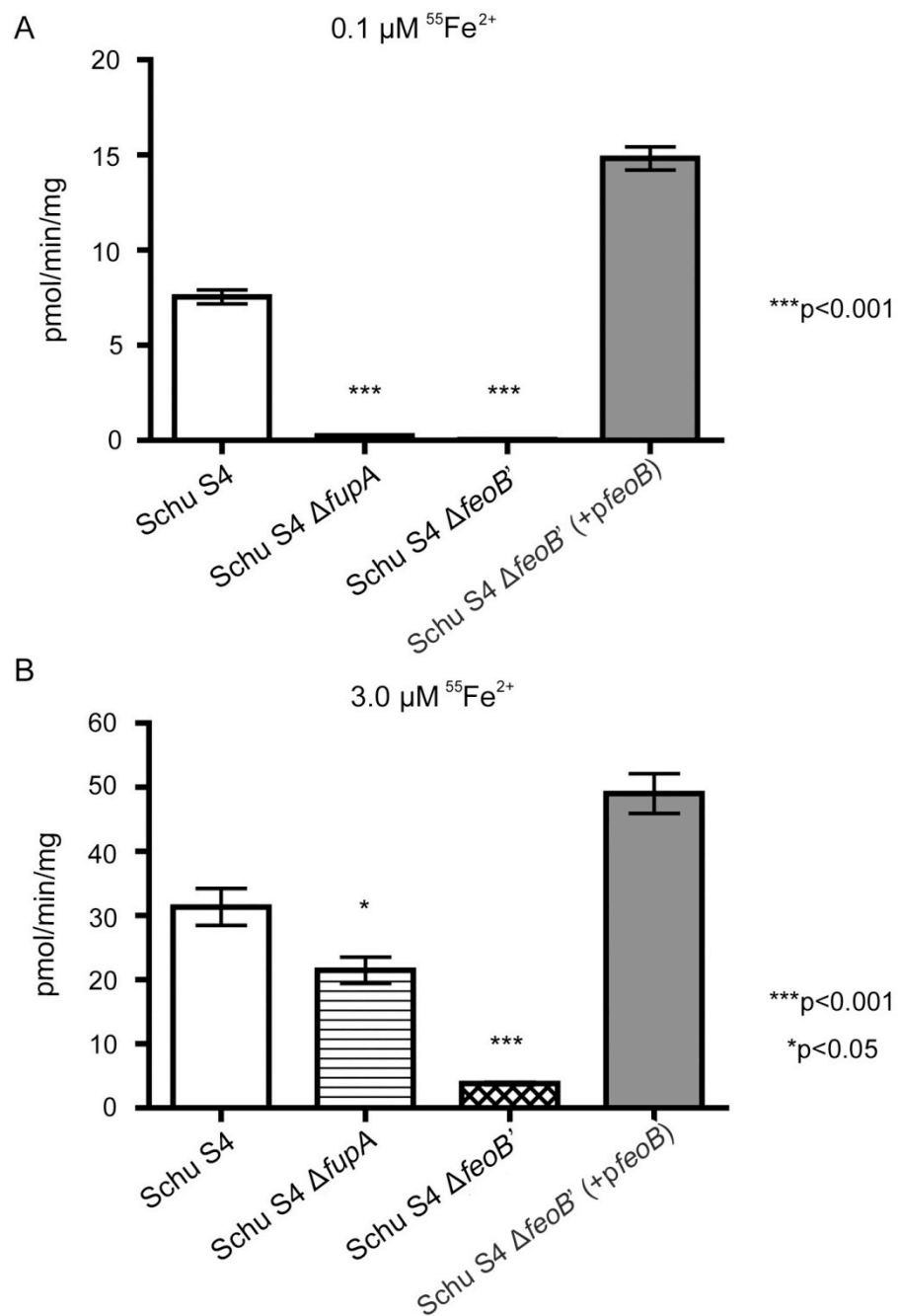
Figure 25

A

J774

Schu S4 (MOI 26)
Schu S4 Δ*fslA* (MOI 20)
Schu S4 Δ*feoB'* (MOI 14)
Schu S4 Δ*feoB'* Δ*fslA* (MOI 25)

***p<0.001

B

HepG2

Schu S4 (MOI 140)
Schu S4 Δ*fslA* (MOI 120)
Schu S4 Δ*feoB'* (MOI 80)
Schu S4 Δ*feoB'* Δ*fslA* (MOI 105)

**p<0.01
***p<0.001

138
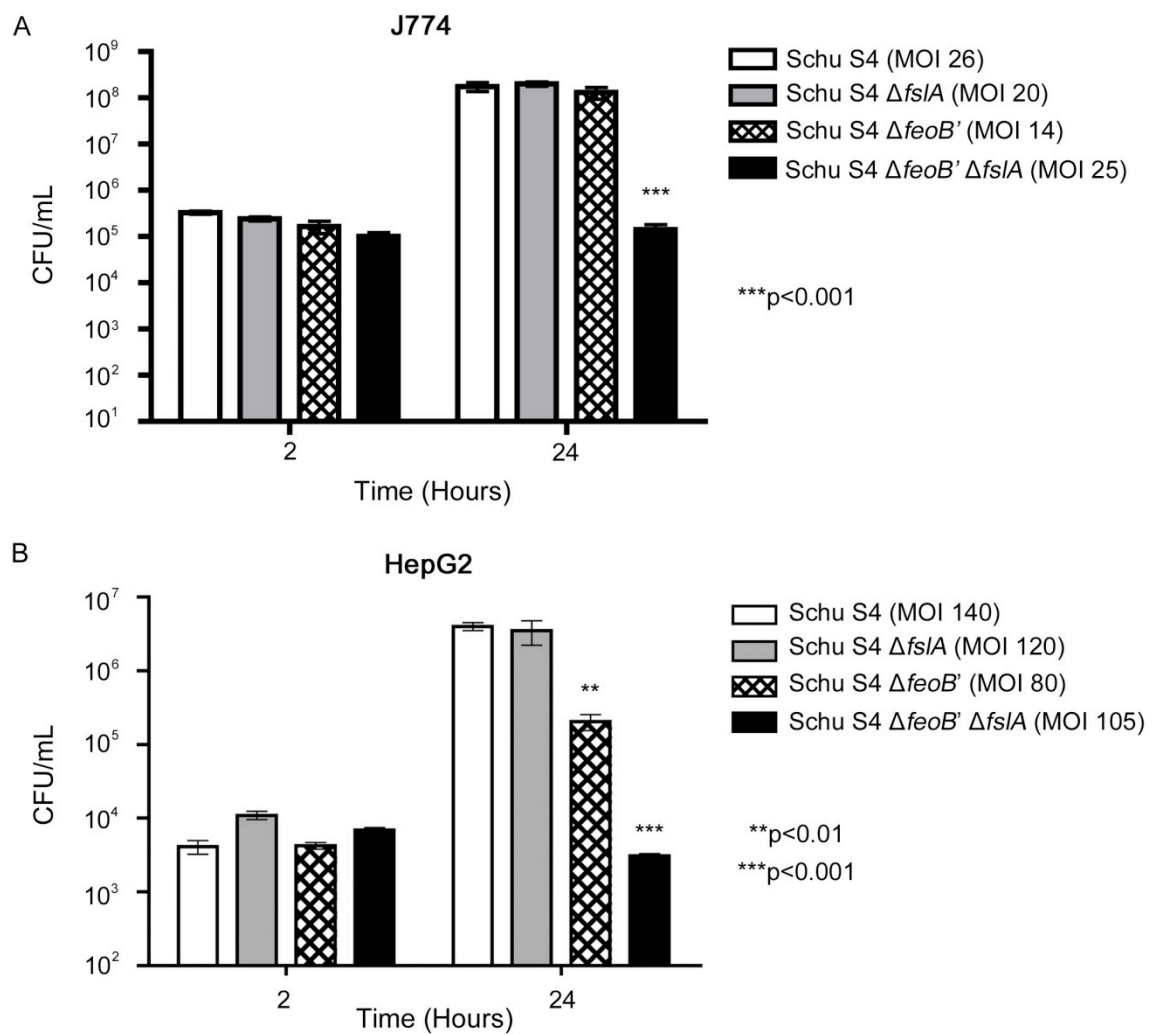
Figure 26: Schu S4 Δ*feoB'* Δ*fslA* is attenuated for virulence.

Three groups of C57BL/6 mice were used to study the virulence of Schu S4 iron

acquisition mutants. Frozen stocks of Schu S4, Δ*feoB'*, and Δ*feoB'* Δ*fslA* strains

were thawed and 25 CFU was administered by subcutaneous route. The CFU

determination was accomplished by plating on MHA+ and additional purified *F.*

tularensis siderophore for the Schu S4 Δ*feoB'* Δ*fslA* mutant. Survivors were

challenged with a lethal dose (25 CFU) of Schu S4.

Figure 26
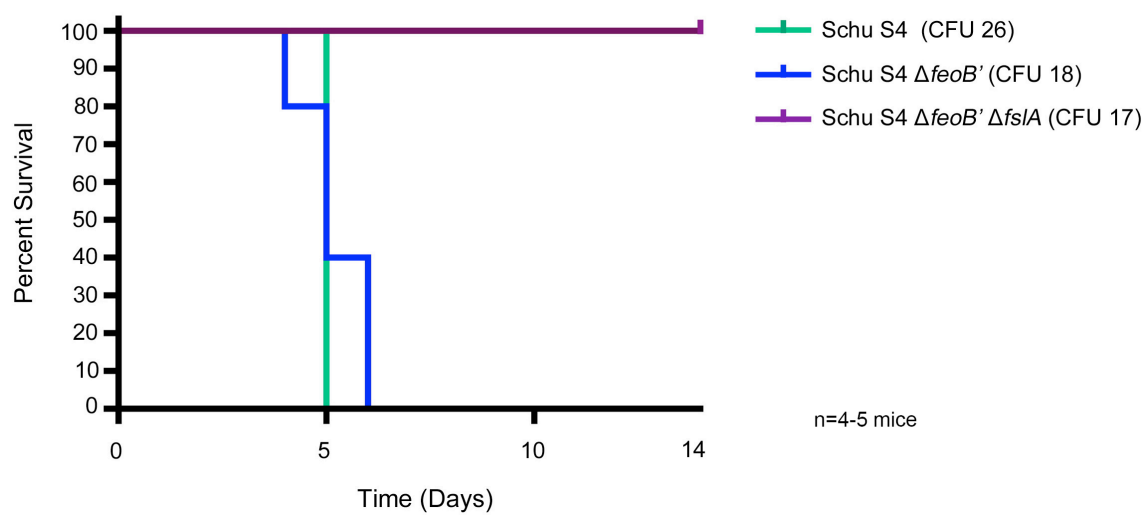
Plot legend:
- Schu S4 (CFU 26)
- Schu S4 Δ*feoB'* (CFU 18)
- Schu S4 Δ*feoB'* Δ*fslA* (CFU 17)

n=4-5 mice

Y-axis: Percent Survival (0, 10, 20, 30, 40, 50, 60, 70, 80, 90, 100)

X-axis: Time (Days) (0, 5, 10, 14)

Appendix The *F. tularensis* siderophore locus (*fsl*) contains all the necessary genes for siderophore biosynthesis and siderophore export

A.0 Abstract.

Siderophores are low molecular mass ferric iron chelators that are synthesized and secreted during iron limitation by both fungi and bacteria. Siderophores are used as a nutritional acquisition tool for bacteria and fungi; however, siderophores can also serve as virulence determinants necessary for pathogens to survive within the host environment. In contrast to some bacterial pathogens, *F. tularensis* expresses only one siderophore which has been purified and identified to be similar in structure to the fungal siderophore rhizoferrin. The *F. tularensis* ferric-siderophore system is predicted to be encoded in the *fslABCDEF* locus and is under the transcriptional control of the ferric uptake regulator (Fur). The analysis of *F. tularensis* siderophore biosynthetic pathway described in this section is based on genetic studies done on LVS Δ*fslA,* LVS Δ*fslC,* and LVS Δ*fsl* in-frame deletion mutants and complements. Siderophore production and secretion were evaluated by CAS assay, bacterial growth under iron limitation in liquid media, and agar plate bioassays. These mutants helped delineate that the *fslA* and *fslC* genes were necessary for siderophore biosynthesis. In addition, the *fslA, fslB,* and *fslC* complementation studies done with LVS Δ*fsl* corroborated the mutant results for siderophore biosynthesis and revealed the genes necessary for export. This work summarizes the results that contributed to the identification of the *fsl* operon genes required for *F. tularensis* siderophore biosynthesis and transport during iron limitation.

A.1 Introduction:

Siderophores are low-molecular mass microbial compounds with very high affinity for ferric iron. These compounds have various iron-binding ligands, which can include hydroxamate, catecholate, and α-hydroxycarboxylate ligands [16]. These siderophore ligands satisfy the six-coordination sites on ferric iron [16]. Bacteria typically encode a variety of siderophores to meet the iron nutritional needs in different niches, including the iron-limiting environment of the host. Siderophores are secreted into the environment, bind ferric iron, and are acquired through specific membrane receptors. While most bacteria generate and acquire their own siderophores, some bacteria avoid siderophore biosynthesis and utilize siderophores secreted from neighboring bacteria [33–35]. The transcription of siderophore biosynthesis genes is tightly regulated in order to restrict the production and secretion of siderophore to conditions of iron limitation [16]. The production, secretion, and uptake of siderophores are energy costly. Over-expression of siderophores during iron-replete conditions may cause a variety of detrimental effects including potentially chelating iron from bacterial enzymes or providing an overabundance of iron that can result in hydroxyl radical production.

Siderophores have also been implicated as virulence factors in various pathogens including *Bacillus anthracis* [51], *Mycobacterium tuberculosis* [49,50], *Escherichia coli* [133], *Yersinia pestis* [126], *Campylobacter jejuni* [23], and *Pseudomonas aeruginosa* [124]. In *P. aeruginosa,* siderophores were shown to regulate their own production as well as other necessary virulence factors [134,135].

To counter the use of siderophores, the mammalian immune system produces siderocalin (also referred to as neutrophil gelatinase associated lipocalin or lipocalin) [136], which is known to target and sequester catechol siderophores such as enterobactin in order to starve bacteria of iron [136]. Bacteria that produce enterobactin such as *E. coli, Salmonella enterica* serovar *typhimurim,* and *Klebsiella pneumoniae* counter this host defense by altering their siderophores through glycosylation to produce salmochelins; this altered structure is not recognized by siderocalin [137,138]. *B. anthracis* produces two siderophores: bacillibactin and petrobactin. Bacillibactin is targeted by host siderocalin but petrobactin is considered a "stealth" siderophore that evades siderocalin and is a virulence factor [139].

Hallman and Mager (1964), identified a growth initiation substance (GIS) in the supernatant of *Francisella* (previously named *Pasturella tularensis*) [74] that was found to promote bacterial growth. A siderophore purified from *F. tularensis* grown under iron limiting conditions [71,75] is predicted to be the GIS initially discovered by Mager's group. This siderophore was confirmed by mass spectrometry to have the same configuration as the α-hydroxycarboxylate siderophore, rhizoferrin (Figure 2) [75], and consists of two citrate molecules linked by amide bonds to a putrescine backbone.

The *F. tularensis fslABCDEF* locus contains genes encoding proteins predicted to be required for siderophore biosynthesis and export (Figure 3) [75], (also designated *figABCDEF* [71]), and is conserved in the *F. tularensis* strains Schu S4 and LVS and the *F. novicida* strain U112 [71]. Siderophore production is

similar between the three strains, however, they use different mechanisms for uptake [98]. Amino acid sequence analysis revealed FslA to belong to the non-ribosomal peptide synthetases (NRPS)-independent (NIS) family of siderophore synthetases [75]. The NIS synthetases require ATP to catalyze the formation of an amide bond between a carboxylic acid and an amino group [26,28]. *F. tularensis* requires *fslA*, the predicted NIS synthetase [75], for siderophore production in culture supernatants as determined by the universal colorimetric Chrome Azurol S (CAS) assay developed by Schwyn and Neilands [108]. Related siderophore synthetase genes were found in loci necessary for biosynthesis of *Corynebacterium diphtheriae's* siderophore, corynebactin [140] and *Staphylococcus aureus's* siderophore, staphyloferrin A [141,142]. Corynebactin and staphyloferrin A are classified as α-hydroxycarboxylate siderophores and are structurally similar to rhizoferrin except that their backbones consist of lysine and ornithine, respectively.

Amino acid sequence searches suggested that FslC is a PLP dependent decarboxylase that potentially functions in siderophore biosynthesis. Amino acid sequence analysis also indicated that the proteins FslB and FslD are most similar to inner membrane resistance-associated permeases/efflux transporter proteins of the major facilitator superfamily (MFS). MFS proteins have been shown to transport siderophores through the inner membrane of some Gram-negative bacteria including *Legionella pneumophila* and *Acinetobacter baumannii* [16,94,95,143]. FslB is predicted to export the siderophore to the periplasm, from where the siderophore is secreted out into the environment through an unknown

outer membrane protein. Once iron is bound, the ferric-siderophore complex is recognized by the siderophore receptor FslE that allows for siderophore entry. Unpublished results from our lab have delineated that FslE and FslD are required for utilization of ^{55}Fe-siderophore.The predicted model for *F. tularensis* siderophore biosynthesis and export is shown in Figure 27.

Halmann and Mager 1967 and our unpublished work showed that ^{14}C-ornithine precursor was incorporated into the *F. tularensis* siderophore under iron limiting conditions [144]. Ornithine and citrate are products of bacterial metabolism and are the likely precursors for siderophore biosynthesis. The predicted model for *F. tularensis* siderophore biosynthesis requires FslA and FslC to synthesize the siderophore in the bacterial cytoplasm in one of three potential siderophore biosynthetic pathways (Figure 28). In the first pathway (Figure 28, 1), FslC catalyzes the decarboxylation of ornithine to putrescine and FslA catalyzes the condensation of putrescine and two citrate molecules to form the final *F. tularensis* siderophore product. In the second pathway (Figure 28, 2), FslA catalyzes the amide bond formation between ornithine's free amine group and citrate to form intermediate I. Decarboxylation of the carboxyl group frees the amine group to produce intermediate II and allows for the final catalytic reaction with FslA and citrate to produce the siderophore. The third pathway (Figure 28, 3) branches off from intermediate I with amide bond formation with another citrate molecule thus producing intermediate III. Intermediate III structure is similar to the *S. aureus* siderophore, staphyloferrin A [145,146]. From intermediate

III, FslC catalyzes the decarboxylation of the ornithine backbone to putrescine thus producing the final *F. tularensis* siderophore product.

We attempted to express and purify FslA and FslC (data not shown); these attempts were modeled after studies by Berti and Thomas (2009) that focused on the expression and purification of the achromobactin siderophore NIS synthetases: AcsC (Type B), AcsA (Type C) and AcsD (Type A) [147]. We planned to also purify FslC in the same manner as the PLP-dependent decarboxylase purified from *Methanococcus jannaschii,* which has also been successfully expressed and purified [148]. The LVS *fslA* and LVS *fslC* genes were cloned individually into the expression plasmids pHIS-parallel and pGST-parallel. The individual plasmids were then introduced into Rosetta (DE3) *Escherichia coli* (Novagen) by transformation and grown to exponential phase, and protein expression was induced. The recombinant FslA and FslC proteins were both expressed with a 5' his$_6$-tag and 5' gst-tag and then purified by affinity chromatography. Recombinant proteins were analyzed on SDS PAGE by Coomassie staining and Western blot for purity. The proteins purified in this manner were rapidly degraded, indicating that special strategies may be required to reconstitute *F. tularensis* siderophore biosynthesis *in vitro.*

The siderophore biosynthetic pathway for the rhizoferrin or its enantiomer has not been determined to date. However, the related siderophore, staphyloferrin A, which contains an ornithine backbone flanked by two citrate molecules has been delineated [142]. Our studies on the biosynthetic pathway of *F. tularensis* siderophore were based on the *fsl* strains: LVS Δ*fslA,* Δ*fslC,* and Δ*fsl*

146

in-frame deletion mutants and complements, and reconstitution of siderophore

biosynthesis *in vitro* with plasmids containing wild-type copies of the *fsl* genes.

The work discussed in this section helped determine the *F. tularensis* genes

required for siderophore biosynthesis and export.

A.2 Results

F. tularensis growth on iron rich and iron limiting agar plates

An in-frame deletion of *fslC,* LVS Δ*fslC,* was generated through a two-step

mutagenesis procedure that was previously described for the LVS Δ*fslA* mutant

[75]. Growth of ten-fold serially diluted wild-type LVS and the *fsl* mutants were

compared on ferrous iron supplemented MHA+ (top) and iron limiting CDM-Fe

plates (bottom) (Figure 29). LVS on CDM-Fe is capable of growing only to 10^{-2}

dilution. This growth phenotype of LVS is different than the *F. tularensis* subsp.

tularensis strain Schu S4, which is capable of growing out to single colonies on

iron limiting CDM-Fe agar plates. The inability of LVS to grow to single colonies

on CDM-Fe is potentially due to a non-iron related nutrient limitation that is not

observed with iron replete MHA+. The LVS Δ*fslA* and LVS Δ*fslC* mutants were

capable of growing out to single colonies on iron rich media like wild-type LVS.

On iron limiting CDM-Fe plates, all the strains grew out to the 10^{-2} dilution but

were unable to grow out to single colonies. These observations demonstrate that

LVS Δ*fslA* and LVS Δ*fslC* mutants are not defective for growth on iron rich MHA+

agar.

Liquid growth of *F. tularensis*

In order to define growth differences in liquid culture, wild-type LVS, LVS Δ*fslA*

and LVS Δ*fslC* growth curves were determined under iron limiting (0.125 µg/mL,

0.168 µM) and iron replete (2.5 µg/mL, 3.36 µM) liquid CDM (Figure 30).

Bacterial cultures were grown overnight in chelex-treated CDM (che-CDM)

supplemented with limiting iron in order to deplete bacterial internal iron stores.

All strains displayed similar growth curves in high iron, thus demonstrating the ability to obtain iron and grow in iron replete conditions even with the loss of the *fslA* and *fslC* genes. Under iron limiting conditions, there was a growth defect in LVS Δ*fslA* as previously demonstrated [75]. LVS Δ*fslC* mutant showed a different slope than wild-type, demonstrating a slower growth rate early in the course of the growth curve. We presume that the LVS Δ*fslC* mutant is inefficient at iron acquisition initially which affects liquid growth; however, the LVS Δ*fslC* mutant eventually obtains the same end biomass as wild-type LVS.

Detection of siderophore production by the CAS assay

The Chrome Azurol S assay (CAS) is a general assay developed by Schwyn and Neilands [108] used to measure the presence of siderophore. LVS, LVS Δ*fslA*, and LVS Δ*fslC* were grown in iron limiting che-CDM overnight and then washed with che-CDM prior to inoculation into high or low ferric iron che-CDM conditions. Bacterial cultures were allowed to grow overnight and their supernatants were collected after centrifugation. In high iron, as expected, all three strains were defective for siderophore production as assessed by Specific CAS activity, which is the level of CAS activity normalized to optical density of bacteria (OD_{600}) (Figure 31). The *F. tularensis* siderophore is secreted only under iron limiting conditions [75] (Figure 31A and 31B) or in the absence of the ferric uptake regulator, Fur [82]. Culture supernatants from LVS Δ*fslA* and LVS Δ*fslC* strains grown in iron-limiting CDM conditions did not have any Specific CAS activity. Complementation of the LVS Δ*fslC* mutant with a plasmid containing a wild-type *fslC* gene restored the production of siderophore, as has been previously

demonstrated for the complementation of the LVS Δ*fslA* mutant with a wild-type copy of the *fslA* gene [75]. Under iron limiting conditions, *F. tularensis* requires the dual action of *fslA* and *fslC* for *F. tularensis* siderophore biosynthesis.

F. tularensis agar plate bioassays

Siderophore plate bioassays were used to evaluate siderophore production and siderophore utilization [75,98] of wild-type LVS, LVS Δ*fslA* and LVS Δ*fslC* strains (Figure 32). Strains were grown in iron limiting liquid che-CDM overnight, serially diluted to a dilution that does not support growth (10^{-3}) and LVS (Figure 32, left) and LVS Δ*fslC* (Figure 32, right) were spread over CDM-Fe plates. Donor strains (LVS, LVS Δ*fslA*, and LVS Δ*fslC*) were spotted on both LVS and LVS Δ*fslC* seeded plates in order to determine whether they had the capability to promote growth of seeded strains. LVS was able to secrete siderophore and promote growth of the seeded LVS and LVS Δ*fslC* strains, while the LVS Δ*fslA* mutant was unable to secrete siderophore and no growth halos were detected on either seeded plate. The LVS Δ*fslC* mutant promoted the growth of LVS and LVS Δ*fslC* seeded strains but with a severely reduced capability compared to wild-type LVS. Since the LVS Δ*fslC* mutant was shown to be defective in siderophore production in liquid (Figure 31), this growth promotion of seeded bacteria may be due to the secretion of a siderophore "intermediate" that is not detected by the CAS assay. From these bioassay studies, we can conclude that the LVS Δ*fslC* strain is capable of receiving wild-type siderophore from LVS. It may also be able to secrete a putative siderophore "intermediate" that has limited growth potentiating capabilities on CDM-Fe agar.

150

F. tularensis intracellular replication within *ex vivo* host cells

The siderophore may be important for iron acquisition by *F.* tularensis within the intracellular niche. To test the role of siderophore during infection, the ability of LVS and *fsl* biosynthesis mutants to enter and replicate within J774A.1 murine macrophages and A549 alveolar epithelial cells was assessed (Figure 33). LVS, LVS Δ*fslA*, and LVS Δ*fslC* were incubated with tissue culture cells at MOIs of 10 and 100 for J774A.1 (Figure 33A) and A549 (Figure 33B), respectively. Tissue culture cells were lysed at 2 hours post infection for J774A.1 (Figure 33A) or 3 hours post infection for A549 (Figure 33B) to determine the initial entry capabilities and 24 hours post infection for replication and growth. LVS siderophore deficient strains LVS Δ*fslA* and LVS Δ*fslC* mutants were not defective for entry or intracellular replication in either cell type. These results demonstrate that an alternative iron acquisition mechanism is available for LVS, LVS Δ*fslA*, and LVS Δ*fslC* to utilize within these tissue culture cell lines.

LVS Δ*fsl* complementation studies demonstrate the necessity of *fslABC*

We have shown that both FslA and FslC are required for siderophore production in culture supernatants through the CAS assay. The *fsl* operon encodes two predicted MFS proteins, FslB and FslD. Results from our lab indicated that FslD is involved in siderophore-mediated iron uptake by the bacteria (Ramakrishnan unpublished). We considered the possibility that FslB is required for export of the siderophore and developed a complementation assay to test this. An in-frame deletion of the *fslABCDEF* locus (LVS Δ*fsl*) was generated with the two-step mutagenesis procedure that was previously described for the LVS deletion

mutants. Growth of the LVS Δ*fsl* strain was compared to wild-type LVS and LVS

Δ*fslA*. There were no observed deficiencies on growth on agar or in liquid culture

(data not shown) or on MHA+/- plates (Figure 34). LVS Δ*fsl* was complemented

with high copy plasmids containing combinations of the *fsl* genes: *fslAC, fslAB,*

and *fslABC* (Figure 35). Specific CAS activities of spent supernatants from LVS

Δ*fsl* complements were compared to LVS strains containing empty vectors (+V)

and wild-type LVS grown under iron limitation (LVS Low-Fe). Only the LVS Δ*fsl*

(+ p*fslABC*) strain was capable of secreting siderophore, and the levels in the

supernatant were high even after growth in iron-replete media.

A.3 Discussion

The wild-type strains of *F. tularensis* subsp. *holarctica* (LVS) and *F. novicida*
(U112) are able to grow in low iron *in vitro* due to their ability to secrete
siderophore, while the Δ*fslA* mutants of these strains were unable to grow under
the same conditions [71,75]. The Δ*fslC* mutant of U112 is also unable to grow in iron
limited liquid conditions [85] while our LVS Δ*fslC* strain initially displays a slower
growth rate but ultimately reaches the same density as wild-type LVS (Figure
30). It is interesting to note that these differences in growth are only seen in liquid
cultures. The delayed growth phenotype of the LVS Δ*fslC* mutant in low iron
(0.168 µM) *in vitro* may be due to the slow secretion of the siderophore
intermediate that was seen in the siderophore plate bioassays (Figure 32). The
delay followed by recovery also suggests that the bacteria may transition to
utilize the Feo system over time which corresponds with the bacteria's ability to
reach wild-type LVS density. While ferric iron is the dominant iron form in aerobic
environments, there is ferrous iron present in limiting quantities as well. The slow
growth rate of the LVS Δ*fslC* mutant may be due to the limiting quantities of
ferrous iron in the low iron che-CDM environment thus postponing the transition
to the Feo iron acquisition system. Attempts to confirm the presence of the
predicted siderophore intermediate from iron starved LVS Δ*fslC* supernatants by
mass spectrometry where unsuccessful (data not shown); this is potentially due
to low siderophore intermediate yield from the mutant, and also the
intermediate's low affinity to the columns that were tested and its subsequent
loss during the purification protocol.

Interestingly, intracellular replication assays within J774A.1 [71] demonstrated a difference between the U112 and LVS strains. There was a defect in growth of the U112 Δ*figA* (Δ*fslA*) strain at the 24-hour time point while no defect was observed in this study for intracellular replication with the LVS Δ*fslA* mutant (Figure 33 and Figure 11) or the Schu S4 Δ*fslA* mutant (Figure 25) in J774A.1. This may represent differences in the capabilities of *F. tularensis* strains LVS and Schu S4 to utilize the other iron acquisition system, Feo, within this tissue culture cell line when devoid of the ferric-siderophore acquisition system. The *F. tularensis* Schu S4 *fslA* gene was found to have increased expression within primary murine macrophages, which suggests its importance in siderophore production in an intracellular environment [70]. Given these differences, it would be of interest to screen for changes in expression of genes associated with siderophore biosynthesis and secretion to help discern this discrepant result between LVS and U112.

Within bone marrow derived macrophages (BMM) [70] Schu S4 did reveal differences in expression of the genes located within the *fsl* locus. It is of interest to note that genes associated with polyamine metabolism/biosynthesis were also up-regulated. These include spermidine synthase (FTT0431) and arginine decarboxylase (FTT0432) [70], which are important enzymes involved in polyamine production through the catabolism of L-arginine and spermidine [70]. This is of interest since polyamines are found in a variety of siderophore structures including putrescine within the *F. tularensis* siderophore [75].

154

FslA and FslC are required for siderophore biosynthesis as determined by the CAS assay and FslB is required for siderophore as determined by complementation of the LVS Δ*fsl* locus. Of the three potential biosynthetic pathways proposed for the *F. tularensis* siderophores, we believe that the second pathway (Figure 28, 2) aligns best with the data presented. Starting with ornithine and citrate the FslA synthetase catalyzes the amide bond formation between ornithine's free amine group and citrate to form intermediate 1. This intermediate we predict to be the siderophore intermediate secreted in the LVS Δ*fslC* bioassays (Figure 32). The intermediate lacks a citrate molecule and it is expected to have a lower affinity for iron and may not be taken up as well by the bacteria. This inefficiency in growth suggests that less ferric iron would be acquired by the cell during exponential growth phase which would result in the slower growth rate with this mutant relative to LVS. The decarboxylation of the carboxyl group frees the amine group to produce intermediate II and allow for the final catalytic reaction with FslA and citrate to produce the siderophore. The third pathway (Figure 28, 3) is the least likely to occur due to the formation of the intermediate III after intermediate I. Intermediate III is the *S. aureus* siderophore, staphyloferrin A [145,146]. Staphyloferrin A is a CAS positive molecule [145] and would have been detected in the supernatant of the Δ*fslC* mutant.

Precursors to siderophore biosynthesis arise from bacterial products, especially those proceeding from aerobic metabolism including the citric acid cycle [25]. Some bacterial siderophores including agrobactin and parabactin contain polyamines within their structure [149]. *F. tularensis* siderophore contains

the polyamine putrescine as its backbone. Polyamines are positively charged molecules that are essential for eukaryotic and prokaryotic functions including DNA replication, protein synthesis, and protein modification [149]. Polyamines are important for maintenance of DNA transcription and translation of proteins [149,150] and for normal bacterial metabolism especially within the citric acid cycle and for arginine biosynthesis. To maintain intracellular homeostasis, polyamines are regulated to limit positive charge intracellularly. They are thus regulated both at the level of transcription and by feedback inhibition of enzymes including ornithine decarboxylase (ODC) at the post-translational level [150]. *F. tularensis* is capable of sensing, reacting, and utilizing the intracellular metabolites of the host cell. *F. tularensis* has been shown to recognize the polyamine precursor spermine [151] and to require spermidine for growth in the chemically defined media [117].

The components of *F. tularensis* siderophore come from bacterial metabolism and potentially from the cytoplasm of the host. In all, from the complementation of the Δ*fsl* locus with the *fsl* genes, we've confirmed (Figure 27), that FslA and FslC are required for siderophore biosynthesis and further need the MFS protein FslB to export the siderophore into the environment. This iron acquisition system is conserved between the *F. tularensis* subspecies and related *F. novicida* species thus demonstrating an effective and necessary siderophore for optimal growth and survival.

A.4 Experimental Methods

Media

Francisella tularensis subspecies *holarctica*, live vaccine strain (LVS) was received from K. Elkins (CBER). Liquid cultures were grown in liquid Chamberlin's defined media (CDM) [117] at 37°C with shaking. Liquid growth under iron limitation was achieved in chelex-100 treated CDM (che-CDM) supplemented with $MgSO_4$ (0.55 nM), $CaCl_2$ (5 µM) with the addition of low (0.125 g/mL, 0.168 µM) or high ferric iron (2.5 µg/mL, 3.36 µM). Growth was monitored by optical densitometry at 600 nm (OD_{600}) with a plate reader (BioTek ELx800). Growth in low and high che-CDM liquid was examined with bacteria cultures grown to exponential phase, washed three times with che-CDM (with no additional iron added) and inoculated at an OD_{600} of 0.01. Bacteria stocks used for intracellular replication assays were grown in iron limiting che-CDM and frozen at exponential stage of growth. Stocks were stored in -80°C and titers were determined prior to use. All strains were maintained on modified Muller Hinton agar (MHA) and supplemented with 2.5% horse serum, 1% glucose, 0.1% cysteine, and either ferric pyrophosphate (FePPi) or ferrous sulfate ($FeSO_4$, 2 µg/mL) and grown at 37°C under aerobic conditions. Iron limiting agar (CDM-Fe) was prepared by the addition of agar to CDM and no additional iron salts. For complementation of LVS mutants, liquid and agar media were supplemented with kanamycin (15 µg/ml).

Escherichia coli strain MC1061.1 (*araD*139 Δ(*ara-leu*)7696 *galE*15 *galK*16 Δ(*lac*)X74 *rpsL* (Str^1) *hsdR2* (rK$^-$mK$^+$) *mcrA mcrB1 recA*) was received from Chang Hahn (University of Virginia) and was used for cloning. *E. coli* was maintained on Luria broth and agar plates with the addition of ampicillin, 50 µg/mL and 100 µg/mL respectively.

Growth of ten-fold serial dilutions on plates

Bacterial strains were grown to mid-log phase overnight at 37°C with shaking. Cultures were then were washed in che-CDM, adjusted to an OD_{600} of 1 and ten-fold serially diluted in che-CDM to the 10^{-6} dilution. Five microliters of each dilution was spotted onto iron limiting CDM-Fe plates and MHA plates supplemented with or without FePPi. Plates were incubated for four days at 37°C in aerobic conditions.

Generation of LVS mutants and complements

All LVS deletion mutants were generated with a two-step mutagenesis procedure used previously to generate the LVS Δ*fslA* mutant [75]. Respective suicide vectors were introduced into LVS through electroporation. LVS was grown in 5 mL of CDM overnight till culture reached mid-log phase of growth. The OD_{600} was determined, cultures were spun at 10,000 rpm for 8 minutes, and the cells were washed three times in 0.5 M sucrose to remove excess salts. Cells were electroporated with a Bio Rad Gene Pulser II Electroporation System set at 2.5 kV, 600 ohms resistance, and 10 µF conductance in 0.1 cm cuvettes (Bio Rad).

Cells were then incubated in rich media (TSB/c) for 4-6 hours and then plated on MHA ($FeSO_4$) supplemented with kanamycin.

To generate an inframe *fslC* mutant a suicide vector, pJOSH (~11 kb) was derived from pGIR463 [82], a derivative of the pUC plasmid, pSL1180 [120]. The plasmid pGIR463 contains a *Bacillus subtillis sacB* gene, an ampicillin resistance marker, and restrictions sites for the insertion of DNA fragments of interest. The 5' and 3' flanking regions of *fslC* were amplified from LVS genomic DNA using the primers F154/F155 and F156/F157 with Fast Taq High Fidelity DNA polymerase (Roche), respectively. The 5' (1.8 kB) and 3' (2 kB) regions were ligated into pGIR463 as NheI-BspEI and BspEI-SacI fragments, respectively, to generate the plasmid pJOSH. This plasmid was introduced into LVS by electroporation and selected on MHA plates supplemented with kanamycin. An isolate with the plasmid integrated into the 3'-flanking region was confirmed with PCR (F140/ F134 and F133/F165). Following isolation on MHA with sucrose, the presence of the in-frame deletion in the LVS Δ*fslC* mutant (GR44) was determined through PCR.

The suicide vector, pRJ24 was derived from the plasmid pGIR463 and was used to generate an inframe *fsl* deletion mutant in LVS. The downstream 3' flanking region of *fslF* (1.8 kB) was amplified using LVS genomic DNA (F321/F322) with Fast Start Hi Fidelity Taq (Roche). The fragment was digested and ligated into BspEI and NotI restriction sites of pGIR463. The upstream 5' flanking region of *fslA* (1.8 kB) was then PCR amplified from LVS genomic DNA with the primers F424/F425 with Fast Start Hi Fidelity Taq (Roche) and cloned as

159

a NheI-NotI fragment to generate pRJ24. pRJ24 was introduced into LVS

through electroporation and plated on MHA with kanamycin. Primers F161/F327

were used to determine that the plasmid integrated in the 3'-flanking region of

fslF. Selection on MHA with sucrose was used to promote removal of the suicide

vector containing the *fsl* locus. The LVS Δ*fsl* locus mutant (GR47) was confirmed

with PCR using the primer set F107/ F187.

LVS Δ*fslC* was complemented with a high copy plasmid pFNLTP6 [121]

containing a wild-type LVS copy of *fslC.* The *fslC* gene was amplified with

primers F336 and F337 and the PCR fragment was ligated into pFNLTP6 at

EcoRI and BamHI sites to generate plasmid pNMP028. pNMP028 was

electroporated into LVS Δ*fslC* and was maintained on MHA supplemented with

kanamycin.

LVS Δ*fsl* mutants were complemented with the high copy plasmid,

pFNLTP6 [121] containing wild-type *fsl* genes. To generate the complementing

plasmids: pFNLTP6_*fslAC*, pFNLTP6_*fslAB*, and pFNLTP6_*fslABC,* the plasmid

pGIR458 [75] was used which contains a wild-type copy of Schu S4 *fslA* cloned in

pFNLTP6*.* To generate pFNLTP6_*fslAC, fslC* was amplified with primers F440

and F441 and ligated into pGIR458 at SacI and BamHI sites to generate

pNMP096. To generate pFNLTP6_*fslAB, fslB* was amplified with primers F115

and F442 and ligated into pGIR458 at NotI and SacI. To generate

pFNLTP6_*fslABC, fslBC* was amplified with primers F115 and F441 and ligated

into pGIR458 at NotI and BamHI sites. Cultures were grown in CDM

supplemented with kanamycin.

Detection of Siderophore:

The Chrome Azurol S (CAS) assay [108] is a colorimetric assay for determining the presence of a siderophore in liquid media or on agar plates. *Francisella* strains were grown in iron-replete (2.5 µg/ml FePPi) and iron-deplete (0.125 µg/mL FePPi) liquid media. Supernatants from late logarithmic cultures were tested for the presence of siderophore using the CAS solution (100 µL) and 2 µL of shuttle solution in wells of a 96-flat bottom well plate. Supernatant and CAS were incubated for 30 minutes at room temperature and absorbance was promptly detected at 630 nm (A_{630}) on a plate reader (BioTek Elx800). A reference blank with water was used to calculate CAS activity with the formula ((A_{630} water-A_{630})/A_{630} water). Specific CAS activity was normalized to bacterial cell density (OD_{600}) with the formula (CAS Activity/OD_{600}). All strains were tested in triplicate. CAS assays on Δ*fsl* complements were completed on strains grown in iron replete media.

Agar plate bioassays

Siderophore plate bioassays [75] were used to determine siderophore production and siderophore utilization of *F. tularensis* wild-type, Δ*fslA,* and Δ*fslC* mutants. Iron limiting agar plates (CDM-Fe) were seeded by spreading (100 µL) of wild-type (for siderophore production) or mutant strains (for siderophore utilization) at a dilution that could not support growth (10^{-3}) and allowed to dry. Siderophore donor strains were spotted (2.5 µL) on the seeded plates and are incubated for 2

to 4 days. The "halo" of colonies surrounding the donor strain indicates that the seeded strain can grow utilizing siderophore being produced by the donor strain.

Purification of *F. tularensis* siderophore

F. tularensis siderophore resembles the structure of rhizoferrin [75]. The procedure for identifying and purifying *F. tularensis* siderophore was as described in Sullivan *et al.* (2006). The supernatant of LVS culture grown in iron limiting che-CDM was run through a series of columns to purify *F. tularensis* siderophore. The supernatants were first passed through: XAD-2 (Amberlite) methanol-activated beads, and then cation-exchange Dowex 50W-X8 beads. After adjusting the pH to 7 with sodium hydroxide, the extract was run on an anion exchange AG1-X8 formate column. After washing with water, *F. tularensis* siderophore was eluted with 1.5 M ammonium formate, lyophilized and resupended in MilliQ water. *F. tularensis* siderophore concentration was compared to deferoxamine standards in a Cu-CAS assay [118].

Intracellular growth assays

Bacterial intracellular replication was assessed in murine macrophage like cells J774A.1 (ATCC TIB-67) as previously described [98] and A549 human alveolar epithelial cells. J774A.1 cells were maintained in high glucose Dulbecco's modified Eagle's medium (DMEM) supplemented with 10% FBS and grown at 37°C with 5% CO_2 and split 1:10 per passage. A549 cells were maintained in DMEM F12 supplemented with 10% FBS and split 1:10 per passage. Tissue culture cells were counted with a hemocytometer and seeded at a concentration

of 2 x 10^5 cells per well in 24-well plates the day before the assay. Bacteria were

added at a multiplicity of infection (MOI) of 10 (J774A.1) or 100 (A549) into four

wells per group and plates were centrifuged at 950 x g for 10 minutes at room

temperature to promote bacterial invasion. Cells were incubated at 37°C for one

hour (J774A.1) or two hours (A549), washed twice with PBS and incubated with

50 μg/mL of gentamicin in DMEM+FBS for 1 hour at 37°C. Cells were washed

twice with PBS and lysed with 1 mL of water and pipetting at 2, 3, 7 and 24 hours

post infection. Lysates serially diluted in CDM and plated on MHA plates to

determine intracellular bacterial numbers as colony-forming units (CFU).

Intracellular replication assays were repeated three times to ensure consistency

in results.

A.5 Appendix Tables

Table 7. Strains in this study

Strain Description	Strain Name	Alternative Strain Name	Source
LVS	LVS	Wild-type	K. Elkins (CBER) [75]
LVS Δ*fslA*	GR7	-	
LVS Δ*fslC*	GR44	NMP021	This study
LVS + pFNLTP6 (+V)	GR58	NMP029	This study
LVS Δ*fslA* + pFNLTP6 (+V)	GR60	NMP030	This study
LVS Δ*fslC* + pFNLTP6 (+V)	GR84	NMP031	This study
LVS Δ*fslC* + pNMP028 (+p*fslC*)	GR83	NMP032	This study
LVS Δ*fsl*	GR47	NMP121	This study
LVS Δ*fsl* + pFNLTP6 (+V)	GR74	NMP128	This study
LVS Δ*fsl* + pNMP096 (+p*fslAC*)	GR71	NMP123	This study
LVS Δ*fsl* + pNMP098 (+p*fslAB*)	GR73	NMP127	This study
LVS Δ*fsl* + pNMP100 (+p*fslABC*)	GR72	NMP125	This study
GR7 + pNMP122 (+p*fslA*)	GR79	NMP135	This study

Table 8. Plasmids

Plasmid Description	Plasmid name	Source
pJOSH (suicide plasmid for in-frame deletion of *fslC*)	pJOSH	This study
pFNLTP6 (replicating plasmid vector with kanamycin resistance marker)	pFNLTP6	Tom Zahrt [121]
pGIR463_*suc_fsl* (suicide plasmid for the in-frame deletion of the *fslABCDEF* locus)	pRJ24	This study
pFNLTP6_+*fslC*	pNMP028	This study
pFNLTP6_+*fslAC*	pNMP096	This study
pFNLTP6_+*fslAB*	pNMP098	This study
pFNLTP6_+*fslABC*	pNMP100	This study
pFNLTP6_+*fslA*	pGIR458	[75]
pMP831_+*fslA*	pNMP122	This study
pUC plasmid pSL1180		[120]
pGIR457 (suicide plasmid for the inframe deletion of *fslA*)	pGIR457	[75]
pGIR458 (pFNLTP6 with *fslA*)	pGIR458	[75]

Table 9. Primers

Name	Sequence[2]
F156	5' ctactgtccggaCTCAGAGTTAGACAAACACATC 3'
F157	5' ctactggagctcTGCAGTTACATAATGTCCAAC 3'
F154	5' ctactggctagcTCTATACCTACTCTATGGTATAG 3'
F155	5' ctactgtccggaAACACTCTTTGAA 3'
F133	5' ctactgggatccATGTCTAAACTAAGCGATTCAAAG 3'
F165	5' GACAAAAGCGTTACCCAAAGAG 3'
F140	5' GGATATTTTAGCTGATATTGCTG 3'
F134	5' ctactggaattcATTGATGTGTTTGTCTAACTCTGAG 3'
F336	5'ctactggaattcAGGAATTAATAAATGTCTAAACTAAGC 3'
F337	5' ctactgggatccACCTATTATTATTGATGTGTTTGTC 3'
F440	5'ctactggagctcTTAAATCATCTAATTTTAAAAATAAGG 3'
F441	5' ctactgggatccTTATTGATGTGTTTGTCTAACTC 3'
F115	5' ctactggcggccgcTGTTAAATGCAAATCCTGTCG 3'
F442	5' ctactggagctcCTATTTAGACATTTATTAATTCC 3'
F441	5' ctactgggatccTTATTGATGTGTTTGTCTAACTC 3'
F321	5' ctactgtccggaGTTGGTGATATTGCTATAGAGC 3'
F322	5' ctactggcggccgcATGCTAAGAAAGTGATAG 3'
F424	5' ctactggctagcTTTGTGAAACAACCTTACCAACC 3'
F425	5' ctactgtccggaTCAGAAAAGCTGTTGTGAGATTG 3'
F161	5' ctactggctagcATAATTAGACTCTAAGTAC 3'
F327	5' GTTCCTGCTGAGATTCTGC 3'
F107	5' CATGCGCTGCAGGATGAACTG 3'
F187	5' TCAAAAACTGCCGTAGCACC 3'

---

[2] Uppercase letters signify sequences corresponding to genomic DNA.

A.6 Appendix Figures

Figure 27: Predicted model for *F. tularensis* LVS siderophore mediated iron uptake.

The model depicts the predicted roles of each of the Fsl proteins in siderophore synthesis and export. The FslA and FslC proteins synthesize the siderophore from the precursors ornithine and citrate. The siderophore is exported out of the cytoplasm through the inner membrane through FslB and out of the outer membrane through an unknown outer membrane protein (OMP). The siderophore receptor binds the ferric siderophore through the dual effect of FslE and FupA/B. FslD is required for transport of the ferric-siderophore through the inner membrane.
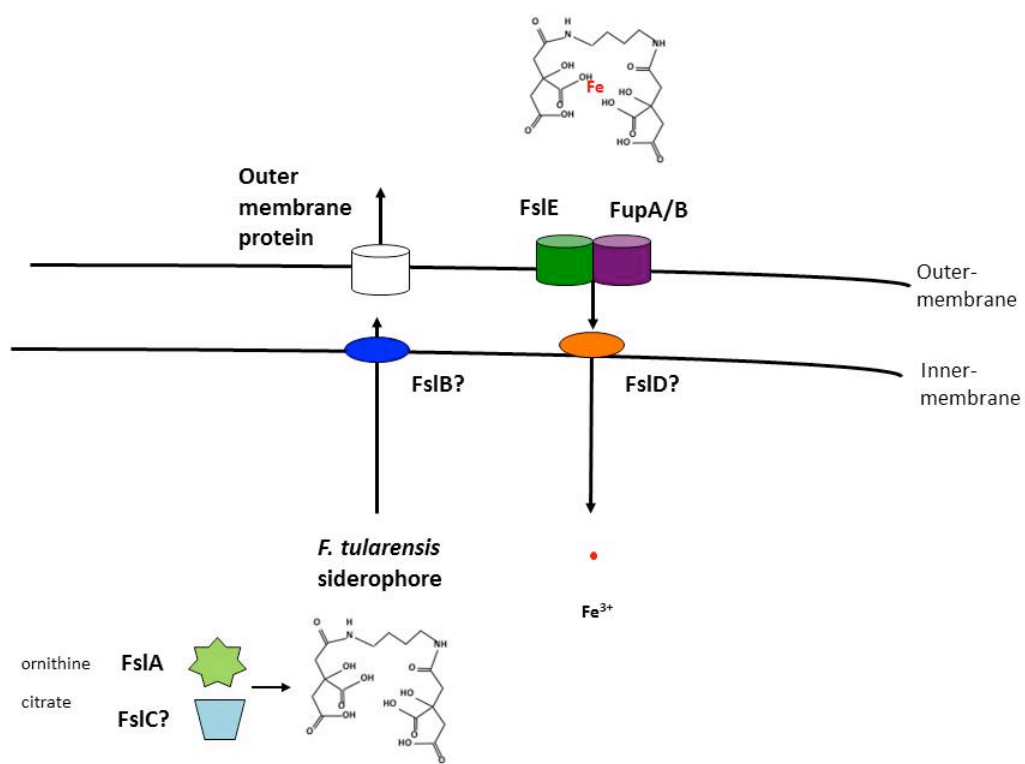
Figure 27

Figure 28: Predicted siderophore biosynthesis pathway.

There are three predicted pathways (1-3) that involve the precursors ornithine

and citrate acted upon by the *F. tularensis fsl* enzymes FslA and FslC to

synthesize the *F. tularensis* siderophore. Three potential intermediates can be

synthesized based on the presence of certain *F. tularensis* enzymes (I, II, III).
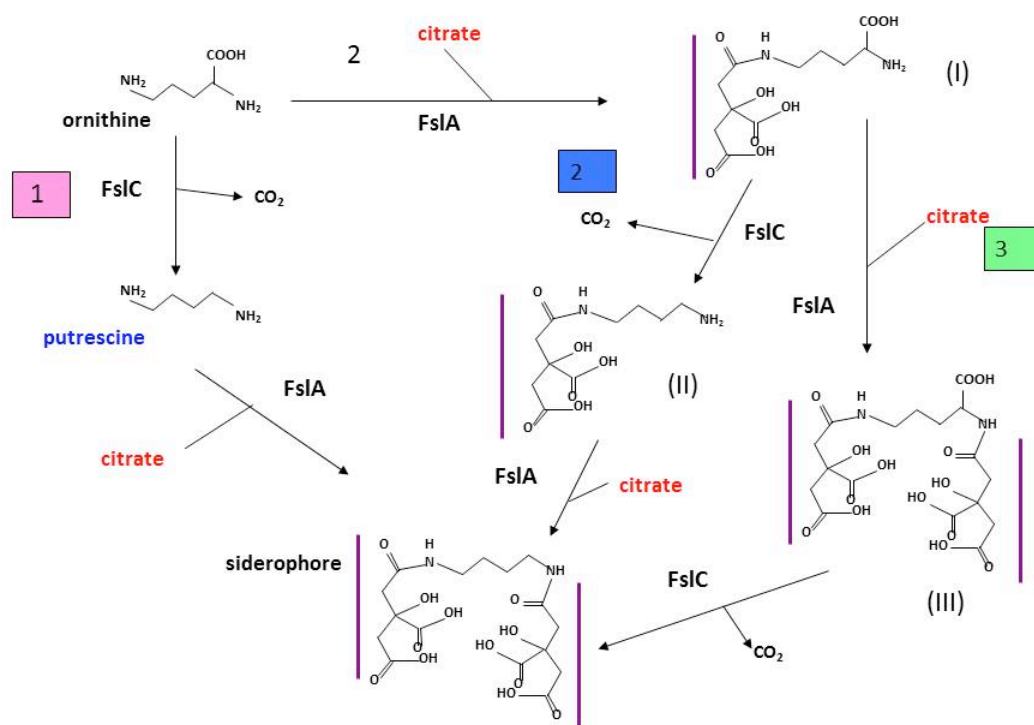
Figure 28

Figure 29: Growth of LVS, LVS Δ*fslA,* and LVS Δ*fslC* mutants on iron replete MHA (MHA+) and iron limiting chemically defined agar (CDM-Fe). LVS, Δ*fslA*, and Δ*fslC* mutants were ten-fold serially diluted in che-CDM and plated on FePPi supplemented MHA agar (MHA+) and iron limiting CDM agar (CDM-Fe) plates. Growth was monitored over 3 days at 37°C under aerobic conditions.
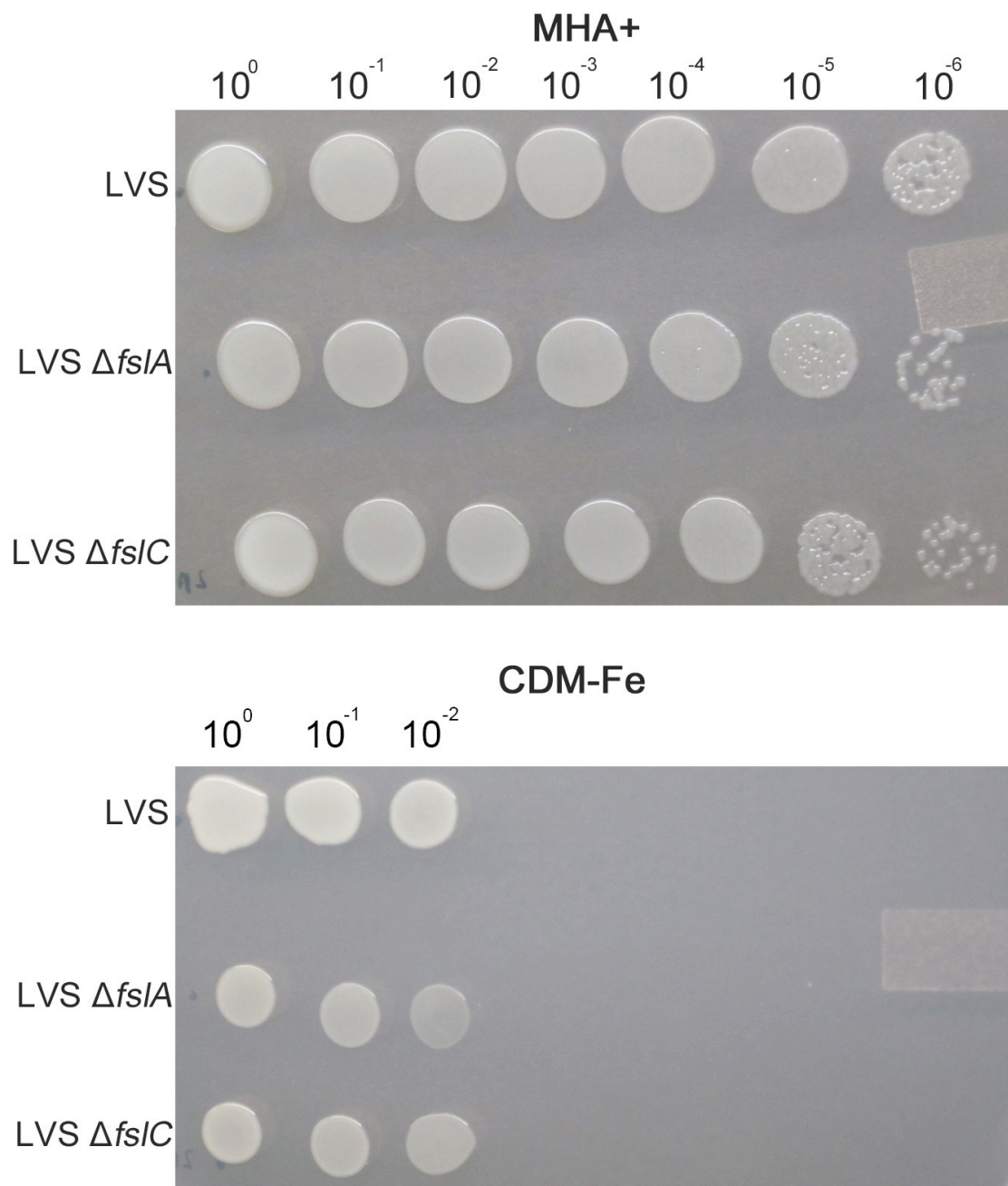
Figure 29

Figure 30:

Growth of LVS, LVS Δ*fslA,* and LVS Δ*fslC* mutants in iron replete and iron limiting chemically defined media.

LVS, Δ*fslA*, and Δ*fslC* mutants were iron starved overnight in iron limiting che-CDM and then inoculated into either high ferric iron (iron replete) or low ferric iron (iron deplete) che-CDM. Growth in liquid was measured as a change in optical density at 600 nm (OD_{600}). Values were plotted as the means ± S.E.
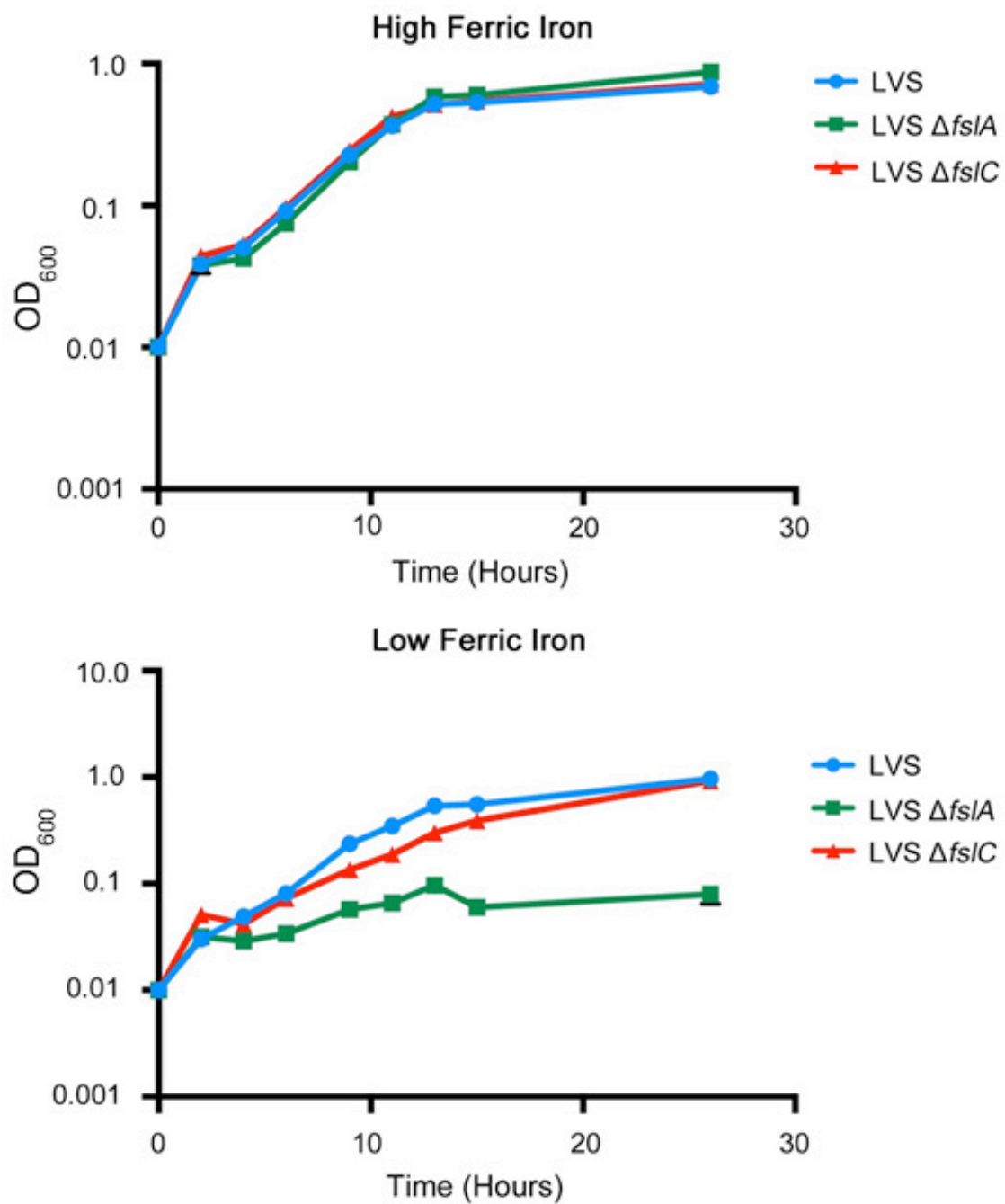
Figure 30

Figure 31: The LVS Δ*fslC* mutant is defective for siderophore production by the CAS assay.

LVS, Δ*fslA*, and Δ*fslC* mutants were grown overnight under high ferric iron (iron replete) (**A**) or low ferric iron (iron deplete) (**B**) conditions. Bacteria contained either empty vector (+V) or the plasmid containing a wild-type copy of *fslC* (+p*fslC*). Culture supernatants were obtained and tested in the CAS assay. Specific CAS activity was determined by normalizing values to OD_{600}.

Figure 31
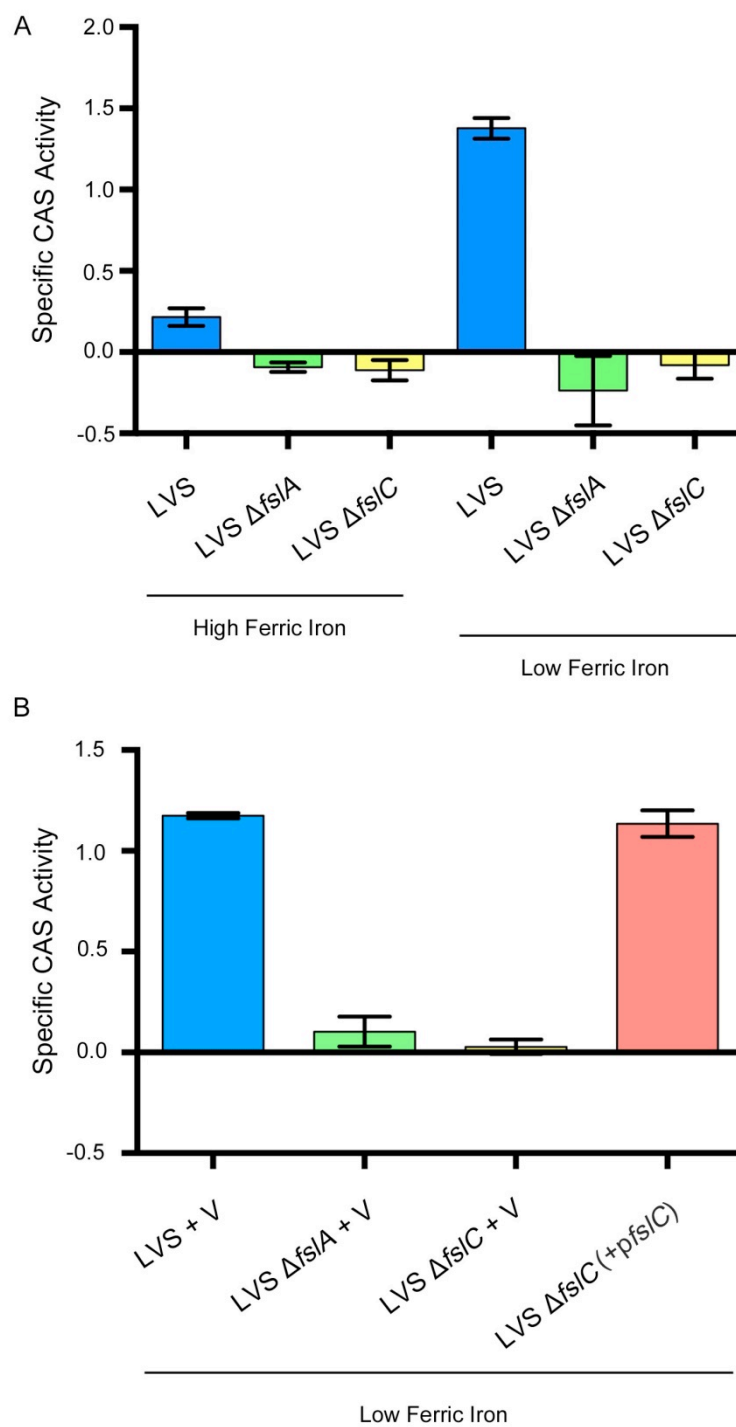
Figure 32: The LVS Δ*fslC* mutant secretes a siderophore intermediate in CDM-Fe siderophore plate bioassays.

CDM-Fe plates were spread with either LVS or Δ*fslC* to serve as the seeded strain. *F. tularensis* donor strains, LVS, LVS Δ*fslA,* and LVS Δ*fslC*, were spotted on the plates and cultures were incubated for 2-4 days. Growth around the spotted donor strain was denoted as the ability of the donor strain to produce and secrete siderophore.

Figure 32

Seed with LVS

Seed with Δ*fslC*
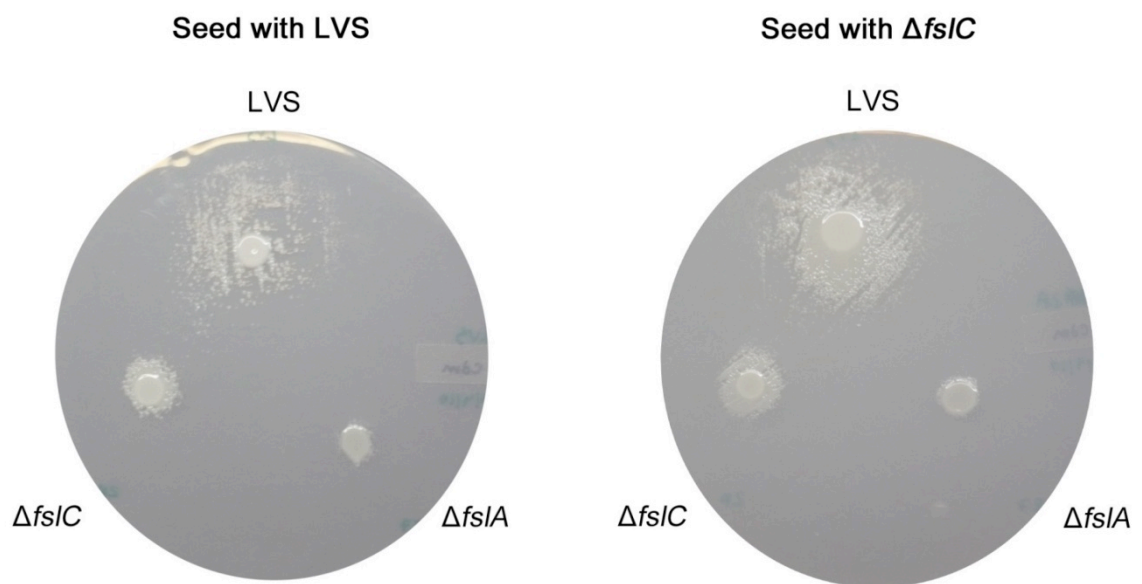
Figure 33: The LVS Δ*fslA* and LVS Δ*fslC* mutants are not defective for replication within J774A.1 murine macrophage cells.

LVS, LVS Δ*fslA,* and LVS Δ*fslC* bacterial stocks were diluted to an MOI of 10 and 100 for infection of J774A.1 murine macrophages (**A**) and A549 human alveolar epithelial cells (**B**), respectively. Cells were infected for the indicated times then subsequently lysed and plated on MHA+ agar plates to determine CFU/mL. Values were expressed as the means ± S.E. Significance was calculated relative to LVS values and LVS Δ*fslA,* and LVS Δ*fslC* were found to be insignificant in comparison to LVS.

Figure 33

A — Intracellular Replication within J774A.1 cells

B — Intracellular Replication within A549 cells
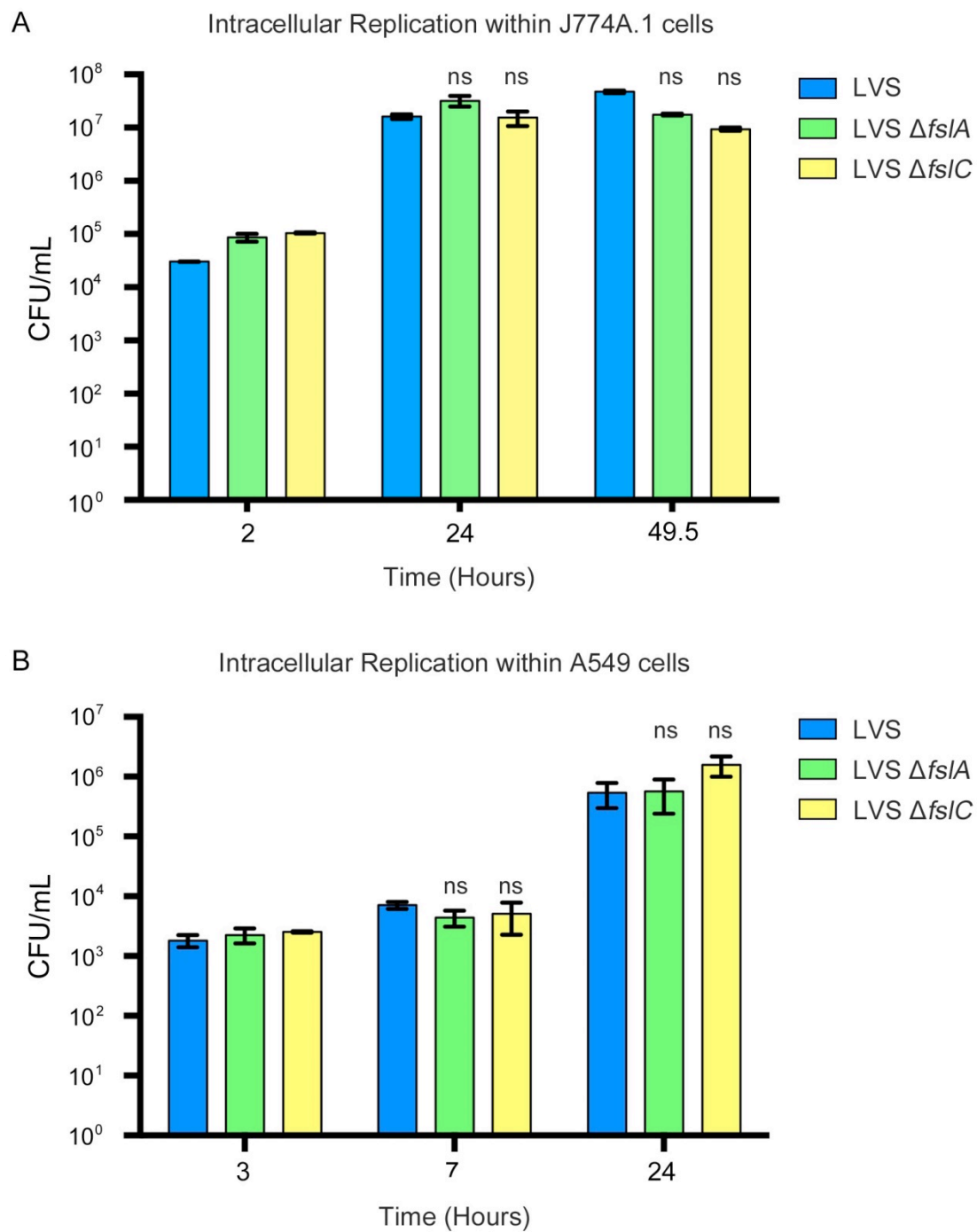
Figure 34: The LVS Δ*fsl* mutant growth on MHA agar.

LVS, Δ*fslA,* and Δ*fsl* strains were ten-fold serially diluted in che-CDM and plated

on MHA agar supplemented with (MHA+) or without (MHA-) FePPi iron. Growth

was monitored over 3 days at 37°C under aerobic conditions.

Figure 34

MHA+

MHA-
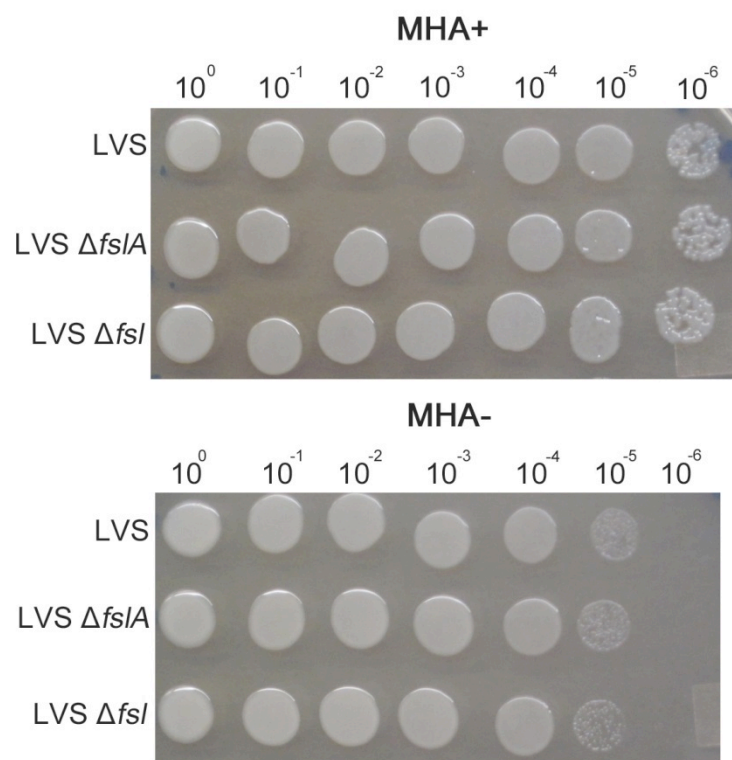
Figure 35: LVS requires the genes *fslA, fslB,* and *fslC* for siderophore production and export.

LVS, Δ*fslA,* and Δ*fsl* mutants containing plasmids with or without *fsl* genes were grown under high ferric iron (iron replete) except for the LVS low iron control which was grown on iron deplete che-CDM broth. Bacterial strains carried either an empty vector (+V) or the plasmid containing wild-type *fslAC, fslAB,* or *fslABC*. Culture supernatants were obtained and tested in the CAS assay. Specific CAS activity was determined by normalizing values to OD_{600}.

Figure 35
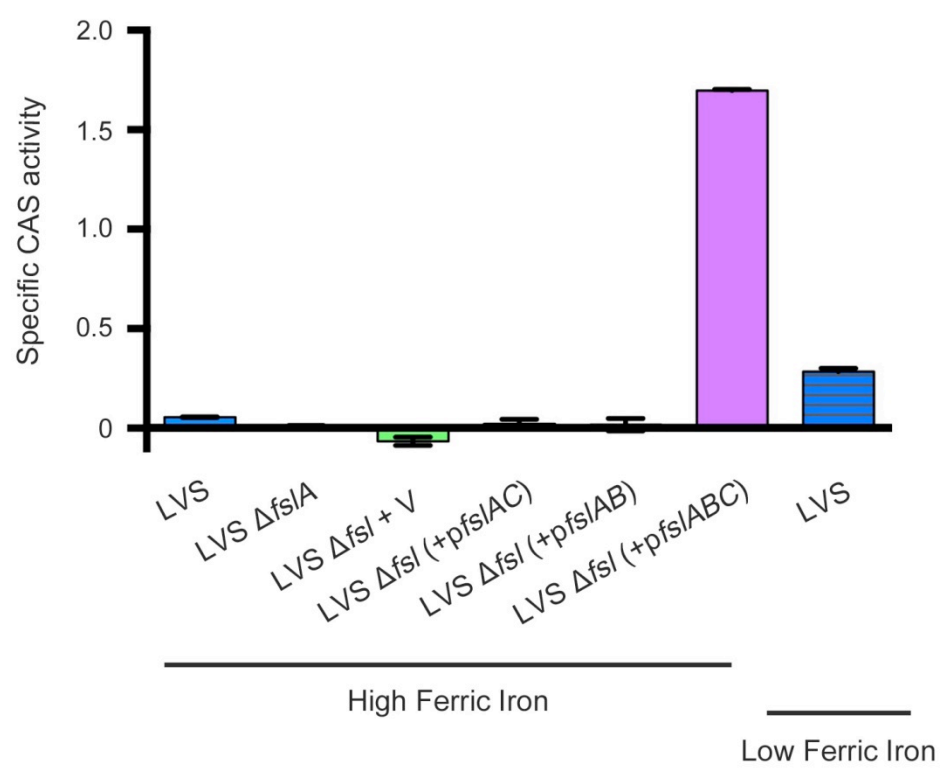
Thesis Discussion:

The mammalian host environment is iron limiting which is primarily attributed to the sequestration of iron by regulatory proteins and iron dependent redox enzymes [1]. This iron restrictive environment substantially reduces the ability for invading bacteria to grow and colonize the host. In order to survive such an environment, bacteria employ diverse iron acquisition mechanisms to obtain iron. Some of these iron acquisition systems are considered virulence determinants and are necessary for bacterial survival in host niches [13,16,17].

The ability of *F. tularensis* to thrive within the iron-limiting environment of the host demonstrates the efficiency of this bacterium in obtaining essential iron for growth and survival. One mechanism in the *F. tularensis* arsenal is the capability of producing a ferric-siderophore under iron limitation [71,75]. Our studies have demonstrated that the *Francisella* siderophore locus (*fslABCDEF*) contains genes necessary for siderophore biosynthesis, transport, and uptake of ferric-siderophore. *F. tularensis* siderophore biosynthesis requires FslA and FslC, and siderophore export requires FslB (Figure 36). The presence of a ferric-siderophore in this bacterium initially led us to hypothesize that the *F. tularensis* siderophore was a potential virulence factor comparable to the ferric siderophores expressed by other pathogenic bacteria such as *B. anthracis* [51] and *M. tuberculosis* [49,50]. However, the *F. tularensis* siderophore was subsequently shown to not be essential for virulence in the Schu S4 Δ*fslA* strain in mouse studies [89] and also in our current studies involving *F. tularensis* Δ*fslA* mutants in tissue culture intracellular replication assays (Figures 11, 25, and 33) [109]. The lack of *F. tularensis* Δ*fslA* virulence in the mouse model instead suggests that *F. tularensis* has another efficient iron acquisition system available at its disposal, which has been shown in LVS [107,109] and Schu S4 to be the Feo iron acquisition system.

Our studies with the FeoB deficient mutants, LVS Δ*feoB'* and Schu S4 Δ*feoB'*, demonstrated that the Feo iron acquisition system is necessary for *Francisella* growth. These studies have expanded our knowledge of *Francisella*'s ferrous iron transport mechanism. We have previously demonstrated that *Francisella* requires the outer membrane ferrous transport proteins, FupA and FupA/B, for high affinity ferrous iron acquisition in Schu S4 and LVS strains, respectively [97,100]. As demonstrated with ^{55}Fe uptake assays in LVS Δ*feoB'*, LVS Δ*fslA* Δ*feoB'*, and Schu S4 Δ*feoB'* strains, ^{55}Fe was unable to enter at both high and low iron concentrations (Figure 16 and Figure 23). Our current model predicts that ferrous iron entry into *Francisella* is highly regulated at the outer and inner membrane (Figure 36). Ferrous iron enters through the outer membrane proteins FupA (Schu S4) or FupA/B (LVS), and is further transported into the cytoplasm through FeoB. FeoA is also present in *Francisella* and future studies determining its function and necessity for optimal ferrous iron transport should be investigated.

The ability of the *F. tularensis* single deletion mutants, LVS Δ*feoB'* and Schu S4 Δ*feoB'*, to continue to thrive in our mouse studies (Figure 18 and Figure 26) demonstrated the importance of the *F. tularensis* siderophore for iron acquisition. The extracellular pathogen *S. aureus* produces a siderophore, staphyloferrin A (Figure 28, Intermediate III) that is structurally related to the *F. tularensis* siderophore (Figure 2 and Figure 28, siderophore). *S. aureus* is capable of utilizing transferrin as an iron source through the use of this iron acquisition system [152]. LVS was shown by Pan *et al.* (2010) to co-localize intracellularly with endocytosed transferrin bound TfR1 receptors within J774A.1 cells [105]. In addition to regulating iron entry into its own cell, *F. tularensis* has the ability to increase the intracellular labile iron pool of host cells through TfR1 [105]. Removal of iron from transferrin by *F. tularensis* was studied in Olakanmi *et al.* (2010) [113]. ^{59}Fe-transferrin was incubated with *F. tularensis* and ^{59}Fe was shown to incorporate into the bacteria [113]. The incubation period was considerably long and potentially allowed

for the degradation of ^{59}Fe-transferrin; this could provide ferric iron for siderophore binding rather than a direct siderophore interaction with the transferrin molecule. Transferrin may still act as an iron source for *F. tularensis* especially late in infection when bacteria have been reported to exist extracellularly in the blood [153], however, the physiological concentration of *F. tularensis* siderophore and further *F. tularensis* siderophore mediated binding of iron from transferrin should be further investigated. We predict that the labile iron pool, which contains transient levels of iron, is the most likely source of iron intracellularly. In our experimental design, only soluble ferric iron, ferrous iron, and ferric-siderophore were provided *in vitro,* but the use of iron bound by host proteins such as hemoglobin, ferritin, or iron bound metalloproteins containing heme or Fe-S clusters were not tested. These iron sources are potential viable alternatives for *F. tularensis* iron attainment and should be explored in future studies.

Neither the Δ*fslA* mutant nor the Δ*feoB'* mutant demonstrates a defect in intracellular growth in J774A.1 cells (Figure 11 and 25) thus suggesting *Francisella* is able to acquire ferric iron through the ferric-siderophore or ferrous iron system to survive within macrophages. Mutants lacking the Feo iron acquisition system had limited ability to grow within hepatocytes, but this growth defect did not hinder the overall *F. tularensis* virulence in mice (Figure 26). This is likely in part due to the ability of the *F. tularensis* Δ*feoB'* mutant to grow and replicate in macrophages, which are considered to be the essential cell type for initial *F. tularensis* growth and replication [60]. Future studies exploring dissemination of these *F. tularensis* single deletion mutants in the mouse model may provide a better understanding of which cell types provide sufficient iron sources for use by the different iron acquisition systems for *Francisella* growth and survival.

Pathogenic bacteria demonstrate severe defects in virulence and viability through the removal of multiple iron acquisition systems [47,48]. This was observed in *Francisella*

through the generation of the double deletion iron acquisition mutants, LVS Δ*fslA* Δ*feoB'*

and Schu S4 Δ*fslA* Δ*feoB'*. The deletion of both systems simultaneously in LVS and

Schu S4 generated a mutant that was defective for iron acquisition and was only viable

in the presence of exogenous siderophore (Figure 13 and Figure 24). Upon entry in host

cells, the ability of *F. tularensis* to escape from the phagosome to the cytoplasm is not

predicted to be iron independent and thus the double deletion is predicted to not remain

in the initial phagosome. Our intracellular replication studies demonstrated that the LVS

double deletion mutant was surprisingly able to survive in tissue culture cells up to 48

hours post infection without a change in the levels of the initial inoculum (Figure 11) [109].

One possibility for the lack of change in *F. tularensis* numbers is a balance of double

deletion mutants growing and dying over time. Although we did not find a third iron

acquisition mechanism *in vitro,* it is possible that an iron bound molecule within our

tissue culture cells may provide minimal iron quantities to allow for replication of the

double deletion and simultaneously the lack of iron may cause another percentage of the

population to die from iron starvation. Since the double deletion mutant is defective for

iron acquisition, a second explanation for this intracellular growth phenotype may be due

to a state of dormancy that allows the bacteria to persist inside the host cell in the

absence of an iron source. The double deletion mutant may be able to remain in the

hostile environment of the cytoplasm or it may also potentially re-enter a host vacuole to

protect itself. It is also possible that the bacteria escape the host cell and try and re-enter

another host cell type. To date we did not identify cell types that limit the growth and

replication of *F. tularensis,* but it is conceivable that in the presence of a nutrient limiting

environment, *F. tularensis* may sequester itself and wait for iron to become available.

The intracellular location of *F. tularensis* Δ*fslA* Δ*feoB'* over time would be best

investigated through tissue culture microscopy studies. A third possibility is for iron to

bind to other divalent metal uptake systems with minimal iron affinity otherwise known as

low-affinity, iron uptake systems. Low-affinity systems have not been well described in other bacteria, but in the presence of iron-replete conditions it is believed that bacteria do not require the expression of high affinity ferric or ferrous iron uptake systems to acquire iron. The double deletion mutants' inability to grow and replicate in iron-replete conditions suggest that low affinity iron acquisition systems are also not being utilized in *F. tularensis.*

It was initially predicted that if the Δ*fslA* Δ*feoB'* mutants were able to grow in tissue culture cells or in the C57BL/6 mouse, then an iron bound protein source could be available within the host to provide iron through an unknown *F. tularensis* iron acquisition system. However, the LVS and Schu S4 double deletion mutants were unable to grow or replicate *in vitro* and were attenuated for virulence in the mouse model. We therefore conclude that the ferric-siderophore and Feo iron acquisition systems are the major iron systems present in *F. tularensis.* These two iron acquisition systems in *F. tularensis* are necessary for optimal iron retrieval and viability and thereby potentiate bacterial virulence. Figure 36 models our current understanding of the iron acquisition mechanisms for *F. tularensis* strains LVS (A) and Schu S4 (B). A third *F. tularensis* iron acquisition system could still potentially have gone undetected in our *in vitro*, *ex vivo*, mouse infection studies, or *in silico* means on the *Francisella* DNA level.

The most significant implications from my work stem from the generation of the LVS and Schu S4 double deletion mutants. These iron acquisition mutants are promising live vaccine candidates, especially the Schu S4 double deletion mutant which provided substantial protection against a lethal challenge of wild-type Schu S4 (Figure 26). Iron limitation is a cue for some bacteria to upregulate not only iron acquisition systems but also virulence factors that may promote bacterial survival within the harsh environment of the mammalian host [13]. RNA sequencing (RNA-seq) profiles of the double deletion mutants during different stages of infection of mammalian cells, especially later time

189

points such as 24 and 48 hours, may provide information about how the mammalian

systems are differentially regulated. We predict from our studies that the double deletion

mutants express bacterial proteins in these iron starved conditions that may be

recognized by the host and contribute to the host's adaptive immune response. Such

studies could provide answers about how the double deletion mutants are capable of

surviving within the mammalian host for long periods of time and would provide

substantial insight into what other factors are contributing to *Francisella's* virulence

within a mammalian host. Future investigators may utilize this information from the

Francisella double deletion mutants for the generation of more effective vaccines against

this pathogenic bacterium.

Figure 36:

The model depicts the predicted roles of the ferric-siderophore system (left) and ferrous iron transport (right) for LVS (**A**) and Schu S4 (**B**). The FslA and FslC proteins synthesize the siderophore from the precursors ornithine and citrate. The siderophore is exported out of the cytoplasm through the inner membrane through FslB and out of the outer membrane through an unknown outer membrane protein (OMP). The siderophore receptor binds the ferric siderophore and its components vary between LVS (FslE and FupA/B) and Schu S4 (FslE) strains. FslD is required for transport of the ferric-siderophore through the inner membrane. Ferrous iron enters the outer membrane through an outer membrane ferrous iron transporter and its components vary between LVS (FupA/B) and Schu S4 (FupA). Entry through the inner membrane requires the inner membrane permease FeoB and potentially the cytoplasmic protein FeoA, both of which are components of the ferrous iron transport system (Feo).

Figure 36
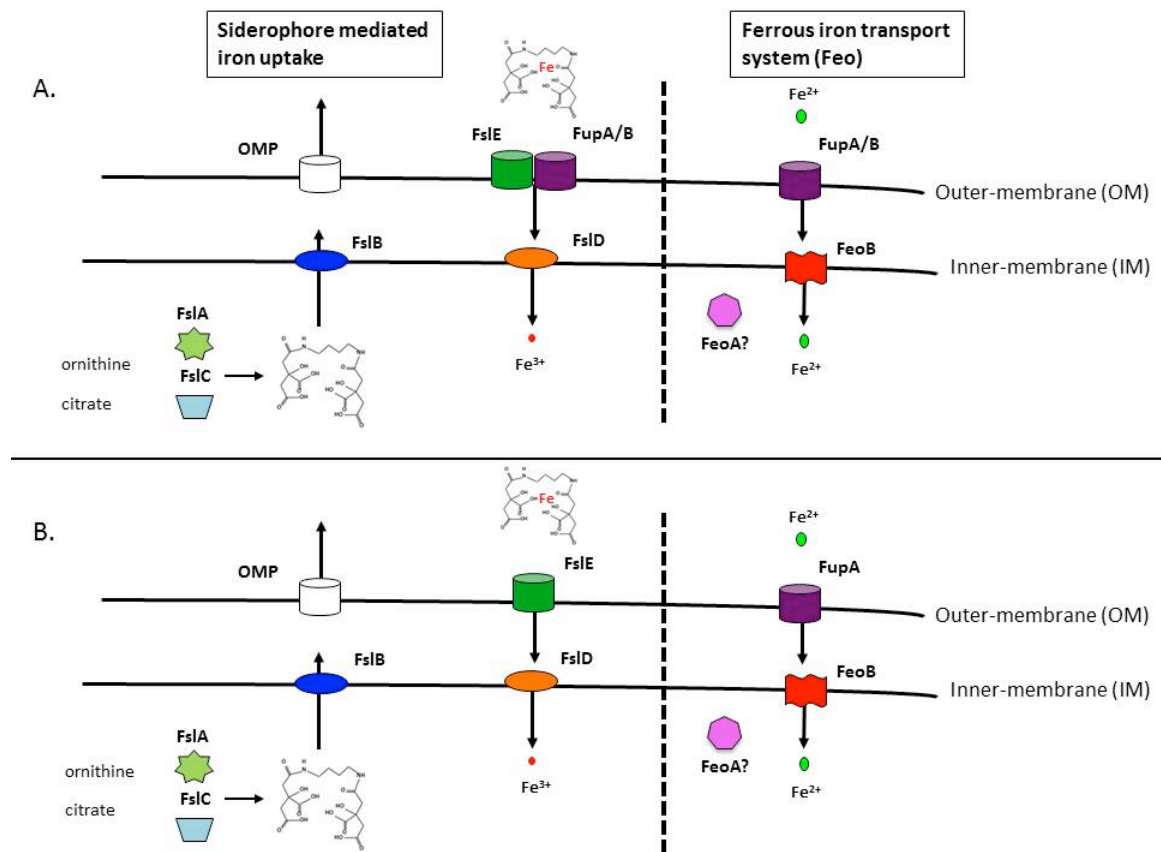
Cited Literature:

1. *Iron and Infection: molecular, physiological, and clinical aspects.* 1–176 (John Wiley & Sons, 1987).

2. Ratledge, C. & Dover, L. G. Iron metabolism in pathogenic bacteria. *Annu. Rev. Microbiol.* **54,** 881–941 (2000).

3. Theil, E. C. & Goss, D. J. Living with iron (and oxygen): questions and answers about iron homeostasis. *Chem. Rev.* **109,** 4568–79 (2009).

4. Caza, M. & Kronstad, J. W. Shared and distinct mechanisms of iron acquisition by bacterial and fungal pathogens of humans. *Front. Cell. Infect. Microbiol.* **3,** 80 (2013).

5. Rapisarda, C. *et al.* Transferrin receptor 2 is crucial for iron sensing in human hepatocytes. *Am. J. Physiol. Gastrointest. Liver Physiol.* **299,** G778–G783 (2010).

6. Kakhlon, O. & Cabantchik, Z. I. The labile iron pool: characterization, measurement, and participation in cellular process(1). *Free Radic. Biol. Med.* **33,** 1037–1046 (2002).

7. Kehl-fie, T. E. & Skaar, E. P. Nutritional immunity beyond iron: a role for manganese and zinc. *Curr. Opin. Chem. Biol.* **14,** 218–224 (2010).

8. Andreini, C., Bertini, I., Cavallaro, G., Holliday, G. L. & Thornton, J. M. Metal ions in biological catalysis: from enzyme databases to general principles. *J. Biol. Inorg. Chem.* **13,** 1205–18 (2008).

9. Schaible, U. E. & Kaufmann, S. H. E. Iron and microbial infection. *Nat. Rev. Microbiol.* **2,** 946–53 (2004).

10. Palaneeswari, M. S., Ganesh, M., Karthikeyan, T., Devi, A. J. M. & Mythili, S. V. Hepcidin-minireview. *J. Clin. Diagn. Res.* **7,** 1767–71 (2013).

11. Cellier, M. F., Courville, P. & Campion, C. Nramp1 phagocyte intracellular metal withdrawal defense. *Microbes Infect.* **9,** 1662–70 (2007).

12. Ganz, T. & Nemeth, E. Iron sequestration and anemia of inflammation. *Semin Hematol* **46,** 387–393 (2009).

13. Litwin, C. M. & Calderwood, S. B. Role of iron in regulation of virulence genes. *Clin. Microbiol. Rev.* **6,** 137–149 (1993).

14. Waldron, K. J. & Robinson, N. J. How do bacterial cells ensure that metalloproteins get the correct metal? *Nat. Rev. Microbiol.* **7,** 25–35 (2009).

15. Andrews, S. C., Robinson, A. K. & Rodríguez-Quiñones, F. Bacterial iron homeostasis. *FEMS Microbiol. Rev.* **27,** 215–237 (2003).

16. Miethke, M. & Marahiel, M. A. Siderophore-based iron acquisition and pathogen control. *Microbiol. Mol. Biol. Rev.* **71,** 413–51 (2007).

17. Latunde-Dada, G. O. Iron metabolism: microbes, mouse, and man. *Bioessays* **31,** 1309–17 (2009).

18. Hantke, K. Is the bacterial ferrous iron transport FeoB a living fossil? *Trends Microbiol.* **11,** 192–195 (2003).

19. Hantke, K. Iron and metal regulation in bacteria. *Curr. Opin. Microbiol.* **4,** 172–7 (2001).

20. Delany, I., Rappuoli, R. & Scarlato, V. Fur functions as an activator and as a repressor of putative virulence genes in Neisseria meningitidis. *Mol. Microbiol.* **52,** 1081–90 (2004).

21. Crosa, J. H. & Walsh, C. T. Genetics and assembly line enzymology of siderophore biosynthesis in bacteria. *Microbiol. Mol. Biol. Rev.* **66,** 223–249 (2002).

22. Braun, V. & Hantke, K. Recent insights into iron import by bacteria. *Curr. Opin. Chem. Biol.* **15,** 328–34 (2011).

23. Palyada, K., Threadgill, D. & Stintzi, A. Iron acquisition and regulation in Campylobacter jejuni. *J. Bacteriol.* **186,** 4714–4729 (2004).

24. Fillat, M. F. The FUR (ferric uptake regulator) superfamily: diversity and versatility of key transcriptional regulators. *Arch. Biochem. Biophys.* **546,** 41–52 (2014).

25. Winkelmann, G. Microbial siderophore-mediated transport. *Biochem. Soc. Trans.* **30,** 691–696 (2002).

26. Kadi, N. & Challis, G. L. Chapter 17. Siderophore biosynthesis a substrate specificity assay for nonribosomal peptide synthetase-independent siderophore synthetases involving trapping of acyl-adenylate intermediates with hydroxylamine. *Methods Enzymol.* **458,** 431–57 (2009).

27. Hider, R. C. & Kong, X. Chemistry and biology of siderophores. *Nat. Prod. Rep.* **27,** 637–57 (2010).

28. Oves-Costales, D., Kadi, N. & Challis, G. L. The long-overlooked enzymology of a nonribosomal peptide synthetase-independent pathway for virulence-conferring siderophore biosynthesis. *Chem. Commun. (Camb).* 6530–41 (2009).

29. Held, K. G. & Postle, K. ExbB and ExbD do not function independently in TonB-dependent energy transduction. *J. Bacteriol.* **184,** 5170–5173 (2002).

30. Cianciotto, N. P. Iron acquisition by Legionella pneumophila. *Biometals* **20,** 323–31 (2007).

31. Larsson, P. *et al.* The complete genome sequence of Francisella tularensis, the causative agent of tularemia. *Nat. Genet.* **37,** 153–9 (2005).

32. Schalk, I. J. & Guillon, L. Fate of ferrisiderophores after import across bacterial outer membranes: different iron release strategies are observed in the cytoplasm or periplasm depending on the siderophore pathways. *Amino Acids* **44,** 1267–77 (2013).

33. D'Onofrio, A. *et al.* Siderophores from neighboring organisms promote the growth of uncultured bacteria. *Chem. Biol.* **17,** 254–64 (2010).

34. Luckey, M., Pollack, J. R., Wayne, R., Ames, B. N. & Neilands, J. B. Iron uptake in Salmonella typhimurium: utilization of exogenous siderochromes as iron carriers. *J. Bacteriol.* **111,** 731–8 (1972).

35. Schubert, S., Fischer, D. & Heesemann, J. Ferric enterochelin transport in Yersinia enterocolitica: molecular and evolutionary aspects. *J. Bacteriol.* **181,** 6387–6395 (1999).

36. Cassat, J. E. & Skaar, E. P. Iron in infection and immunity. *Cell Host Microbe* **13,** 509–19 (2013).

37. Anzaldi, L. L. & Skaar, E. P. Overcoming the heme paradox: heme toxicity and tolerance in bacterial pathogens. *Infect. Immun.* **78,** 4977–89 (2010).

38. Cartron, M. L., Maddocks, S., Gillingham, P., Craven, C. J. & Andrews, S. C. Feo--transport of ferrous iron into bacteria. *Biometals* **19,** 143–57 (2006).

39. Kammler, M., Schön, C. & Hantke, K. Characterization of the ferrous iron uptake system of Escherichia coli. *J. Bacteriol.* **175,** 6212–9 (1993).

40. Kim, H., Lee, H. & Shin, D. The FeoA protein is necessary for the FeoB transporter to import ferrous iron. *Biochem. Biophys. Res. Commun.* **423,** 733–738 (2012).

41. Kim, H., Lee, H. & Shin, D. The FeoC protein leads to high cellular levels of the Fe(II) transporter FeoB by preventing FtsH protease regulation of FeoB in Salmonella enterica. *J. Bacteriol.* **195,** 3364–70 (2013).

42. Marlovits, T. C., Haase, W., Herrmann, C., Aller, S. G. & Unger, V. M. The membrane protein FeoB contains an intramolecular G protein essential for Fe (II) uptake in bacteria. *Proc. Natl. Acad. Sci. U. S. A.* **99,** 16243–8 (2002).

43. Weaver, E. A., Wyckoff, E. E., Mey, A. R., Morrison, R. & Payne, S. M. FeoA and FeoC are essential components of the Vibrio cholerae ferrous iron uptake system, and FeoC interacts with FeoB. *J. Bacteriol.* **195,** 4826–35 (2013).

44. Velayudhan, J. *et al.* Iron acquisition and virulence in Helicobacter pylori: a major role for FeoB, a high-affinity ferrous iron transporter. *Mol. Microbiol.* **37,** 274–286 (2000).

45. Naikare, H., Palyada, K., Panciera, R., Marlow, D. & Stintzi, A. Major role for FeoB in Campylobacter jejuni ferrous iron acquisition, gut colonization, and intracellular survival. *Infect. Immun.* **74,** 5433–44 (2006).

46. Robey, M. & Cianciotto, N. P. Legionella pneumophila feoAB promotes ferrous iron uptake and intracellular infection. *Infect. Immun.* **70,** 5659–5669 (2002).

47. Perry, R. D., Mier Jr., I. & Fetherston, J. D. Roles of the Yfe and Feo transporters of Yersinia pestis in iron uptake and intracellular growth. *Biometals* **20,** 699–703 (2007).

48. Runyen-Janecky, L. J., Reeves, S. A., Gonzales, E. G. & Payne, S. M. Contribution of the Shigella flexneri Sit, Iuc, and Feo iron acquisition systems to iron acquisition in vitro and in cultured cells. *Infect. Immun.* **71,** 1919–1928 (2003).

49. Reddy, P. V. *et al.* Disruption of mycobactin biosynthesis leads to attenuation of Mycobacterium tuberculosis for growth and virulence. *J. Infect. Dis.* **208,** 1255–65 (2013).

50. De Voss, J. J. *et al.* The salicylate-derived mycobactin siderophores of Mycobacterium tuberculosis are essential for growth in macrophages. *Proc. Natl. Acad. Sci. U. S. A.* **97,** 1252–7 (2000).

51. Cendrowski, S., MacArthur, W. & Hanna, P. Bacillus anthracis requires siderophore biosynthesis for growth in macrophages and mouse virulence. *Mol. Microbiol.* **51,** 407–17 (2004).

52. Sjöstedt, A. Tularemia: history, epidemiology, pathogen physiology, and clinical manifestations. *Ann. N. Y. Acad. Sci.* **1105,** 1–29 (2007).

53. Foley, J. E. & Nieto, N. C. Tularemia. *Vet. Microbiol.* **140,** 332–8 (2010).

54. Kingry, L. C. & Petersen, J. M. Comparative review of Francisella tularensis and Francisella novicida. *Front. Cell. Infect. Microbiol.* **4,** 35 (2014).

55. Petersen, J. M., Mead, P. S. & Schriefer, M. E. Francisella tularensis: an arthropod-borne pathogen. *Vet Res* **40,** 7 (2009).

56. Akimana, C. & Kwaik, Y. A. Francisella-arthropod vector interaction and its role in patho-adaptation to infect mammals. *Front. Microbiol.* **2,** 34 (2011).

57. Oyston, P. C. F. Francisella tularensis: unravelling the secrets of an intracellular pathogen. *J. Med. Microbiol.* **57,** 921–30 (2008).

58. Ellis, J., Oyston, P. C. F., Green, M. & Titball, R. W. Tularemia. *Clin. Microbiol. Rev.* **15,** 631–646 (2002).

59. Rohmer, L. *et al.* Comparison of Francisella tularensis genomes reveals evolutionary events associated with the emergence of human pathogenic strains. *Genome Biol.* **8,** R102 (2007).

60. Elkins, K. L., Cowley, S. C. & Bosio, C. M. Innate and adaptive immune responses to an intracellular bacterium, Francisella tularensis live vaccine strain. *Microbes Infect.* **5,** 135–42 (2003).

61. Sjöstedt, A. Virulence determinants and protective antigens of Francisella tularensis. *Curr. Opin. Microbiol.* **6,** 66–71 (2003).

62. Clemens, D. L., Lee, B. & Horwitz, M. A. Francisella tularensis enters macrophages via a novel process involving pseudopod loops. *Infect. Immun.* **73,** 5892–5902 (2005).

63. Golovliov, I., Baranov, V., Krocova, Z., Kovarova, H. & Sjöstedt, A. An attenuated strain of the facultative intracellular bacterium Francisella tularensis can escape the phagosome of monocytic cells. *Infect. Immun.* **71,** 5940–5950 (2003).

64. Clemens, D. L., Lee, B. & Horwitz, M. A. Virulent and avirulent strains of Francisella tularensis prevent acidification and maturation of their phagosomes and escape into the cytoplasm in human macrophages. *Infect. Immun.* **72,** 3204–3217 (2004).

65. Santic, M., Asare, R., Skrobonja, I., Jones, S. & Abu Kwaik, Y. Acquisition of the vacuolar ATPase proton pump and phagosome acidification are essential for escape of Francisella tularensis into the macrophage cytosol. *Infect. Immun.* **76,** 2671–7 (2008).

66. Fortier, A. H. *et al.* Growth of Francisella tularensis LVS in macrophages: the acidic intracellular compartment provides essential iron required for growth. *Infect. Immun.* **63,** 1478–83 (1995).

67. Barker, J. R. & Klose, K. E. Molecular and genetic basis of pathogenesis in Francisella tularensis. *Ann. N. Y. Acad. Sci.* **1105,** 138–59 (2007).

68. Pechous, R. D. *et al.* A Francisella tularensis Schu S4 purine auxotroph is highly attenuated in mice but offers limited protection against homologous intranasal challenge. *PLoS One* **3,** e2487 (2008).

69. Qin, A. & Mann, B. J. Identification of transposon insertion mutants of Francisella tularensis tularensis strain Schu S4 deficient in intracellular replication in the hepatic cell line HepG2. *BMC Microbiol.* **6,** 69 (2006).

70. Wehrly, T. D. *et al.* Intracellular biology and virulence determinants of Francisella tularensis revealed by transcriptional profiling inside macrophages. *Cell. Microbiol.* **11,** 1128–1150 (2009).

71. Deng, K., Blick, R. J., Liu, W. & Hansen, E. J. Identification of Francisella tularensis genes affected by iron limitation. *Infect. Immun.* **74,** 4224–36 (2006).

72. Lenco, J. *et al.* Proteomics analysis of the Francisella tularensis LVS response to iron restriction: induction of the F. tularensis pathogenicity island proteins IglABC. *FEMS Microbiol. Lett.* **269,** 11–21 (2007).

73. Meibom, K. L. & Charbit, A. Francisella tularensis metabolism and its relation to virulence. *Front. Microbiol.* **1,** 140 (2010).

74. Halmann, M. & Mager, J. An endogenously produced substance essential for growth initiation of Pasteurella tularensis. *J. Gen. Microbiol.* **49,** 461–468 (1967).

75. Sullivan, J. T., Jeffery, E. F., Shannon, J. D. & Ramakrishnan, G. Characterization of the siderophore of Francisella tularensis and role of fslA in siderophore production. *J. Bacteriol.* **188,** 3785–95 (2006).

76. Drechsel, H. *et al.* Rhizoferrin — a novel siderophore from the fungus Rhizopus microsporus var. rhizopodiformis. *Biol. Met.* **4,** 238–243 (1991).

77. Münzinger, M. *et al.* S, S-rhizoferrin (enantio-rhizoferrin) – a siderophore of Ralstonia (Pseudomonas) pickettii DSM 6297 – the optical antipode of R, R-rhizoferrin isolated from fungi. *Biometals* **12,** 189–193 (1999).

78. Carrano, C. J. *et al.* Coordination Chemistry of the Carboxylate Type Siderophore Rhizoferrin: The Iron(III) Complex and Its Metal Analogs. *Inorg. Chem.* **35,** 6429–6436 (1996).

79. Drechsel, H. & Winkelmann, G. The configuration of the chiral carbon atoms in staphyloferrin A and analysis of the transport properties in Staphylococcus aureus. *Biometals* **18,** 75–81 (2005).

80. Wandersman, C. & Delepelaire, P. Bacterial iron sources: from siderophores to hemophores. *Annu. Rev. Microbiol.* **58,** 611–47 (2004).

81. O'Brien, S., Hodgson, D. J. & Buckling, A. Social evolution of toxic metal bioremediation in Pseudomonas aeruginosa. *Proc. R. Soc. London B Biol. Sci.* **281,** (2014).

82. Ramakrishnan, G., Meeker, A. & Dragulev, B. fslE is necessary for siderophore-mediated iron acquisition in Francisella tularensis Schu S4. *J. Bacteriol.* **190,** 5353–61 (2008).

83. Weiss, D. S. *et al.* In vivo negative selection screen identifies genes required for Francisella virulence. *Proc. Natl. Acad. Sci. U. S. A.* **104,** 6037–42 (2007).

84. Asare, R. & Abu Kwaik, Y. Molecular complexity orchestrates modulation of phagosome biogenesis and escape to the cytosol of macrophages by Francisella tularensis. *Environ. Microbiol.* **12,** 2559–86 (2010).

85. Kiss, K., Liu, W., Huntley, J. F., Norgard, M. V & Hansen, E. J. Characterization of fig operon mutants of Francisella novicida U112. *FEMS Microbiol. Lett.* **285,** 270–7 (2008).

86. Moule, M. G., Monack, D. M. & Schneider, D. S. Reciprocal analysis of Francisella novicida infections of a Drosophila melanogaster model reveal host-pathogen conflicts mediated by reactive oxygen and imd-regulated innate immune response. *PLoS Pathog.* **6,** e1001065 (2010).

87. Asare, R. & Kwaik, Y. A. Exploitation of host cell biology and evasion of immunity by francisella tularensis. *Front. Microbiol.* **1,** 145 (2010).

88. Su, J. *et al.* Genome-wide identification of Francisella tularensis virulence determinants. *Infect. Immun.* **75,** 3089–101 (2007).

89. Lindgren, H. *et al.* The 58-kilodalton major virulence factor of Francisella tularensis is required for efficient utilization of iron. *Infect. Immun.* **77,** 4429–36 (2009).

90. Traub, A., Mager, J. & Grossowicz, N. Studies on the nutrition of Pasteurella tularensis. *J. Bacteriol.* **70,** 60–69 (1955).

91. Paulsen, I. T., Brown, M. H. & Skurray, R. A. Proton-dependent multidrug efflux systems. *Microbiol. Rev.* **60,** 575–608 (1996).

92. Tanabe, T., Nakao, H., Kuroda, T., Tsuchiya, T. & Yamamoto, S. Involvement of the Vibrio parahaemolyticus pvsC gene in export of the siderophore vibrioferrin. *Microbiol. Immunol.* **50,** 871–876 (2006).

93. Furrer, J. L., Sanders, D. N., Hook-Barnard, I. G. & McIntosh, M. A. Export of the siderophore enterobactin in Escherichia coli: involvement of a 43 kDa membrane exporter. *Mol. Microbiol.* **44,** 1225–34 (2002).

94. Allard, K. A., Viswanathan, V. K. & Cianciotto, N. P. lbtA and lbtB are required for production of the Legionella pneumophila siderophore legiobactin. *J. Bacteriol.* **188,** 1351–1363 (2006).

95. Chatfield, C. H., Mulhern, B. J., Viswanathan, V. K. & Cianciotto, N. P. The major facilitator superfamily-type protein LbtC promotes the utilization of the legiobactin siderophore by Legionella pneumophila. *Microbiology* **158,** 721–35 (2012).

96. Huntley, J. F., Conley, P. G., Hagman, K. E. & Norgard, M. V. Characterization of Francisella tularensis outer membrane proteins. *J. Bacteriol.* **189,** 561–74 (2007).

97. Ramakrishnan, G., Sen, B. & Johnson, R. Paralogous outer membrane proteins mediate uptake of different forms of iron and synergistically govern virulence in Francisella tularensis tularensis. *J. Biol. Chem.* **287,** 25191–202 (2012).

98. Sen, B., Meeker, A. & Ramakrishnan, G. The fslE homolog, FTL_0439 (fupA/B), mediates siderophore-dependent iron uptake in Francisella tularensis LVS. *Infect. Immun.* **78,** 4276–85 (2010).

99. Twine, S. *et al.* A mutant of Francisella tularensis strain SCHU S4 lacking the ability to express a 58-kilodalton protein is attenuated for virulence and is an effective live vaccine. *Infect. Immun.* **73,** 8345–8352 (2005).

100. Ramakrishnan, G. & Sen, B. The FupA/B protein uniquely facilitates transport of ferrous iron and siderophore-associated ferric iron across the outer membrane of Francisella tularensis live vaccine strain. *Microbiology* **160,** 446–57 (2014).

101. Boisset, S., Caspar, Y., Sutera, V. & Maurin, M. New therapeutic approaches for treatment of tularaemia: a review. *Front. Cell. Infect. Microbiol.* **4,** 40 (2014).

102. Hamblin, K. A., Wong, J. P., Blanchard, J. D. & Atkins, H. S. The potential of liposome-encapsulated ciprofloxacin as a tularemia therapy. *Front. Cell. Infect. Microbiol.* **4,** 79 (2014).

103. Pechous, R. D., McCarthy, T. R. & Zahrt, T. C. Working toward the future: insights into Francisella tularensis pathogenesis and vaccine development. *Microbiol. Mol. Biol. Rev.* **73,** 684–711 (2009).

104. Oyston, P. C. F., Sjostedt, A. & Titball, R. W. Tularaemia: bioterrorism defence renews interest in Francisella tularensis. *Nat Rev Micro* **2,** 967–978 (2004).

105. Pan, X., Tamilselvam, B., Hansen, E. J. & Daefler, S. Modulation of iron homeostasis in macrophages by bacterial intracellular pathogens. *BMC Microbiol.* **10,** 64 (2010).

106. Lau, C. K. Y., Ishida, H., Liu, Z. & Vogel, H. J. Solution structure of Escherichia coli FeoA and its potential role in bacterial ferrous iron transport. *J. Bacteriol.* **195,** 46–55 (2013).

107. Thomas-Charles, C. A. *et al.* FeoB-mediated uptake of iron by Francisella tularensis. *Infect. Immun.* **81,** 2828–37 (2013).

108. Schwyn, B. & Neilands, J. B. Universal chemical assay for the detection and determination of siderophores. *Anal. Biochem.* **160,** 47–56 (1987).

109. Pérez, N. M. & Ramakrishnan, G. The reduced genome of the Francisella tularensis live vaccine strain (LVS) encodes two iron acquisition systems essential for optimal growth and virulence. *PLoS One* **9,** e93558 (2014).

110. Fortier, A. H., Slayter, M. V, Ziemba, R., Meltzer, M. S. & Nacy, C. A. Live Vaccine Strain of Francisella tularensis: infection and immunity in mice. *Infect. Immun.* **59,** 2922–2928 (1991).

111. Pechous, R. *et al.* Construction and characterization of an attenuated purine auxotroph in a Francisella tularensis live vaccine strain. *Infect. Immun.* **74,** 4452–61 (2006).

112. Santiago, A. E. *et al.* Characterization of rationally attenuated Francisella tularensis vaccine strains that harbor deletions in the guaA and guaB genes. *Vaccine* **27,** 2426–36 (2009).

113. Olakanmi, O. *et al.* Gallium disrupts iron uptake by intracellular and extracellular Francisella strains and exhibits therapeutic efficacy in a murine pulmonary infection model. *Antimicrob. Agents Chemother.* **54,** 244–53 (2010).

114. Larsson, P. *et al.* Molecular evolutionary consequences of niche restriction in Francisella tularensis, a facultative intracellular pathogen. *PLoS Pathog.* **5,** e1000472 (2009).

115. Sjödin, A. *et al.* Genome characterisation of the genus Francisella reveals insight into similar evolutionary paths in pathogens of mammals and fish. *BMC Genomics* **13,** 268 (2012).

116. Kieffer, T. L., Cowley, S., Nano, F. E. & Elkins, K. L. Francisella novicida LPS has greater immunobiological activity in mice than F. tularensis LPS, and contributes to F. novicida murine pathogenesis. *Microbes Infect.* **5,** 397–403 (2003).

117. Chamberlain, R. E. Evaluation of Live Tularemia Vaccine Prepared in a Chemically Defined Medium. *Appl. Microbiol.* **13,** 232–5 (1965).

118. Shenker, M. Rapid Method for Accurate Determination of Colorless Siderophores and Synthetic Chelates. *Soil Sci. Soc. Am. J.* **59,** 1612 (1995).

119. Eberl, L. *et al.* Analysis of the multimer resolution system encoded by the parCBA operon of broad-host-range plasmid RP4. *Mol. Microbiol.* **12,** 131–141 (1994).

120. Brosius, J. Superpolylinkers in cloning and expression vectors. *DNA* **8,** 759–77 (1989).

121. Maier, T. M. *et al.* Construction and characterization of a highly efficient Francisella shuttle plasmid. *Appl. Environ. Microbiol.* **70,** 7511–7519 (2004).

122. Imlay, J. A. & Linn, S. DNA damage and oxygen radical toxicity. *Science* **240,** 1302–1309 (1988).

123. Pomposiello, P. J. & Demple, B. Global adjustment of microbial physiology during free radical stress. *Adv. Microb. Physiol.* **46,** 319–41 (2002).

124. Meyer, J. M., Neely, A., Stintzi, A., Georges, C. & Holder, I. A. Pyoverdin is essential for virulence of Pseudomonas aeruginosa. *Infect. Immun.* **64,** 518–523 (1996).

125. Neilands, J. B. Siderophores. *Arch. Biochem. Biophys.* **302,** 1–3 (1993).

126. Bearden, S. W., Fetherston, J. D. & Perry, R. D. Genetic organization of the yersiniabactin biosynthetic region and construction of avirulent mutants in Yersinia pestis. *Infect. Immun.* **65,** 1659–1668 (1997).

127. Salomonsson, E. *et al.* Reintroduction of two deleted virulence loci restores full virulence to the live vaccine strain of Francisella tularensis. *Infect. Immun.* **77,** 3424–31 (2009).

128. Chong, A. *et al.* The early phagosomal stage of Francisella tularensis determines optimal phagosomal escape and Francisella pathogenicity island protein expression. *Infect. Immun.* **76,** 5488–99 (2008).

129. Qin, A., Scott, D. W., Rabideau, M. M., Moore, E. A. & Mann, B. J. Requirement of the CXXC motif of novel Francisella infectivity potentiator protein B FipB, and FipA in virulence of F. tularensis subsp. tularensis. *PLoS One* **6,** e24611 (2011).

130. Forbes, J. R. & Gros, P. Iron, manganese, and cobalt transport by Nramp1 (Slc11a1) and Nramp2 (Slc11a2) expressed at the plasma membrane. *Blood* **102,** 1884–1892 (2003).

131. Soe-Lin, S. *et al.* Nramp1 promotes efficient macrophage recycling of iron following erythrophagocytosis in vivo. *Proc. Natl. Acad. Sci. U. S. A.* **106,** 5960–5 (2009).

132. Jones, C. M. *et al.* Self-poisoning of Mycobacterium tuberculosis by interrupting siderophore recycling. *Proc. Natl. Acad. Sci. U. S. A.* **111,** 1945–50 (2014).

133. Williams, P. H. Novel iron uptake system specified by ColV plasmids: an important component in the virulence of invasive strains of Escherichia coli. *Infect. Immun.* **26,** 925–932 (1979).

134. Crosa, J. H. Signal Transduction and Transcriptional and Posttranscriptional Control of Iron-Regulated Genes in Bacteria. *Microbiol. Mol. Biol. Rev.* **61,** 319–336 (1997).

135. Lamont, I. L., Beare, P. A., Ochsner, U., Vasil, A. I. & Vasil, M. L. Siderophore-mediated signaling regulates virulence factor production in Pseudomonas aeruginosa. *Proc. Natl. Acad. Sci. U. S. A.* **99,** 7072–7 (2002).

136. Goetz, D. H. *et al.* The neutrophil lipocalin NGAL is a bacteriostatic agent that interferes with siderophore-mediated iron acquisition. *Mol. Cell* **10,** 1033–1043 (2002).

137. Müller, S. I., Valdebenito, M. & Hantke, K. Salmochelin, the long-overlooked catecholate siderophore of Salmonella. *Biometals* **22,** 691–5 (2009).

138. Fischbach, M. A., Lin, H., Liu, D. R. & Walsh, C. T. How pathogenic bacteria evade mammalian sabotage in the battle for iron. *Nat. Chem. Biol.* **2,** 132–8 (2006).

139. Abergel, R. J. *et al.* Anthrax pathogen evades the mammalian immune system through stealth siderophore production. *Proc. Natl. Acad. Sci. U. S. A.* **103,** 18499–18503 (2006).

140. Zajdowicz, S. *et al.* Purification and structural characterization of siderophore (corynebactin) from Corynebacterium diphtheriae. *PLoS One* **7,** e34591 (2012).

141. Beasley, F. C. *et al.* Characterization of staphyloferrin A biosynthetic and transport mutants in Staphylococcus aureus. *Mol. Microbiol.* **72,** 947–63 (2009).

142. Cotton, J. L., Tao, J. & Balibar, C. J. Identification and characterization of the Staphylococcus aureus gene cluster coding for staphyloferrin A. *Biochemistry* **48,** 1025–35 (2009).

143. Dorsey, C. W., Tolmasky, M. E., Crosa, J. H. & Actis, L. A. Genetic organization of an Acinetobacter baumannii chromosomal region harbouring genes related to siderophore biosynthesis and transport. *Microbiology* **149,** 1227–1238 (2003).

144. Halmann, M. & Mager, J. An endogenously produced substance essential for growth initiation of Pasteurella tularensis. *J. Gen. Microbiol.* **49,** 461–468 (1967).

145. Meiwes, J. *et al.* Isolation and characterization of staphyloferrin A, a compound with siderophore activity from Staphylococcus hyicus DSM 20459. *FEMS Microbiol. Lett.* **55,** 201–5 (1990).

146. Konetschny-Rapp, S., Jung, G., Meiwes, J. & Zähner, H. Staphyloferrin A: a structurally new siderophore from staphylococci. *Eur. J. Biochem.* **191,** 65–74 (1990).

147. Berti, A. D. & Thomas, M. G. Analysis of achromobactin biosynthesis by Pseudomonas syringae pv. syringae B728a. *J. Bacteriol.* **191,** 4594–604 (2009).

148. Ray, S. S. *et al.* Cocrystal structures of diaminopimelate decarboxylase: mechanism, evolution, and inhibition of an antibiotic resistance accessory factor. *Structure* **10,** 1499–508 (2002).

149. Tabor, C. W. & Tabor, H. Polyamines in microorganisms. *Microbiol. Rev.* **49,** 81–99 (1985).

150. Filippou, P. S. *et al.* Effect of polyamines and synthetic polyamine-analogues on the expression of antizyme (AtoC) and its regulatory genes. *BMC Biochem.* **8,** 1 (2007).

151. Russo, B. C. *et al.* A Francisella tularensis locus required for spermine responsiveness is necessary for virulence. *Infect. Immun.* **79,** 3665–76 (2011).

152. Beasley, F. C., Marolda, C. L., Cheung, J., Buac, S. & Heinrichs, D. E. Staphylococcus aureus transporters Hts, Sir, and Sst capture iron liberated from human transferrin by Staphyloferrin A, Staphyloferrin B, and catecholamine stress hormones, respectively, and contribute to virulence. *Infect. Immun.* **79,** 2345–55 (2011).

153. Forestal, C. A. *et al.* Francisella tularensis has a significant extracellular phase in infected mice. *J. Infect. Dis.* **196,** 134–7 (2007).